IN-18
3794
72 P

NASA Contractor Report 189172

# Cryogenic On-Orbit Liquid Depot Storage Acquisition and Transfer (COLD–SAT) Experiment Subsystem Instrumentation and Wire Harness Design Report

Lawrence G. Edwards
*Analex Corporation*
*Brook Park, Ohio*

March 1994

(NASA-CR-189172) CRYOGENIC ON-ORBIT LIQUID DEPOT STORAGE ACQUISITION AND TRANSFER (COLD-SAT) EXPERIMENT SUBSYSTEM INSTRUMENTATION AND WIRE HARNESS DESIGN REPORT Final Report (Analex Corp.) 72 p

N94-29405

Unclas

G3/18 0003794

Prepared for
Lewis Research Center
Under Contract NAS3–25776

National Aeronautics and
Space Administration

# CRYOGENIC ON-ORBIT LIQUID DEPOT STORAGE ACQUISITION AND TRANSFER (COLD–SAT) EXPERIMENT SUBSYSTEM INSTRUMENTATION AND WIRE HARNESS DESIGN REPORT

Lawrence G. Edwards
Analex Corporation
Brook Park, Ohio

## SUMMARY

This report describes an instrumentation and wire harness design for the COLD–SAT experiment subsystem. The design incorporates transducers, signal conditioning systems, and wire harness components that were chosen, whenever possible, based on their past successful use with liquid hydrogen ($LH_2$) and on previous spaceflight systems. Electrical current excitation levels and data acquisition ranging were designed to meet the temperature measurement requirements using space-flight qualified platinum resistance thermometers with existing 8-bit space-flight qualified data acquisition systems. Cone shaped $LH_2$ temperature and liquid/vapor sensors were recommended to minimize false measurements in low-gravity conditions. The need for a 12-bit data acquisition system to provide improve resolution and accuracy for critical measurements is addressed, and an experimental data unit design is presented. Error analyses were performed on all instrument candidates, and the influence of physical parameters such as temperature and pressure on the overall measurement accuracies was determined. Most experimenters' measurement requirements can be met by the design; however, some measurement techniques and instrumentation need development. Two-phase flow detection, leak detection systems, and mass gauging are areas that need development. Heat conduction to the $LH_2$ tanks was recognized as a chief concern early in the design effort. Wire materials, wire multiplexing techniques, and cryogenic operable pressure transducers were selected to minimize this problem.

A list identifying all measurements and the transducers to be used to make the measurements is presented. Schematic drawings showing the locations of the transducers are presented, and a total system wire harness was designed to show the feasibility and hardware requirements of the system.

## INTRODUCTION

Acquiring the technology to store and transfer cryogens in space is mandatory for future long-duration space flight missions. COLD–SAT, an acronym for cryogenic orbiting liquid depot for storage, acquisition, and transfer, is a spacecraft-experiment system designed to obtain this technology. The spacecraft will contain a $LH_2$ supply tank, a large receiver tank, and a small receiver tank. Experiments investigating $LH_2$ tank pressure control, receiver tank chilldown methods, and receiver tank fill techniques will be conducted. The success of the COLD–SAT experiments will be directly related to the measurements made and the accuracy with which the measurement data are acquired and processed. The instrumentation, signal conditioning, and measurement techniques used to make the various measurements is critical in determining the success of the mission.

The instrumentation must be capable of surviving the stresses of launch and the environment of space and be reliable over the course of the COLD–SAT mission. The instrumentation must not interfere with or distort the processes it measures. Transducers must operate in liquid and gaseous hydrogen environments. Electrical wiring materials and techniques must minimize heat conduction to the cryogenic tanks.

This report presents a detailed design for the instrumentation, signal conditioning, and wire harness. In developing the design, instrumentation candidates capable of meeting the measurement requirements were compared, and recommendations were proposed based on error analysis, reliability, and performance histories. The location, mounting techniques, and electrical harnessing of the instruments are addressed. Experiment signal conditioners and telemetry interface systems that are designed to maximize the return of experimental data while minimizing interference with experiment phenomena are presented. System component weights and power requirements were estimated. Specific instrumentation models are not identified in this report to avoid the appearance of NASA or Analex Corp. endorsement of commercial products.

This report is meant to be used in conjunction with the overall COLD–SAT Technical Memorandum report which contains detailed descriptions of the spacecraft, experiment requirements, and mission philosophy.

This report documents the NASA Lewis Research Center in-house COLD–SAT instrumentation and wire harness design effort conducted under Contract NAS3–25776. The feasibility design was completed for presentation at a nonadvocate review of the total COLD–SAT program held in June 1990. The findings of the review committee were that the project was feasible. The program, however, was found unacceptable due to cost.

## ACKNOWLEDGMENTS

The author is grateful to all the members of the COLD–SAT design team, NASA Lewis Research Center's Cryogenic Fluid Technology Office, Analex Corp., editors, and the numerous others who have contributed to the completion of the design effort.

## COLD-SAT EXPERIMENT INSTRUMENTATION AND ELECTRONICS SUBSYSTEM TT&C

### Interface Definition

The experiment system instrumentation and electronics subsystem consists of the transducers required to convert physical process parameters, such as temperature, pressure, flow rate, and acceleration, into electrical equivalent signals. The transducers require electrical excitation signals, which are provided by power supplies contained in the signal-conditioning electronic boxes. The output signal of the transducers must be conditioned to a form compatible for input to the spacecraft telemetry tracking and command (TT&C) subsystem. This is accomplished by amplifiers, filters, and analog-to-digital signal converters. The experiment system contains three high-resolution, 12-bit analog-to-digital converter signal conditioning units, called experiment data units, or EDU's. The experiment system instrumentation and electronics subsystem also contains the instrumentation and electrical component wire harnesses, sensor mounting hardware, heaters, liquid-level capacitive probe signal conditioning unit, accelerometer, and fluid mixer power unit. Table 1 lists the experiment system electronic boxes with their estimated weights and power requirements. Figure 1 is an artist's concept of the COLD–SAT spacecraft that shows the location of the electronic bays.

The experiment electrical and electronic boxes receive power from the spacecraft electrical system. Heaters, valves, mixer motor, and most instrumentation receive electrical power through the TT&C system. The TT&C system contains a command telemetry unit (CTU) and two remote command telemetry units (RCTU's), which provide transducer electrical power, sensor output signal conditioning, and 8-bit analog-to-digital signal conversion. The TT&C system also contains relay sequencer units (SEQ's), which distribute electrical power to the experiment subsystem valves and heaters. Figure 2 is a block diagram of the COLD–SAT experiment system and its interface with the TT&C system. The total number of sensors and the number of sensors assigned to each signal conditioner is shown.

## Transducers

Transducers consist of the sensors and built-in compensation networks required to convert physical properties into equivalent electrical signals. Temperature, pressures, flow rates, acceleration, liquid level, vapor detection, mixer motor speed, power, and valve status transducers are required for monitoring the physical properties and status of the COLD–SAT experiment fluids and systems.

## Data Acquisition Systems

Figure 3 is a simplified block diagram representation of a COLD–SAT experiment data acquisition system (DAS). The DAS acquires the analog output signals of the transducers, conditions the signals by means of amplifiers, filters, and translators and converts the signal to an equivalent digital form required by the TT&C system.

To minimize circuitry, electronic multiplexers are used to switch the transducer output to a single instrumentation amplifier stage where the signal is converted to a 0- to 5-V level. The voltage output of the amplifier stage is converted to an equivalent digital form for the telemetry system by analog-to-digital converters. The convertors are defined by the number of binary digits (bits) they use to represent an analog signal range. The resolution, or smallest detectable change, of the DAS is equal to the span of the measurement system divided by the decimal equivalent of the number of bits. COLD–SAT experiment measurements will be monitored with two types of DAS systems: 8-bit analog-to-digital systems, located in the TT&C telemetry units, and 12-bit analog-to-digital systems, designated as experimental data units (EDU's).

*Telemetry tracking and command 8-bit data acquisition systems.*—The TT&C system provides most of the signal conditioning electronics for the COLD–SAT instrumentation. The TT&C system uses 8-bit analog-to-digital converters located in the systems command and remote command telemetry units (RCTU's). The 8-bit converters set the measurement resolution to 1 part in 256 of the analog measurement range. The maximum error between the analog input and its digitized equivalent can be as great as 1/2 the resolution value, or ±0.195 percent of the full-scale range. This error component is known as the quantization error (ref. 1). The system's multiplexers have leakage current components that produce measurement errors due to the voltage drop they produced across resistive components in the circuit. Each signal conditioning card contains eight multiplexers that can result in a total leakage current component eight times greater than the specified value of one multiplexer. The uncertainties of the signal conditioning electronics were included in the measurement error analysis and influenced the selection of a sensor type. Table 2 lists the estimated root sum square (rss) signal conditioning uncertainties for the anticipated sensor measurement ranges. The values were based on existing 8-bit flight qualified data acquisition system capabilities. The rss method of combining uncertainties was used for all measurement error analysis because of the unlikely probability that all uncertainties are coherent (ref. 2).

*Experimental data units .*—Three EDU's were designed with 12-bit analog-to-digital converters to provide improved accuracy and resolution and to meet measurement requirements incapable of being met by the 8-bit systems. The EDU design and 8-bit signal conditioning system designs were identical except for the use of a 12-bit analog-to-digital converter and only one multiplexer per circuit card. The EDU's would provide excitation and signal conditioning electronics for the flow-measurement systems, accelerometer, and high-resolution tank-pressure measurement transducers. Figure 4 is a simplified block diagram of an EDU measurement system. Figure 5 shows the major signal conditioning errors of the two types of DAS units estimated for the 30-mV measurement range. The use of a 12-bit analog-to-digital converter and only one multiplexer per card reduced the quantization error to 0.012 percent of the range and reduced the leakage current influence by 1/8th. The qualification of a 12-bit analog-to-digital converter for space flight is required for this system to be feasible.

## Harnessing

The experiment subsystem instrumentation and electrical power component harness consists of the electrical wiring and connectors required to connect the transducers and electrical powered components to their associated signal conditioners, power supplies, and relay boxes.

Most of the instrumentation and electric powered components will be thermally bonded to the $LH_2$ tanks. The temperature gradient experienced by the component wiring will result in a large thermal energy input into the tanks and an excessive boiloff loss of hydrogen if copper wire were used. To minimize this problem, unconventional wire material will be used to electrically connect the cryogenic tank instrumentation and hardware to the warm copper wire harness of the spacecraft wire trays. Manganin wire will be used for instrumentation wiring. Phosphor bronze wiring will be used for valves and heater applications.

Manganin has a distinct advantage over other wire materials for cryogenic use because of its very low thermal conductivity at low temperatures (ref. 3). Unfortunately, being a poor thermal energy conductor also results in manganin being a poor electrical conductor. However, the current requirements for most of the instrumentation is below 15 mA, and 24 American wire gauge (AWG) diameter manganin wire is adequate. Four-wire measurements will be made on temperature sensors to eliminate the wire voltage drop of the sensors' current carrying leads from the voltage-measurement circuit. The constant current operation of pressure transducers will eliminate wire voltage-drop influence from this measurement.

Phosphor bronze wire provides a combination of fairly low thermal conductivity with reasonable resistivity and was selected for valves, motors, and heaters that have current ratings that would require excessively large-diameter manganin wire (ref. 4). The use of phosphor bronze wire would reduce the electrical components harness weight and limit heat conduction to a tolerable level.

Connectors and receptacles used for cryogenic tank wire feedthroughs will be similar to the type used on D–1A Centaur launch vehicles. Bulkhead connector assemblies exposed to temperatures below –55 °F will conform to George C. Marshall Space Flight Center specification 40M38294. Connectors exposed to temperatures above –55 °F will be series MIL–C–38999.

## MEASUREMENT REQUIREMENTS

The COLD–SAT experiment matrix consists of eight primary experiments. From the primary experiment data requirements the following measurements were identified to be necessary:

- High-resolution $LH_2$ and $GH_2$ temperatures (type A)
- Tank structure temperatures (type AB)
- Hydrogen liquid-vapor level
- Liquid-vapor two-phase flow detection
- Tank pressures and flow device pressure drops
- Liquid-hydrogen flow rates
- Mixer flow rates
- Thermodynamic vent systems (TVS) and vent flow rates
- Spacecraft acceleration
- Valve status indication
- Electrical power supplied to heaters and mixer motors.

Transducers were selected for each type of measurement based on measurement range, accuracy, and reliability. Signal conditioning techniques were developed to achieve best possible measurement accuracy based on a measurement error analysis. Table 3 lists the required measurements, the measurement range, transducer type, and numbers. Calculated measurement uncertainties and desired sampling rates are also listed. A detailed measurement list, which provides traceability of each measurement to its primary experiment requirement document, is located in the appendix.

## Temperature Measurement Requirement

Two primary temperature measurement requirements were determined from the experiment requirements.

*High-resolution $LH_2$ and $GH_2$ temperatures (type A).*—The capability of measuring and resolving small temperature gradients existing from the $LH_2$ tank walls into the bulk of the fluid and also at the $LH_2$–$GH_2$ interface is required. Temperature sensors capable of fulfilling this requirement would provide temperature measurements of structure and fluid in the saturated and subcooled hydrogen temperature ranges. An uncertainty less than or equal to ±0.2 °R for the 20 to 50 °R temperature range is required for these measurements. This high-accuracy temperature measurement was designated as type A.

The saturation temperature of hydrogen varies from 30.8 °R at 5 psia to 45.4 °R at 50 psia (ref. 5). This pressure range covers the operating range of the cryogenic tanks and thermodynamic vent systems. The temperature measurement accuracy over this range was considered critical.

*Tank structure temperatures.*—Temperature measurements of tanks, structure components, and fluids during chilldown experiments and periodically during the course of the COLD–SAT mission must be measured. A total temperature range measurement from 36 to 540 °R is required. This total temperature range measurement was designated type AB.

## Temperature Sensor Candidates

A number of temperature transducer types exist that could be used to measure the required temperature ranges (ref. 6). Three popular thermoresistive temperature sensors used for cryogenic temperature measurements are germanium resistance thermometers (GRT), platinum resistance thermometers (PRT), and silicon diodes. Thermoresistive temperature measurement is based on the change in a metal or semiconductor impedance as a function of temperature.

Other temperature measurement sensors include thermocouples and thermistors. Thermocouples were not considered because of their low sensitivities and poor accuracies. Thermistors were not considered because of their rapidly changing sensitivities and the need for multiple range-switching signal-conditioning systems.

*Platinum resistance thermometers.*—Platinum resistance thermometers (PRT's) belong to the resistance temperature detector (RTD) family. Resistance temperature detection is based on the increase in resistivity of a metal conductor with increase in temperature. Ideally, the metal used for the temperature sensor would be pure and would be mounted in a strain-free manner. The resistance of the sensor, then, would be dependant only on temperature and metal geometry. The basic relation between sensor resistance, geometry, and temperature is

$$R_t = \sigma L/A = R_o\left[1+\alpha\left(T-T_o\right)\right] \tag{1}$$

where $A$ is the area, $L$ is the length, $R_t$ is the resistance, $R_o$ is the ice point resistance, $T$ is the temperature, $T_o$ is the ice point temperature, $\sigma$ is the resistivity, $\alpha$ is the temperature coefficient of resistance.

Platinum resistance thermometers are classified according to their water ice point resistance ($R_o$) values and can range in value from tens to thousands of ohms. They have been used extensively in aerospace and cryogenic applications and have also been mounted and used in special cone-shaped probes designed for use in low-gravity environments to minimize false ullage temperature readings (ref. 7).

*Germanium resistance thermometers.*—Germanium resistance thermometers (GRT's) typically consist of a specially grown and doped germanium crystal mounted in a strain-free manner within a copper metal can. Four wire leads of very-small-gauge copper or low-thermal-conductivity wire are attached to the sensor to provide electrical excitation and output signal sensing connections. Germanium resistance thermometers have negative resistivity temperature coefficients, and their values of resistance and sensitivity can vary by several orders of magnitude over the temperatures from 18 to 180 °R. To prevent self-heating errors, manufacturers recommend that the sensor be excited by a power source such that the potential across the sensor is kept at 10 mV or less. Measurements taken with GRT's would be limited to type A. A different type of temperature sensor would be required to monitor the warmer temperature ranges.

*Silicon diode temperature sensors.*—Silicon diode temperature sensors are nonlinear semiconductor devices that exhibit negative temperature coefficients of resistivity. They exhibit very high sensitivity (millivolts per degree) at cryogenic temperatures and good sensitivity above the cryogenic range. The sensors are small and rugged, and their high impedance may allow two-wire measurements to be made for less accurate measurement requirements. Silicon diodes are attractive as total range temperature sensors that could monitor the chilldown rate of the COLD–SAT tank structures. The low 10-μA excitation recommended for silicon diode operation virtually eliminates sensor self-heating errors.

## Temperature Measurement Error Sources

*Temperature sensor calibration inaccuracy.*—Calibration of the temperature sensors is required to accurately characterize the specific sensor's resistance versus temperature characteristic and to obtain measurement uncertainties of ≤0.2 °R. Inaccuracies in the calibration process are due to temperature standard, calibration media, and measurement equipment errors. Commercial temperature sensor calibration uncertainties are typically less than ±0.05 °R.

*Interpolation errors.*—The voltage output response of the calibrated temperature sensor is converted to its temperature equivalent by use of a polynomial equation. The accuracy of the temperature interpolation equation is dependant on the calibration measurement accuracy and the number of calibration points. Interpolation error can also occur when linear interpolation is used between calibrated points. Interpolation errors of less than ±0.04 °R can be obtained by proper specification of the number of calibration points and the temperature increment size on the calibration table.

*Data acquisition system error.*—The largest uncertainty in the COLD–SAT temperature measurement is due to data acquisition system limitations. The DAS voltage measurement error for the temperature sensor candidates was estimated using the DAS voltage measurement range errors listed in table 2. Table 4 lists the estimated excitation signals, output signal levels, and data acquisition inaccuracies for the sensor candidates.

A concern exists regarding the ability to flight qualify a 10-μA constant current source required for the silicon diode sensors. However, for comparison purposes a 10-μA flight-qualified current source was considered feasible with an excitation error of less than ±0.1 percent.

To prevent self-heating errors, the recommended excitation level for GRT sensors is a current that produces a potential drop across the sensor of 10 mV or less. An electronic power supply that would automatically regulate the sensor current so that the sensor potential remains at 10 mV would be required. The excitation current would be detected across a precise resistor and temperature would be calculated from the current level magnitude.

*Platinum resistance thermometer temperature measurement design and error analysis.*—The PRT sensitivity to meet the high-accuracy temperature measurement requirement of ±0.2 °R must be greater than the ratio of the voltage measurement range error divided by the inaccuracy requirement of 0.2 °R; that is, assuming a rss error for the 125-mV measurement of 0.36 percent or 0.45 mV:

$$\text{Sensitivity} = \text{mV}/{}^\circ\text{R} \geq (0.45\ \text{mV}/0.2\ {}^\circ\text{R}) \geq 2.25\ \text{mV}/{}^\circ\text{R} \qquad (2)$$

The sensitivity of commercially available ice-point resistance PRT's was calculated as a function of excitation current magnitude. Table 5 lists the typical resistance-temperature relationship for a 1000-Ω PRT.

The change in PRT resistance as a function of temperature was calculated. The product of this value and the excitation current magnitude of 10 mA yields the sensitivity of the sensor at that temperature. The temperature equivalent of the DAS error was calculated by taking the product of the inverse of the sensitivity factor and the millivolt DAS error value. Figure 6 shows that the 1000-Ω ($R_o$) PRT, when excited by a 10-mA constant current, could meet the sensitivity requirement with a DAS uncertainty of ±0.2 °R over the temperature range of 29 to 50 °R. The total rss combination of sensor calibration, interpolation, and DAS error would still be less than ±0.21 at 29 °R.

*Self-heating error considerations.*—A major concern was the magnitude of error that could occur due to self-heating of the PRT sensor by the 10-mA excitation current. Self-heating causes the sensor's temperature to rise to a value greater than the temperature of the environment it is to measure. To minimize self-heating, the sensors would be energized for short duty cycles of approximately 1.0 percent. The effective power dissipated by the sensor would be $1 \times 10^{-4}$ that of its continuous operation duty cycle value.

*Total range PRT temperature measurement (type AB) error analysis.*—The TT&C DAS uses programmable gain amplifiers that will allow dual measurement ranging. This capability allows a large temperature span to be monitored at a reduced accuracy. Error analysis performed on PRT sensors showed that a 1000 $R_0$ PRT excited by a 1-mA constant current source could measure the temperature range from 29 to 560 °R with an 8-bit DAS uncertainty within ±2.0 °R. A DAS range change from the 125-mV range to the 1.25-V range would occur at temperatures above 110 °R. Figure 7 shows the results of this error analysis.

*Silicon diode, 8-bit DAS temperature measurement error analysis.*—The estimated temperature measurement error for a commercially available silicon diode was determined using the manufacturer's diode sensitivity values and the estimated 8-bit DAS, 1.25-V range measurement error. Below 33 °R the diodes output voltage would exceed the 1.25-V range limit, and a DAS range change would be required. The temperature measurement error results for the 1.25-V range are shown in figures 5 and 6.

*High-accuracy liquid hydrogen temperature range measurement.*—The fraction of a volt deviation in the diode output that occurs in the critical $LH_2$ temperature range rides on a 1-V level. To maximize the accuracy and resolution in this critical measurement range a –1.13-V offset could be algebraically summed with the diodes output. This would result in the shifting of the output voltage so that the more sensitive 125-mV measurement range could be used over the range from 33 to 43 °R. An amplifier range change would be required for temperatures below 33 °R and above 43 °R. Figure 8 shows the results of this analysis. The performance of the type A PRT measurement is also shown for comparison purposes.

*GRT - 8-bit temperature measurement design and error analysis.*—The contribution of data acquisition error on temperature measurement error for a GRT system was estimated using the values of sensitivity for a commercially available sensor. The sensor output voltage would be maintained at a 10-mV level, and the resultant current level would be determined from the voltage drop measured across a sensing resistor. The limitation of this measurement system is the accuracy of measuring and maintaining the 10-mV GRT voltage drop.

The estimated 10-mV measurement range error for the 8-bit system is ±0.18 mV. The temperature error analysis results (table 6) show that the temperature equivalent of the voltage uncertainty would exceed ±0.27 at 36 °R. The results are also shown in figure 5 for comparison purposes.

*Wire voltage drop errors.*—Manganin wire was selected for instrumentation hookup wiring because of its low thermal conductivity. Manganin, however, has a greater resistivity than copper, and the voltage drop across the sensor wiring would be a significant source of error. To eliminate this problem, the temperature sensors will be used in four-wire measurement circuits: Two wires supply power to the sensor, and two wires couple the sensor voltage drop to the high-impedance voltage measurement circuit of the DAS. Virtually no current flows in the sensing lead; thus the excitation current ($I$) wire voltage drop ($I \times R$) is eliminated from the voltage measurement. Silicon diodes, because of their very high impedance and low excitation current level, may be used in two-wire systems for low-accuracy measurements.

*Thermoelectric potential effects.*—Thermoelectric potential effects due to temperature gradients across the instrumentation, wiring inhomogeneities, and dissimilar metal junction temperatures may occur. To compensate for this problem, the measurement system would be programmed to periodically take a sensor measurement without current excitation. This would determine the magnitude of the thermocouple effects and allow the offset corrections to be made for high-accuracy measurement requirements.

*Low-gravity influence on measurement error.*—Under low-gravity conditions, surface tension forces dominate, and liquid films could wick over temperature sensors in an otherwise gaseous environment resulting in measurement errors. Special cone shaped sensors designed to wick liquid films away from the sensor tip have been designed to minimize this problem (ref. 7).

## Temperature Sensor Selection

Platinum resistance thermometers were recommended for COLD–SAT because of their successful use in previous aerospace applications and because of the feasibility of highly accurate measurements with minimal change to existing flight-qualified data acquisition measurement systems. Desired specifications for the temperature sensors are detailed in this section.

*High-accuracy type A tank internal fluid temperatures.*—A PRT probe similar to that shown in figure 9 is recommended for immersion temperature measurements. The probe would consist of a 1000-Ω ($R_o$) platinum sensing element mounted in a stainless-steel cone. The cone shape is designed to wick away liquid films from the sensor tip, thereby minimizing false ullage temperature readings under low-gravity conditions. The probe design is very rugged, and the threaded mounting attachment ensures a reliable mount to an instrumentation rake. The probe would be connected with 24-gauge manganin wire to minimize heat conduction. Probes of similar design have been spaceflight qualified by a commercial manufacturer. A simplified schematic of the four-wire PRT excitation and voltage measurement circuit is included in figure 9.

*Hydrogen saturation temperature based on absolute pressure.*—The hydrogen saturation temperature within the cryogenic tanks can be determined from the tank absolute pressure measurement. Figure 10 shows hydrogen saturation temperature versus saturation pressure (ref. 5). A forth-order polynomial was found to fit this graph with a regression factor of 1.0. The uncertainty of inferring temperature (*UT*) from the absolute pressure measurement was calculated by taking the product of the polynomial slope and the uncertainty of the pressure measurement (*UP*) at the pressure (*P*) of interest. Table 7 lists the results of this analysis using the estimated values of pressure measurement uncertainty for a 50 psia range transducer (table 8). This measurement is valid only for fluid and surface measurements at the saturation temperature. The uncertainty in this requirement necessitates the use of multiple temperature sensors located throughout the cryogenic system.

*High-accuracy type A surface temperature measurements.*—Platinum resistance thermometers are recommended for the surface measurements because they are capable of providing total measurement inaccuracies of less than ±0.2 °R over the critical $LH_2$ range from 29 to 46 °R while using an 8-bit data acquisition system.

*Type AB total temperature range measurement.*—Platinum resistance thermometers are recommended to perform the surface temperature measurements over the range from 36 to 540 °R. Total temperature range measurements with inaccuracy less than ±2 °R are feasible with the dual range measurement capability of the data acquisition system.

*Mounting considerations.*—Surface temperature sensors must be attached to the structure in a manner such that intimate thermal contact is obtained with adequate strength to withstand thermal cycling and stresses of launch. Sensors can be mounted with adhesives or mounted in a high-thermal-conductivity holder that can be attached with screws or spot welded to the structure. The sensor leads should be thermally bonded to the structure so that they are at the same surface temperature. Reference reports detailing recommended mounting techniques are available from the various sensor manufacturers.

## Absolute Pressure Measurement Requirements

The absolute pressure of the cryogenic tanks, plumbing systems, and gas pressure supplies must be monitored to determine experiment pressurization rates, system operational status, and fluid thermodynamic state information. Measurement resolution of better than 0.2 psia are desired over the 50-psia operation range of the cryogenic tanks.

Absolute pressure measurements of the cryogenic tanks present unique problems. Standard temperature range transducers could be used by tapping into the system using stainless steel tubes. However, this procedure could result in thermal acoustic oscillations and conduct large amounts of heat energy into the $LH_2$ tanks. A transducer capable of operating at the $LH_2$ temperature range that could be directly installed at the cryogenic tank is desired.

*Absolute cryogenic rated pressure measurement transducer.*—A commercial strain gauge absolute pressure transducer is available that has a compensated cryogenic temperature range 36 to 186 °R. Table 8 lists the specifications for this cryogenic absolute pressure transducer. The transducer can also be calibrated for warmer temperature range operation. This transducer type has been flight qualified for the space shuttle.

*Absolute pressure sensor specifications and error analysis.*—The major sources of pressure measurement error include transducer inaccuracy, temperature effects, data acquisition error, and wiring errors. Transducer inaccuracy consists of the root sum square combination of nonlinearity, hysteresis, and nonrepeatability. This specification is listed as a percent of full-scale range. The transducers also have a specified compensated temperature range in which their performance change is defined as a function of temperature. The influences of temperature on the transducer zero point and slope are expressed in the thermal zero shift and thermal sensitivity shift specifications.

The pressure transducers used on the COLD–SAT experiment system will experience periods of temperature cycling. The transducers must be calibrated at various temperatures, and the influence of temperature effects on zero and sensitivity shifts determined.

*Excitation and wiring errors.*—Manganin wiring is recommended to minimize the heat energy conducted into the cryogenic tanks. Manganin wire of 24 AWG size would have an approximate resistance of 0.7 Ω/ft. The voltage drop across the manganin wire by the current level supplied by the 10-V power supply to the 1000-Ω bridge resistance pressure transducer would be sufficient to change the voltage actually supplied to the transducer. A second voltage measurement directly at the transducer input terminals must be made to determine the actual excitation voltage of the transducer. To eliminate the wire voltage drop problem, the transducers should be calibrated and excited by a equivalent current source equal to the recommended excitation voltage (10 V dc) divided by the transducer bridge resistance.

*Data acquisition error.*—The full-scale output of the pressure sensor candidates is 30 mV. The estimated 8-bit DAS error for this measurement range is ±0.67 percent of full scale with a resolution of 0.39 percent of full scale. This system would result in a DAS error of ±0.365 psia for a 50-psia range measurement with a resolution of 0.196 psia.

High-accuracy pressure measurements will be made with the EDU systems. The EDU system will decrease the DAS error to ±0.36 percent of full scale and improve the resolution to 0.024 percent of full scale. Table 9 lists the resolution values and psia equivalent errors of the rss combination of transducer inaccuracy (0.25 percent of full scale) and DAS inaccuracy (percent of full scale) for the two types of measurement systems as a function of full-scale pressure range.

## Discrete-Point Liquid-Vapor Detection

Liquid-level detectors are required to determine tank liquid level during ground fill operation. In-flight uses include liquid level gauging during acceleration, two-phase flow detection, and low-gravity liquid-vapor distribution profiles of tank fluid.

Discrete-point liquid-vapor detector candidates include thermoresistive elements such as thermistors, carbon resistors, and wire elements. The detectors are excited at an electrical power level at which self-heating of the sensor occurs. Self-heating causes sensor resistance to be significantly different when immersed in liquid from its resistance when immersed in vapor. The sensor resistance change produces a voltage level change that is fed to a comparator circuit. The electronic comparator circuit produces a high- or low-voltage output dependant on the fluid state. The sensor can be used in a bridge circuit configuration and excited by a constant voltage source or singularly excited by a constant current source.

Other methods of determining fluid level include capacitance probes and resistive tape strips. Using these type of detectors with high-wetting fluids under low-gravity conditions could result in inaccurate measurements due to fluid wicking. Discrete-point level sensors could also give erroneous indications of liquid presence under low-gravity conditions due to the presence of a liquid film existing over the sensor. Cone shaped sensors that use the surface tension force experienced by the fluid to wick away the fluid film from the sensor tip are recommended for low-gravity applications.

*Recommended sensor.*—Cone shaped liquid-vapor discrete-point detectors similar in shape to the temperature probe shown in figure 9 have been used on Centaur upper stage vehicles. A sensor similar to that design containing a thermistor sensing tip is proposed. The probe would be supplied with 24 AWG manganin wire leads to reduce conducted heat flow.

*Ground fill liquid hydrogen gauging.*—Ground test results indicate that inaccurate discrete-point detector liquid-level readings can occur during tank fill operations because of the vigorous boiling of the hydrogen. Commercially available capacitance probes, however, have performed satisfactorily. Capacitance probes are used for $LH_2$ gauging for the space shuttle power reactant storage assembly. A capacitance probe that will monitor the fill level from 85 to 100 percent is required for COLD–SAT.

*Two-phase flow detection.*—Two-phase flow detection inside the liquid acquisition device (LAD) channels and at the vent line exits is required. Thermistors that have very high-sensitivities could be mounted inside the channels or at the entrances to the plumbing lines. The sensors would be excited at a power level where sensor self-heating occurs in vapor but not in liquid. Testing and development of sensors, mounting and signal conditioning is needed to optimize two-phase flow detection.

Flowmeters used on the $LH_2$ and vent lines should also give two-phase flow indications. Two-phase flow through a turbine meter is to be avoided and will cause noticeable speed increases. Two-phase flow through a differential pressure flow metering device should also be detectable by pressure surges.

## Liquid Hydrogen Flow-Rate Measurement

Liquid hydrogen flow rates of 50, 100, and 200 lbm/hr are required for the tank chilldown and $LH_2$ transfer experiments. Fluid inventories must also be maintained by integrating the $LH_2$ flow rates over the COLD–SAT experiment time line. Studies performed by independent testing facilities indicate the older flow-measurement techniques using turbine meters or pressure head meters (venturi/orifice) to be the most reliable (ref. 8).

The desired flow rates will be obtained by sizing orifices or venturies to provide the required pressure drops. The pressure drop across a flow-control device is ideally proportional to the flow rate squared and can be monitored with a differential pressure transducer for determining the fluid volumetric flow rate. The use of differential pressure transducers mounted to tubes that are tapped to the flow lines would conduct undesirable levels of heat into the $LH_2$ tanks and present thermal acoustic oscillation problems. A differential pressure transducer capable of operating in $LH_2$ is required.

Turbine flowmeters have also been used successfully on $LH_2$ ground test facilities. Over speeding of the turbine meter by liquid flashing into a vapor is a concern. Target meters in which the flowing liquid imparts a force on the target proportional to the flow rate squared were also considered.

*Liquid hydrogen flow-measurement candidate error analysis.*—Differential pressure and turbine flowmeters measure volumetric flow rate. Therefore, to determine the mass flow rate, the fluid density must be known. The $LH_2$ density will be determined by measuring the fluid's temperature and pressure at the flowmeter inlet. The $LH_2$ density will be determined from thermal dynamic property tables. The $LH_2$ mass flow rate error is a function of the volumetric flow-measurement error and the error in density determination.

*Estimated $LH_2$ density error.*—The influence of temperature and pressure on $LH_2$ density was estimated by determining best fit equations that mathematically described the change in $LH_2$ density as a function of temperature and pressure over the range of interest. Figure 11(a) shows the strong influence of temperature on density for the temperature range from 30.8 to 41.3 °R at a constant pressure of 30 psia. The minor influence of pressure on $LH_2$ density for a constant temperature of 36 °R over the pressure range from 15 to 50 psia is also shown in figure 11(b). The uncertainty in density determination was estimated by equation (3).

$$U\rho = (\partial\rho/\partial T * UT) \tag{3}$$

where $U\rho$ is the uncertainty in density, $UT$ is the uncertainty in temperature, and $\partial\rho/\partial T$ is the change in density as a function of temperature. The uncertainty in temperature measurement over the critical $LH_2$ range for a 1000-Ω ice-point PRT was estimated to be ≤0.2 °R. A density uncertainty of ±0.2 percent, based on the temperature measurement uncertainty of ±0.2 °R, was estimated for mass flow rate measurements. Pressure measurement error was considered insignificant for $LH_2$ conditions.

*Liquid hydrogen flow rate by orifice-differential pressure measurement error analysis.*—Variable reluctance differential pressure transducers have been tested at cryogenic temperatures (ref. 9). The estimated $LH_2$ mass flow-rate error analysis based on the measurement of differential pressure drop across a flow-control orifice by use of a similar variable reluctance differential pressure transducer is given in table 10(a). An orifice and pressure transducer calibration inaccuracy of ±0.5 percent of reading for each component was assumed for this study, and the estimated electronics error of the EDU was assumed to be ±0.4 percent. These values are estimates, and actual $LH_2$ calibration of the system would have to be performed.

*Turbine flow-measurement error analysis.*—Table 10(b) lists the estimated flow-measurement error for a commercial turbine flowmeter assumed calibrated at an accuracy of ±0.5 percent of reading. The assumed EDU measurement inaccuracy is 0.4 percent of range and the estimated density error is ±0.2 percent.

*Target meters.*—The feasibility of using a commercially available target flowmeter was investigated. The pressure drop developed across the target of the investigated meter was proportional to the density of the fluid and the volumetric flow rate squared. The meter had a designed full-scale pressure drop of 7 psi that was too high for the COLD–SAT requirements, and the meter would have to be used at its low operational end where its accuracy would be low.

*Proposed $LH_2$ flow measurement system.*—Venturi or orifice flow-control devices will be sized to provide the required flow rates. The differential pressure developed across the flow-control devices will be monitored by variable-reluctance differential-pressure transducers. Variable-reluctance transducers have been tested successfully at cryogenic temperatures by a number of facilities and have been selected for liquid helium flow-rate measurements for the superfluid helium on-orbit transfer experiments (SHOOT) (ref. 10). A turbine meter located immediately downstream of the supply tank will be used for measurement redundancy and can be disconnected from the transfer line during line chilldown periods to protect it from overspeeding.

## THERMODYNAMIC VENT SYSTEM FLOW-RATE MEASUREMENT REQUIREMENTS

The thermodynamic vent system (TVS) flow rates will be monitored to determine system operation status and to quantify the hydrogen mass expelled. The flow rates will be obtained by the use of flowrestriction devices. The system must be extensively calibrated so that the mass flow will be known as a function of system pressure and temperature. The TVS systems will be designed to provide single-phase hydrogen vapor at their exit. Additional gaseous TVS flow-rate measurements are requested with an inaccuracy less than ±5.0 percent. The TVS vent plumbing design use tee connections located on the radiator tray where the individual tank vent lines join to a common TVS vent line. The individual tank TVS flowmeters could be located on the radiator tray and must be capable of operating within a temperature range 36 to 360 °R.

*Proposed gaseous hydrogen TVS flow-measurement candidate.*—The recommended volumetric flowmeter for the TVS systems is the turbine flowmeter. Commercially available turbine meters are designed for both liquid and gas measurements and are operable down to temperatures of 30 °R.

The turbine meter consists of a rotor mounted by bearings inside the meter housing. Fluid flow through the meter imparts a torque to the rotor blades causing the rotor to spin at a rate proportional to volumetric flow rate. Rotation rate is detected by a magnetic or carrier modulated pickup assembly that detects a change in motional inductance of the coil either as a voltage pulse or as a change in carrier frequency. The meters are calibrated and a proportionality constant ($K$) relating meter output frequency to volume is determined. The deviation of the $K$ factor over the measurement range of the meter from its nominal value is given in the linearity specification. Turbine flowmeters are available with linearity capabilities of ±1.0 percent of full scale over a normal 10:1 flow range. The calibration of the meters under gaseous hydrogen at the actual operating temperature and pressure conditions will be required. Table 11 lists the various COLD-SAT tank TVS flow rate ranges as a function of temperature and pressure. The required size flowmeters are listed that have operating ranges comparable with the TVS ranges.

*TVS flow-measurement density error analysis.*—Turbine meters measure volumetric flow rate. In order to calculate mass flow rate, the density must be determined. Temperature and pressure measurements made at the meter inlet will be used to determine density. Mass flow-rate error is a function of the uncertainty of the turbine volumetric flow measurement and of the uncertainty in density determination based on the temperature and pressure measurement errors.

The influence of temperature and pressure on $GH_2$ density was estimated by finding the best fit equations that mathematically describe the change in hydrogen density as a function of temperature and pressure over the range from 180 to 360 °R and 5 to 20 psia. Figure 12 shows that the hydrogen density is proportional to the pressure-to-temperature ratio (ideal gas law). The uncertainty in density determination was calculated using equation (4). The results of this analysis indicate that a rss density uncertainty of 3.66 percent could occur.

$$U\rho=\left[\left(\frac{\partial\rho}{\partial T}\times UT\right)^2+\left(\frac{\partial\rho}{\partial P}\times UP\right)^2\right]^{0.5} \tag{4}$$

where uncertainty in density is $U\rho$, $\partial\rho/\partial T$ is the change in density as a function of temperature, $\partial\rho/\partial P$ is the change in density as a function of pressure, $UT$ is the uncertainty in temperature, and $UP$ is the uncertainty in pressure.

*TVS flow-measurement error analysis* .—Table 12 lists the error contributions of the various sources involved in the TVS flow measurement. The rss combination is listed and the results show the feasibility of a ±5 percent mass flow-rate measurement.

## Supply and Receiver Tanks Vent Flow-Rate Measurement Requirement

The capability of measuring the vent flow rates of the supply and receiver tanks is required for fluid inventory management and receiver tank chilldown performance. Tank vent flow rates of approximately 50 lbm/hr are estimated.

*Proposed tank vent flow-rate measurement system.*—A flow-regulation device will be required to control the rate of tank pressure decrease so that valve actuation and tank pressure can be controlled. The tanks will be vented at pressures of approximately 50 psia to a near vacuum condition. This large pressure drop across a sonic flow nozzle will result in a choked flow condition at the throat section of the nozzle. The velocity of the vented gas will reach the sonic value and will not be influenced by changes in downstream pressure (ref. 11). The flow rate is dependent only on the upstream pressure. Temperature of the vented gas will be measured so that density and mass flow rates can be calculated. Commercial suppliers of sonic flow nozzles have designed flow nozzles that develop sonic flow with downstream pressures as high as 80 percent of the nozzle inlet pressure.

*Sonic flow-nozzle sizing.*—The required diameter of the nozzle can be estimated as follows:

$$M = \rho A V_s \tag{5}$$

where $M$ is the mass flow rate, $\rho$ is the density, $A$ is the area of nozzle throat, and $V_s$ is the sonic velocity. Table 13 lists the properties of $GH_2$ and their influence on the required diameter of a sonic nozzle for a mass flow rate of 50 lbm/hr (0.0139 lbm/sec) at a inlet pressure of 50 psia.

*Large receiver tank chilldown vent flow-rate measurement.*—The receiver tanks must be chilled down before a $LH_2$ transfer experiment. The proposed method of tank chilldown is to inject a known mass of $LH_2$ into the tank. The $LH_2$ absorbs heat, vaporizes and pressurizes the tank. The tank will be vented when the pressure reaches 30 psia. The desired rate of pressure decrease is 5 psia in 10 sec. This charge-hold-vent process will be repeated until the tank temperature decreases from an initial value of >400 °R to the target temperature of approximately 140 °R. The amount of mass that must be vented from the large receiver tank to lower its pressure from 30 to 25 psia is listed as a function of temperature in table 14. The approximate time required to vent this amount of hydrogen through a 0.151-in.-diameter sonic nozzle is also listed.

*Small receiver tank vent flow-rate measurement.*—The volume of the small receiver is 13.5 $ft^3$ and that of the large receiver 21 $ft^3$. The volume ratio of the two tanks is 0.643. To acquire the same rate of pressure decrease as the large receiver tank, the small receiver vent line would require a sonic nozzle with a diameter of $(0.643)^{1/2}$ that of the large receiver, or 0.121 in.

*Sonic nozzle flow-measurement error analysis.*—The inaccuracy in the vent flow-rate measurements is dependant on the calibration error of the nozzle, typically ±0.75 percent, and on the accuracy of the required absolute pressure and temperature measurements at the entrance to the sonic nozzle. The general formula for mass flow rate $M$ through the nozzle is

$$M = KP/(T)^{1/2} \tag{6}$$

where $P$ is the absolute pressure (in pounds per square inch) at the nozzle inlet, $K$ is the flow coefficient, and $T$ is the nozzle inlet temperature. The uncertainty in the flow measurement $UM$ was estimated as follows:

$$UM = \left\{\left[(\partial M/\partial P)UP\right]^2 + \left[(\partial M/\partial T)UT\right]^2 + UM_{\mathrm{cal}}^2\right\}^{0.5} \tag{7}$$

where $\partial M/\partial P$ is the change in flow with respect to pressure, $UP$ is the uncertainty in pressure, $\partial M/\partial T$ is the change in flow with respect to temperature, $UT$ is the uncertainty in temperature, and $UM_{\mathrm{cal}}$ is the uncertainty in flow calibration. The results of this analysis using the pressure and temperature measurement uncertainties obtained with the proposed PRT temperature sensors and EDU measured 50-psia range pressure transducers are listed in table 15. The results indicate that a < ±5 percent measurement is feasible.

*Acceleration measurement requirement.*—The influence of acceleration levels on the fluid dynamic and thermodynamic properties will be determined during the tank chilldown experiments by accelerating the spacecraft at levels from 10 to 100 μ*g*. The other COLD–SAT experiments will be conducted at acceleration levels where natural convection is insignificant (≤10 μ*g*). The acceleration magnitude along all three axes will be measured.

*Recommended accelerometer system.*—A transducer assembly similar to that used on the space shuttle orbiter program is recommended for COLD–SAT. This assembly consists of three accelerometers and the required power conditioning, analog servoelectronics, signal conditioning and electromagnetic interference electronics. The unit has been used on the space shuttle orbiter programs to measure low level accelerations in the micro-*g* range to 10 milli-*g*.

The three-axis 0- to 5-V output signals of the accelerometer would be measured at the EDU boxes and converted to their digital equivalent levels by the high-resolution 12-bit analog-to-digital converters. A peak hold circuit will register peak transient acceleration levels. The peak detector will be read and reset at a 1-sec rate.

## Mixer Flow-Rate Measurement Requirement

A mixer is required for the active thermodynamic vent system of the supply tank. The mixer pump must be capable of supplying $LH_2$ at flow rates of 3.0 to 12.7 gal/min. The flow rate of the mixer can be obtained by calibrating the mixer shaft rotation rate with respect to flow rate. The mixer shaft rotation rate can be detected by induction or magnetic type pulse detecting sensors.

A speed sensor compatible with the $LH_2$ environment will be supplied with the selected mixer pump. The frequency pulse output of the mixer speed sensor will be proportional to the shaft speed and the flow rate. The frequency output of the speed sensor is supplied to an EDU for signal conditioning and fed to a RCTU/CTU of the TT&C system. Figure 13 shows a block diagram of the rotational speed measurement system. This design is similar to a rotational speed measurement design used in the shuttle/Centaur design.

## Valve Status Indicators

The cryogenic and standard temperature rated valves proposed for the COLD–SAT plumbing system are manufactured with valve position indicating switches. The status of the switches (open/closed) will be monitored by the remote command telemetry units to verify operational status. Only 1 bit is required for digitizing this information.

Figure 14 shows the typical schematic for discrete measurements. This design is similar to the Shuttle/Centaur design. The proposed design uses manganin wiring for the cryogenic valve switches to minimize heat conduction.

## Power Measurements

The voltage and current supplied to the COLD–SAT experiment system heaters and mixers will be measured to determine the power dissipated by the components. The measurements will be made at the relay sequencer units of the TT&C system.

# COLD–SAT EXPERIMENT SUBSYSTEM MODULE INSTRUMENTATION REQUIREMENTS AND ALLOCATIONS

The following sections present brief descriptions of the COLD–SAT experiments and lists the number of transducers allocated to each COLD–SAT module to meet the experiment requirements.

## Supply Module Instrumentation Requirements

The instrumentation allocated for the supply module was dictated by the requirements of the following experiments.

*Experiment 1: tank pressure control experiment.*—The pressurization rate of a cryogenic storage tank depends on the rate and distribution of heat energy into the tank. In space the lack of gravity-induced fluid convection currents can result in nonuniform heating of the cryogen and the formation of temperature stratified layers of fluid. The ullage pressure will be determined by the warmest layer of liquid and the tank pressurization rate will be high.

The tank pressure-control experiments will investigate the rate of tank pressurization as a function of heat flux, tank fill, and acceleration levels. Methods to reduce thermal stratification by means of active and passive thermodynamic vent systems (TVS) will be evaluated.

*Key measurements.*—Quantification of the heat energy entering the tank will be determined by measuring the temperatures and temperature gradients existing throughout the supply tank module. The internal tank fluid state (liquid or vapor) and temperatures will be monitored using specially designed probes for low-gravity applications. Absolute tank pressure and differential pressure drops across flow-control devices, acceleration level, mixer motor speed, valve status, and heater power levels will be monitored.

Table 16 list the type, number, and location of the instrumentation proposed for the supply tank module. A measurement list detailing the description, range, accuracy, and sample rate for each measurement is given in the appendix. The supply tank module contains the $LH_2$ supply tank and gas pressurization system. The accelerometer is listed under this module for convenience only. The accelerometer will be located in the midelectronic bay.

## Receiver Modules Instrumentation Requirements

The instrumentation proposed for the large receiver and the small receiver modules was dictated by the requirements of the following experiments.

*Experiment 2: No-vent fill of cryogenic tanks in low gravity.*—The objectives of the no-vent fill experiments were to characterize the influence of the thermodynamic state of the liquid, the liquid flow rate, and the liquid-injection technique on the maximum amount of tank liquid fill that can be obtained.

*Experiment 3: Cryogenic tank chilldown in low gravity.*—The first step in the $LH_2$ transfer process is to chill down the receiver tank to a temperature at which a continual no-vent-fill fluid transfer can be obtained. Tank chilldown experiments will consist of injecting known charge magnitudes of $LH_2$ into the receiver tank. The $LH_2$ will vaporize and absorb heat from the receiver tank and thermally bonded structure. After a sufficient hold time the tank will be vented and the remaining fluid will again absorb heat from the structure. This process of charge-hold-vent will be repeated until a target temperature is reached, at which point a no-vent fill transfer could be performed. The influence of $LH_2$ charge flow rate, acceleration, and spray method will be evaluated to determine the optimum method of tank chilldown.

*Experiment 4: Fill of liquid acquisition devices in low gravity.*—The capability of filling a warm LAD and refill a cold LAD will be performed on the large receiver tank. Tables 17 and 18 list the type, number, and location of the instrumentation selected for the large and small receiver modules. A measurement list containing the description, range, accuracy, and sample rate for each large and small receiver module measurement is located in the appendix.

### Instrumentation Redundancy

Large quantities of temperature, pressure, and liquid-vapor point sensors have been allocated to the COLD–SAT tank modules. The loss of any one specific sensor would not significantly jeopardize the experimental measurement data acquisition or accuracy. Three absolute pressure transducers are assigned to each tank for voting purposes. High-accuracy $LH_2$ flow measurements will be determined by differential pressure measurements across the flow-control elements. A turbine flowmeter is also assigned for secondary total flow measurement. The thermodynamic vent system and vent lines will be instrumented, and flow rates will be determined from calibration data as a function of temperature and pressure. Turbine flowmeters will also provide TVS flow-rate measurements.

The instrumentation for each module is distributed equally among the three command telemetry units and the three EDU's so that if a signal conditioning board failure occurs, sensor loss would be distributed among the three modules so as to minimize the loss of experimental data.

## COLD–SAT EXPERIMENT INSTRUMENTATION AND ELECTRICAL HARNESS DESIGN

Electrical wiring is required to supply the excitation power to the sensors and to couple the sensor output signal to the DAS's. Most of the instrumentation will be thermally bonded to the cryogenic tanks and a large heat input to the tanks would occur if copper wire is used. To minimize heat input, manganin wire was chosen for instrumentation wiring. Phosphor bronze wiring was chosen for valves and heater applications. The influence of temperature on the thermal conductivity of copper, manganin, and phosphor bronze is shown in figure 15.

Connectors and receptacles used for cryogenic tank wire feedthroughs must be capable of operation at $LH_2$ temperatures. The candidate connector assemblies will be similar to the type used on D–1A Centaur. Bulkhead connector assemblies exposed to temperatures below –55 °F will be series 40M38294. Connectors exposed to temperatures above –55 °F will be series MIL–C–38999. Detailed descriptions of the designed experiment system instrumentation and electrical wire harness is included in the following sections.

### Wire Material Selection

Copper wire is an excellent electrical conductor and also a very good thermal energy conductor. However, the large number of instrumentation wires thermally bonded to the COLD–SAT supply tank would result in excessive conducted heat input and boiloff of $LH_2$ during the mission. Copper wire, therefore, is not practical, and a material with a lower thermal conductivity is desired. Manganin, a copper alloy consisting of 87 percent copper, 11 percent manganese, and the remainder nickel, has a much lower thermal conductivity than copper. Manganin is commonly used for cryogenic temperature measurements to prevent thermal conduction temperature measurement errors. The resistivity of manganin is considerably greater than copper and four-wire measurements where two wires supply power to the sensor and two wires sense the potential across the sensor must be used for accurate results. The heat conducted down the additional manganin wiring is still far lower than that conducted down two wire copper systems.

Manganin wire of 24 AWG size has been selected for the cryogenic instrumentation wiring harnesses. The current requirements of the selected instrumentation is generally 10 mA or less, and the 24 AWG gauge size should be more than adequate. This gauge size should also provide the strength and maintenance properties desirable for interconnection harnessing.

Valves and heaters will require larger diameter wire because of their greater current carrying requirements (1 to 5 A). Manganin wire of 12 to 10 gauge would be required to provide this current carrying capacity. This size wire would present a large weight increase.

Phosphor bronze is a copper wire alloy commonly used in cryogenic applications. This wire is beneficial for cryogenic applications requiring current carrying capacities unpractical for manganin. 18–AWG phosphor bronze wire was selected to represent the typical wire material for valve and heater leads that will be thermally bonded to the cryogenic tanks.

## Wire Construction Model

The wire construction was modeled after MIL–W–81381, which specifies a fluorocarbon and polyimide insulation rated for +200 °C. The estimated weight of 24 AWG manganin and 18 AWG phosphor bronze wire based on the specification data is listed in table 19. Table 20 lists the estimated diameters of the various wire bundles.

## Instrumentation and Power Wire Requirements

Table 21 is a summary of the required type and number of wire for each COLD–SAT tank module. Tables 22 to 24 list the number and termination locations of the supply, large receiver, and small receiver module wiring.

## Signal Conditioner Assignments

The instrumentation and electrical actuated components of the modules were divided between the various signal conditioning units and sequencer boxes so as to minimize the loss of measurement data in case of a harness or electronic system failure. Tables 25 and 26 list the wire allocations.

## Cryogenic Tank Wire Connectors and Feedthroughs

The internal tank instrumentation wiring will penetrate the pressure vessels through hermetically sealed electrical wire feedthroughs. The connector style selected is similar to the type used on D–1A Centaur. The desired modification is to have the feedthrough assembly supplied in a weld-mount style. Six feedthrough assemblies are required for the supply tank: four for the large receiver, and three are required for the small receiver.

## Multiplexer Wire Reduction Techniques

A large number of temperature and liquid/vapor sensors are installed inside the cryogenic tanks. The sensors require two to four wires each. The large number of wires penetrating the cryogenic tanks increases the conducted heat leak and require large numbers of cryogenic tank feedthroughs.

Methods of using four-channel differential joint Army Navy (JAN)-qualified analog multiplexers were developed that use common excitation lines to reduce the number of wires penetrating the tanks. Figure 16(a) is a schematic of a multiplexed four-wire temperature measurement method in which the required number of wires is reduced from 64 to 40 wires for the 16 sensors.

Large numbers of liquid-level point detectors are also required to determine the fluid-phase distribution throughout the COLD–SAT tanks. To reduce the number of wires penetrating the tanks, the sensors will be connected in parallel to common excitation lines inside the cryogenic tanks. Figure 16(b) shows how the multiplexers could be used to select and excite the desired sensor to be measured. The number of wires penetrating the tanks by this method is 1/4 the number required for individually wired detectors.

## Wire Harness Construction

The COLD–SAT experiment subsystem will be assembled in separate tank modules. The instrumentation will be mounted on the LAD instrumentation rakes and checked for proper operation before mounting the LAD in the tank. The internal tank instrumentation wiring will be connected to the cryogenic plug, and electrical contact to the external harness will be made through the cryogenic receptacle. The instrumentation and power wiring harnesses will be separated and routed from the tank structure to the radiator tray in bundles of 40 to 55 wires. The radiator tray is located on the cold side of the spacecraft and is designed to serve as a heat sink to remove heat energy from the wiring prior to its arrival to the tank. Connector feedthroughs will exist at panels located at module interfaces. The temperature of the radiator tray may be below –100 °F and cryogenic environment resisting connectors as specified in 40M38294 will be required.

The wire harnesses will be routed from the tray to bulkhead connectors located on panels located on the warm side of the spacecraft. This design is to prevent undesirable chilldown of the electronic boxes. From the warm-side panels, the harnesses terminate at their required electronic or power box. Spacecraft warm-side electrical connectors will be selected from Mil–C–38999. Figure 17 shows the overall wire schematic for the COLD–SAT experiment subsystem instrumentation.

## Electromagnetic Interference Concerns

The instrumentation and power wiring should be separated and routed away from noise sources. The wire should be twisted to minimize inductive noise coupling. The low-level signal wiring should be harnessed in shielded bundles until it is inside the multilayer insulation can.

## Heater Requirements

Heaters are required to provide the desired experiment heat flux inputs for the tank pressurization experiments. Heaters are also required to warm the receiver tanks to the required initial temperatures before chilldown experiments. The hydrogen vaporizers will use heaters to warm and maintain their system at their designed operating point. Panel and vent line heaters will be required to maintain their structure at desired operating conditions.

Thin, flexible heaters consisting of etched metal foil resistive elements laminated between layers of Kapton insulation are commercially available. Goddard Space Flight Center has qualified similar heaters for aerospace applications from –65 to 200 °C.

The listed lower temperature range of operation of commercially available Kapton-insulated heaters is –200 °C. Discussions with manufacturing representatives indicate that the heaters should be capable of operation at $LH_2$ temperatures as long as appropriate installation adhesives and techniques are used. Testing would be required to qualify an adhesive for this application.

## CONCLUSIONS

An instrumentation and wire harness for the COLD–SAT experiment subsystem was designed. The transducers, signal conditioning systems, and wire harness components of the design were recommended, when at all possible, based on past $LH_2$ and space-flight histories. Electrical current excitation levels and data acquisition ranging were designed to meet the temperature measurement requirements using space flight qualified platinum resistance thermometers with minimal changes to existing 8-bit space flight qualified data acquisition systems. Cone shaped $LH_2$ temperature and liquid/vapor sensors were recommended to minimize false measurements in low-gravity conditions. The need for a 12-bit data acquisition system to provide improve resolution and accuracy for critical measurements was addressed, and an EDU design was presented. The 12-bit system was identical to the 8-bit system but with only one multiplexer for each circuit card and the 12-bit analog-to-digital converter. Error analyses were performed on all instrument candidates, and the influence of physical parameters such as temperature and pressure on the overall measurement accuracies was investigated. The results indicated that most of the experimenters' measurement requirements were feasible; however, two-phase flow detection, leak detection systems, and mass gauging are areas that need development.

Heat conduction to the $LH_2$ tanks was a chief concern. Wire materials, wire multiplexing techniques, and cryogenic operable pressure transducers were selected and developed to minimize this problem.

## REFERENCES


1. Zuch, E.L.: Data Acquisition and Conversion Handbook: A Technical Guide to A/D - D/A Converters and their Applications. Datel Intersil, Ma, 1979.
2. Abernethy, R.B.; Benedict, R.P.; and Dowdell, R.B.: ASME Measurement Uncertainty. J. Fluids Eng., vol. 107, June 1985, pp. 161–164.
3. Weast, R.C.; Astel, M.J.; and Beyer, W.H., eds.: CRC Handbook of Chemistry and Physics. 68th ed., CRC Press, Inc. Boca Raton, FL, 1987, p. E–9.
4. Touloukian, Y.S., Powell, R. W.; Ho, C.Y.; and Klemans, P.G.: Thermophysical Properties of Matter. Vol. 1: Thermal Conductivity, Metallic Elements and Alloys. IFI/Plenum, Washington, DC, 1970.
5. McCarty, R.D.: Hydrogen Technological Survey: Thermophysical Properties. NASA SP–3089, 1975.
6. Liptak, B.G.; and Venczel, K.: Instrument Engineers Handbook, Rev. ed., Chilton Book Co., Radnor, PA, 1982.
7. Berns, J.A.; Yeh, F.C.; and Nussel, R.C.: Photographic Investigation of Liquid Behavior on Temperature and Liquid/Vapor Sensors Used in Low-Gravity Environment. NASA TM X–1438, 1967.
8. Baird, R.S.: Flowmeter Evaluation For On-Orbit Operations. NASA TM–100465, 1988.
9. Kashani, A.: Shoot Flowmeter and Pressure Transducers. Cryogenics, Vol. 30, Mar. 1990, pp. 286–291.
10. DiPirro, M.J.; and Kittel, P.: The Superfluid Helium On-Orbit Transfer (SHOOT) Flight Experiment. Advances In Cryogenic Engineering, Vol. 31, Plenum Press, New York. 1988.
11. John, J.E.A.; and Haberman, W.L.: Introduction to Fluid Mechanics. Second ed., Prentice-Hall, Inc., Englewood Cliffs, NJ, 1980.

## APPENDIX—COLD-SAT EXPERIMENT SUBSYSTEM MEASUREMENT LISTS:

Measurement lists containing the descriptions, ranges, inaccuracies and sampling rates for the COLD-SAT experiment measurements were prepared. The measurements are referenced to the primary COLD-SAT experiment requiring the measurement. Measurement numbers are assigned according to the definitions and nomenclature discussed below.

### COLD-SAT EXPERIMENT SUBSYSTEM MEASUREMENT LIST NOMENCLATURE AND DEFINITIONS:

MEASUREMENT LOCATIONS

S = Supply Module
Lr = Large Receiver
Sr = Small Receiver

MEASUREMENT TYPES

| | |
|---|---|
| A = Acceleration | L = Liquid/Vapor |
| C = Capacitance | P = Pressure |
| E = Voltage | R = Rate (RPM) |
| I = Current | T = Temperature |
| | W = Power |

PRIMARY EXPERIMENTS:

1 = PRESSURE CONTROL
2 = NO-VENT FILL
3 = CHILL DOWN
4 = LAD
8 = PRESSURIZATION

RANGE: The listed experiment range is based on the expected state of the fluid over the course of the experiment.

INACCURACY: The listed inaccuracy is based on the Root Sum Square contributions of sensor inaccuracy and estimated data acquisition error over the measurement range. This result is an estimate and all sensors should be calibrated and evaluated under actual operating conditions.

SAMPLE RATE: The sample rate represents the frequency at which the measurement will be made. The actual sampling time will be considerably less.

TEMPERATURE MEASUREMENT IDENTIFICATION CODE: Temperature sensors were classified according to their range of operation. Type A sensors cover the temperature range from 29 °R to 46 °R. Type B sensors cover the temperature range from 113 °R to 540 °R. Sensors classified as type AB indicate dual ranging of the sensor which extends the range of coverage from 29 °R to 540 °R but at reduced accuracy.

To facilitate locating temperature sensors in the various regions of the tank modules, the sensors were numbered by the following method. Temperature measurement numbers ranging from 1 to 99 indicate measurements located inside the tank pressure vessel. Temperature measurement numbers ranging from 101 to 199 indicate measurements located on the outside pressure vessel wall. Temperature measurement numbers ranging from 201 to 299 indicate measurements located between the multilayer insulation (MLI) and the pressure vessel. Temperature measurement numbers ranging from 301 to 399 indicate measurements located on or outside the MLI structure.

CRYOGENIC TANK INTERNAL FLUID TEMPERATURE MEASUREMENTS: The fluid temperature distribution existing throughout the cryogenic tanks will be measured using Platinum Resistance Thermometers (PRTs). The fluid temperature sensors will be mounted in cone shaped probes similar to those used on Centaur. These probes are designed to wick away liquid films from the sensor tip, minimizing false ullage temperature readings.

The temperature probes in the supply tank are mechanically secured to (7) seven instrumentation rakes. Horizontal rakes are located at 70% and 30% tank volume levels. These rakes will monitor the fluid temperature distribution existing from the tank wall into the fluid bulk. A vertical rake positioned at the 50% volume level will monitor the liquid/vapor interface temperature during a low gravity settling period. The fluid temperature between 90% to 98% volume levels will be measured by temperature probes mounted on vertical rake #5. Four LAD mounted rakes will contain sensors to determine the temperature distribution throughout the 4% to 90% tank volume region.

A minimum LH2 temperature of 30.8° should occur downstream of the Joule Thomson expansion device. The maximum Tank pressure should not exceed 50 PSIA. The H2 saturation temperature for this pressure is 45.5 °R. Type A PRTs are excited and signal conditioned to maximize their sensitivity over this temperature range.

QUANTIFYING THE HEAT ENERGY INPUT INTO THE CRYOGENIC TANKS: The heat energy conducted into the cryogenic tanks will be determined by monitoring the temperature and temperature gradients existing across the module components that are thermally bonded to the tanks. These components consist of the plumbing penetrations, struts, and wire harnesses. Temperature maps of the tank surface, inner MLI surface, and outer MLI surfaces will be obtained to determine the thermal radiative environment of the module.

TANK PANEL LOCATED TEMPERATURE MEASUREMENTS: Aluminum panels are mounted on the surface of the supply and receiver tanks. The panels support plumbing and instrumentation components. The panels are thermally bonded to the tanks and the temperature of the panels and their components will be in the Type A temperature measurement range.

INNER HONEYCOMB WALL TEMPERATURE MEASUREMENTS: The temperature range listed for the inner MLI-Honeycomb structure were determined from the thermal analysis. The range covers the estimated worse case deviations in temperature.

OUTER MLI TEMPERATURE MEASUREMENTS: The temperature range listed for the outer MLI structure was determined from the thermal analysis. The range covers the worse case deviations in temperature.

SUPPLY AND RECEIVER MODULES INSTRUMENTATION LOCATION SCHEMATICS: Figures 18(a) and (b) show the location of the supply tank rake mounted temperature and liquid-vapor sensors. Figure 19 shows the instrumentation rake design and external sensor locations for the large receiver. Figure 20 shows the instrumentation rake design and the external sensor locations for the small receiver.

COLD-SAT EXPERIMENT SUBSYSTEM MEASUREMENT LIST

SUPPLY TANK INTERNAL TEMPERATURE MEASUREMENTS

| MEAS | NUM | DESCRIPTION | RANGE Deg (R) | INACCURACY ± Deg (R) | SAMPLE FREQ. (Hz) | PRI. EXP. |
|---|---|---|---|---|---|---|
| STa | 1 | Horizontal Rake 70% Volume Level | 29 - 46 | < 0.20 | 0.1 | 1 |
| STa | 2 | Horizontal Rake 70% Volume Level | 29 - 46 | < 0.20 | 0.1 | 1 |
| STa | 3 | Horizontal Rake 70% Volume Level | 29 - 46 | < 0.20 | 0.1 | 1 |
| STa | 4 | Horizontal Rake 70% Volume Level | 29 - 46 | < 0.20 | 0.1 | 1 |
| STa | 5 | Horizontal Rake 70% Volume Level | 29 - 46 | < 0.20 | 0.1 | 1 |
| STa | 6 | Horizontal Rake 70% Volume Level | 29 - 46 | < 0.20 | 0.1 | 1 |
| STa | 8 | Horizontal Rake 30% Volume Level | 29 - 46 | < 0.20 | 0.1 | 1 |
| STa | 9 | Horizontal Rake 30% Volume Level | 29 - 46 | < 0.20 | 0.1 | 1 |
| STa | 10 | Horizontal Rake 30% Volume Level | 29 - 46 | < 0.20 | 0.1 | 1 |
| STa | 11 | Horizontal Rake 30% Volume Level | 29 - 46 | < 0.20 | 0.1 | 1 |
| STa | 12 | Horizontal Rake 30% Volume Level | 29 - 46 | < 0.20 | 0.1 | 1 |
| STa | 13 | Vertical Rake 50% Volume Level | 29 - 46 | < 0.20 | 0.1 | 1 |
| STa | 14 | Vertical Rake 50% Volume Level | 29 - 46 | < 0.20 | 0.1 | 1 |
| STa | 15 | Vertical Rake 50% Volume Level | 29 - 46 | < 0.20 | 0.1 | 1 |
| STa | 16 | Vertical Rake 50% Volume Level | 29 - 46 | < 0.20 | 0.1 | 1 |
| STa | 17 | Vertical Rake 50% Volume Level | 29 - 46 | < 0.20 | 0.1 | 1 |
| STa | 18 | Vertical Rake 50% Volume Level | 29 - 46 | < 0.20 | 0.1 | 1 |
| STab | 19 | Rake #1 90% Volume Level | 29 - 46 | < 0.20 | 0.1 | 1 |
| STa | 20 | Rake #1 80% Volume Level | 29 - 46 | < 0.20 | 0.1 | 1 |

| MEAS | NUM | DESCRIPTION | RANGE Deg (R) | INACCURACY ± Deg (R) | SAMPLE FREQ. (Hz) | PRI. EXP. |
|---|---|---|---|---|---|---|
| STa | 21 | Rake #1 72% Volume Level | 29 - 46 | < 0.20 | 0.1 | 1 |
| STa | 22 | Rake #1 56% Volume Level | 29 - 46 | < 0.20 | 0.1 | 1 |
| STa | 23 | Rake #1 48% Volume Level | 29 - 46 | < 0.20 | 0.1 | 1 |
| STa | 24 | Rake #1 32% Volume Level | 29 - 46 | < 0.20 | 0.1 | 1 |
| STa | 26 | Rake #2 88% Volume Level | 29 - 46 | < 0.20 | 0.1 | 1 |
| STa | 27 | Rake #2 78% Volume Level | 29 - 46 | < 0.20 | 0.1 | 1 |
| STa | 28 | Rake #2 68% Volume Level | 29 - 46 | < 0.20 | 0.1 | 1 |
| STaB | 29 | Rake #2 54% Volume Level | 29 - 46 | < 0.20 | 0.1 | 1 |
| STa | 30 | Rake #2 44% Volume Level | 29 - 46 | < 0.20 | 0.1 | 1 |
| STa | 31 | Rake #2 28% Volume Level | 29 - 46 | < 0.20 | 0.1 | 1 |
| STa | 32 | Rake #2 12% Volume Level | 29 - 46 | < 0.20 | 0.1 | 1 |
| STa | 33 | Rake #3 86% Volume Level | 29 - 46 | < 0.20 | 0.1 | 1 |
| STa | 34 | Rake #3 76% Volume Level | 29 - 46 | < 0.20 | 0.1 | 1 |
| STab | 35 | Rake #3 64% Volume Level | 29 - 46 | < 0.20 | 0.1 | 1 |
| STa | 36 | Rake #3 52% Volume Level | 29 - 46 | < 0.20 | 0.1 | 1 |
| STa | 37 | Rake #3 40% Volume Level | 29 - 46 | < 0.20 | 0.1 | 1 |
| STa | 38 | Rake #3 24% Volume Level | 29 - 46 | < 0.20 | 0.1 | 1 |
| STa | 39 | Rake #3 8% Volume Level | 29 - 46 | < 0.20 | 0.1 | 1 |
| STab G | 40 | Rake #4 84% Volume Level | 29 - 46 | < 0.20 | 0.1 | 1 |
| STab G | 41 | Rake #4 74% Volume Level | 29 - 46 | < 0.20 | 0.1 | 1 |

| MEAS | NUM | DESCRIPTION | RANGE Deg (R) | INACCURACY ± Deg (R) | SAMPLE FREQ. (Hz) | PRI. EXP. |
|---|---|---|---|---|---|---|
| STa G | 42 | Rake #4 60% Volume Level | 29 - 46 | < 0.20 | 0.1 | 1 |
| STab G | 43 | Rake #4 50% Volume Level | 29 - 46 | < 0.20 | 0.1 | 1 |
| STa G | 44 | Rake #4 36% Volume Level | 29 - 46 | < 0.20 | 0.1 | 1 |
| STa G | 45 | Rake #4 20% Volume Level | 29 - 46 | < 0.20 | 0.1 | 1 |
| STa G | 46 | Rake #4 4% Volume Level | 29 - 46 | < 0.20 | 0.1 | 1 |
| STa G | 47 | Rake #5 98% Volume Level | 29 - 46 | < 0.20 | 0.1 | 1 |
| STa G | 48 | Rake #5 95% Volume Level | 29 - 46 | < 0.20 | 0.1 | 1 |
| STab G | 49 | Rake #5 92% Volume Level | 29 - 46 | < 0.20 | 0.1 | 1 |
| STab | 50 | Press diffuser | 29 - 46 | < 0.20 | 0.1 | 1 |
| STa | 51 | Forward LAD box | 29 - 46 | < 0.20 | 0.1 | 1 |
| STa | 52 | AFT LAD box | 29 - 46 | < 0.20 | 0.1 | 1 |
| STa | 53 | LAD channel #1 1/3 length | 29 - 46 | < 0.20 | 0.1 | 1 |
| STa | 54 | LAD channel #1 2/3 length | 29 - 46 | < 0.20 | 0.1 | 1 |
| STa | 55 | LAD channel #2 1/3 length | 29 - 46 | < 0.20 | 0.1 | 1 |
| STa | 56 | LAD channel #2 2/3 length | 29 - 46 | < 0.20 | 0.1 | 1 |
| STa | 57 | LAD channel #3 1/3 length | 29 - 46 | < 0.20 | 0.1 | 1 |
| Sta | 58 | LAD channel #3 2/3 length | 29 - 46 | < 0.20 | 0.1 | 1 |
| STa | 59 | LAD channel #4 1/3 length | 29 - 46 | < 0.20 | 0.1 | 1 |
| STa | 60 | LAD channel #4 2/3 length | 29 - 46 | < 0.20 | 0.1 | 1 |
| Sta | 61 | 1/4 inch from TVS line, Channel #1 | 29 - 46 | < 0.20 | 0.1 | 1 |
| STa | 62 | 1/4 inch from TVS line, Channel #2 | 29 - 46 | < 0.20 | 0.1 | 1 |

| MEAS | NUM | DESCRIPTION | RANGE Deg (R) | INACCURACY ± Deg (R) | SAMPLE FREQ. (Hz) | PRI. EXP. |
|---|---|---|---|---|---|---|
| STa | 63 | 1/4 inch from TVS line, Channel #3 | 29 - 46 | < 0.20 | 0.1 | 1 |
| Sta | 64 | 1/4 inch from TVS line, Channel #4 | 29 - 46 | < 0.20 | 0.1 | 1 |
| SUPPLY TANK OUTER WALL TEMPERATURE MEASUREMENTS | | | | | | |
| STa | 101 | LH2 transfer line temperature at supply tank wall | 29 - 46 | < 0.20 | 0.1 | 1 |
| STa | 102 | fill drain line temperature at supply tank | 29 - 46 | < 0.20 | 0.1 | 1 |
| Sta | 103 | passive TVS line temperature at outer supply tank wall | 29 - 46 | < 0.20 | 0.1 | 1 |
| STab | 104 | gas pressurization line temp at supply tank wall | 29 - 46 | < 0.20 | 0.1 | 1 |
| STa | 105 | vent line temperature at supply tank outer wall | 29 - 46 | < 0.20 | 0.1 | 1 |
| Sta | 106 | top dome warm side temperature | 29 - 46 | < 0.20 | 0.1 | 1 |
| STa | 107 | supply tank upper barrel cold side temperature | 29 - 46 | < 0.20 | 0.1 | 1 |
| STa | 108 | AFT dome cold side temperature | 29 - 46 | < 0.20 | 0.1 | 1 |
| Sta | 109 | supply tank lower barrel warm side temperature | 29 - 46 | < 0.20 | 0.1 | 1 |
| STa | 110 | top dome cold side temperature | 29 - 46 | < 0.20 | 0.1 | 1 |
| STa | 111 | AFT dome warm side temperature | 29 - 46 | < 0.20 | 0.1 | 1 |
| Sta | 112 | forward barrel warm side temperature | 29 - 46 | < 0.20 | 0.1 | 1 |
| STa | 113 | aft barrel cold side temperature | 29 - 46 | < 0.20 | 0.1 | 1 |
| Sta | 114 | central barrel +y direction | 29 - 46 | < 0.20 | 0.1 | 1 |
| STa | 115 | central barrel -y direction | 29 - 46 | < 0.20 | 0.1 | 1 |

| MEAS | NUM | DESCRIPTION | RANGE Deg (R) | INACCURACY ± Deg (R) | SAMPLE FREQ. (Hz) | PRI. EXP. |
|---|---|---|---|---|---|---|
| STa | 116 | forward barrel warm side strut near tank wall | 29 - 46 | < 0.20 | 0.1 | 1 |
| STa | 117 | aft barrel cold side strut near tank wall | 29 - 46 | < 0.20 | 0.1 | 1 |
| STa | 118 | harness at PV warm side | 29 - 46 | < 0.20 | 0.1 | 1 |
| STa | 119 | harness at PV cold side | 29 - 46 | < 0.20 | 0.1 | 1 |
| SUPPLY TANK MODULE PANEL LOCATED TEMPERATURE MEASUREMENTS | | | | | | |
| STa | 201 | LH2 transfer line temperature at Flow meter panel J | 29 - 46 | < 0.20 | 0.1 | 1 |
| STa | 202 | LH2 transfer line temperature at Ventri flow control entrance, Panel I | 29 - 46 | < 0.20 | 0.1 | 1 |
| STa | 203 | LH2 transfer line temp. at Orifice flow control bank exit. Panel I | 29 - 46 | < 0.20 | 0.1 | 1 |
| Sta | 204 | LH2 transfer line temp. at panel f entrance. This line section feeds the active TVS mixer pumps | 29 - 46 | < 0.20 | 0.1 | 1 |
| STa | 205 | LH2 transfer line at Panel F exit. Active TVS mixer pumps exit temp. | 29 - 46 | < 0.20 | 0.1 | 1 |
| STa | 206 | passive TVS line Temp. at Joule Thompson dev. Panel H | 29 - 46 | < 0.20 | 0.1 | 1 |
| Sta | 207 | TVs line temp. downstream of JT devices. Panel H | 29 - 46 | < 0.20 | 0.1 | 1 |
| STa | 208 | Joule Thompson dev. heater temp Panel H | 29 - 46 | < 0.20 | 0.1 | 1 |
| STab | 209 | gas pressurization line temperature at Panel J | 29 - 46 | < 0.20 | 0.1 | 1 |
| STa | 210 | ground fill line temperature at Panel E exit | 29 - 46 | < 0.20 | 0.1 | 1 |

| MEAS | NUM | DESCRIPTION | RANGE Deg (R) | INACCURACY ± Deg (R) | SAMPLE FREQ. (Hz) | PRI. EXP. |
|---|---|---|---|---|---|---|
| STa | 211 | vent line temp. at Panel G | 29 - 46 | < 0.20 | 0.1 | 1 |
| INNER HONEYCOMB TEMPERATURE MEASUREMENTS | | | | | | |
| STb | 212 | forward dome warm side temp. of inner honeycome structure | 117-280 | < 1.5 | 0.1 | 1 |
| STb | 213 | forward barrel warm honeycomb temp | 117-280 | < 1.5 | 0.1 | 1 |
| STb | 214 | Aft Dome inner honeybomb temp. cold side | 117-280 | < 1.5 | 0.1 | 1 |
| STb | 215 | Aft barrel inner honeycomb warm side temperature | 117-280 | < 1.5 | 0.1 | 1 |
| STb | 216 | forward dome cold si honeycomb temp. | 117-280 | < 1.5 | 0.1 | 1 |
| STb | 217 | AFT dome warm side honeycomb temp. | 117-280 | < 1.5 | 0.1 | 1 |
| STb | 218 | forward barrel cold side honeycomb temp | 117-280 | < 1.5 | 0.1 | 1 |
| STb | 219 | Aft barrel cold side honeycomb temp | 117-280 | < 1.5 | 0.1 | 1 |
| STb | 220 | central barrel +y direction honeycomb temperature | 117-280 | < 1.5 | 0.1 | 1 |
| STb | 221 | central barrel -y direction honeycomb temperature | 117-280 | < 1.5 | 0.1 | 1 |
| STb | 222 | Forward barrel warm side strut near honeycomb | 117-280 | < 1.5 | 0.1 | 1 |
| STb | 223 | Aft barrel cold side strut near honeycomb | 117-280 | < 1.5 | 0.1 | 1 |
| STb | 224 | harness at honeycomb warm side | 117-280 | < 1.5 | 0.1 | 1 |
| STb | 225 | harness at honeycomb cold side | 117-280 | < 1.5 | 0.1 | 1 |
| HYDROGEN VAPORIZER TEMPERATURE MEASUREMENTS | | | | | | |
| STa | 301 | LH2 transfer line temp. at Vaporizer line inlet | 36 - 41 | < 0.2 | 0.1 | 1 |

| MEAS | NUM | DESCRIPTION | RANGE Deg (R) | INACCURACY ± Deg (R) | SAMPLE FREQ. (Hz) | PRI. EXP. |
|---|---|---|---|---|---|---|
| STab | 302 | vaporizer B coil inlet temperature | 36-530 | < 1.5 | 0.1 | 1 |
| STab | 303 | vaporizer A coil inlet temperature | 36-530 | < 1.5 | 0.1 | 1 |
| Stab | 304 | vaporizer B coil exit temperature | 36-530 | < 1.5 | 0.1 | 1 |
| STab | 305 | vaporizer A coil exit temperature | 36-530 | < 1.5 | 0.1 | 1 |
| STb | 306 | vaporizer B bottle cold side temp. | 485-525 | < 1.5 | 0.1 | 1 |
| STb | 307 | vaporizer A bottle cold side temp. | 485-525 | < 1.5 | 0.1 | 1 |
| STb | 308 | vaporizer B bottle warm side temp. | 485-525 | < 1.5 | 0.1 | 1 |
| STb | 309 | vaporizer A bottle warm side temp. | 485-525 | < 1.5 | 0.1 | 1 |
| Stab | 310 | vaporizer coil exit temp. at vent line | 38-525 | < 1.5 | 0.1 | 1 |
| STb | 311 | helium bottle temperature | 485-525 | < 1.5 | 0.1 | 1 |
| STa | 312 | helium bottle temperature | 485-525 | < 1.5 | 0.1 | 1 |
| STb | 313 | helium bottle temperature | 485-525 | < 1.5 | 0.1 | 1 |
| STb | 314 | helium bottle temperature | 485-525 | < 1.5 | 0.1 | 1 |
| STb | 315 | Gas pressurant flow meter inlet | 485-525 | < 1.5 | 0.1 | 1 |
| OUTER MLI TEMPERATURE MEASUREMENTS | | | | | | |
| STb | 316 | Forward dome outer MLI temperature on warm side | 360-525 | < 1.5 | 0.1 | 1 |
| STb | 317 | Upper barrel outer MLI temperature on cold side | 235-525 | < 1.5 | 0.1 | 1 |
| STb | 318 | AFT dome outer MLI temperature on cold side | 235-525 | < 1.5 | 0.1 | 1 |
| STb | 319 | lower barrel outer MLI temperature on warm side | 360-525 | < 1.5 | 0.1 | 1 |

| MEAS | NUM | DESCRIPTION | RANGE Deg (R) | INACCURACY ± Deg (R) | SAMPLE FREQ. (Hz) | PRI. EXP. |
|---|---|---|---|---|---|---|
| STb | 320 | Forward dome outer MLI temperature on cold side | 235-525 | < 1.5 | 0.1 | 1 |
| STb | 321 | AFT dome outer MLI temperature on warm side | 360-525 | < 1.5 | 0.1 | 1 |
| STb | 322 | upper barrel warm side outer MLI temperature | 360-525 | < 1.5 | 0.1 | 1 |
| STb | 323 | lower barrel outer MLI temperature on cold side | 235-525 | < 1.5 | 0.1 | 1 |
| STb | 324 | central barrel +y direction outer MLI temperature | 235-525 | < 1.5 | 0.1 | 1 |
| STb | 325 | central barrel -y direction outer MLI temperature | 235-525 | < 1.5 | 0.1 | 1 |
| VENT AND GASEOUS FLOW METER TEMPERATURES | | | | | | |
| STb | 326 | ground/ascent vent line temperature | 235-525 | < 1.5 | 0.1 | 1 |
| STb | 327 | temperature at vent relief line | 235-525 | < 1.5 | 0.1 | 1 |
| STb | 328 | Supply tank active TVS flow meter temp | 235-525 | < 1.5 | 0.1 | 1 |
| STb | 329 | Supply tank passive TVS flow meter temp | 235-525 | < 1.5 | 0.1 | 1 |
| STb | 331 | gas pressurant flow meter inlet temp. | 485-525 | < 1.5 | 0.1 | 1 |
| STb | 332 | temperature at balanced TVS vent. (flow) | 235-525 | < 1.5 | 0.1 | 1 |

SUPPLY TANK LIQUID VAPOR POINT MEASUREMENTS

| MEAS | NUM | DESCRIPTION | RESPONSE Deg (R) | SAMPLE FREQ. (Hz) | PRI. EXP. |
|---|---|---|---|---|---|
| SL | 1 | Rake #5 98% Volume | LIQ/VAP | 0.1 | 1 |
| SL | 2 | Rake #5 96% Volume | LIQ/VAP | 0.1 | 1 |
| SL | 3 | Rake #5 95% Volume | LIQ/VAP | 0.1 | 1 |
| SL | 4 | Rake #5 94% Volume | LIQ/VAP | 0.1 | 1 |
| SL | 5 | Rake #5 92% Volume | LIQ/VAP | 0.1 | 1 |
| SL | 6 | Rake #1 90% Volume | LIQ/VAP | 0.1 | 1 |

| MEAS | NUM | DESCRIPTION | RESPONSE Deg (R) | SAMPLE FREQ. (Hz) | PRI. EXP. |
|---|---|---|---|---|---|
| SL | 7 | Rake #2 88% Volume | LIQ/VAP | 0.1 | 1 |
| SL | 8 | Rake #3 86% Volume | LIQ/VAP | 0.1 | 1 |
| SL | 9 | Rake #4 84% Volume | LIQ/VAP | 0.1 | 1 |
| SL | 10 | Rake #1 80% Volume | LIQ/VAP | 0.1 | 1 |
| SL | 11 | Rake #2 78% Volume | LIQ/VAP | 0.1 | 1 |
| SL | 12 | Rake #3 76% Volume | LIQ/VAP | 0.1 | 1 |
| SL | 13 | Rake #4 74% Volume | LIQ/VAP | 0.1 | 1 |
| SL | 14 | Rake #1 72% Volume | LIQ/VAP | 0.1 | 1 |
| SL | 15 | Rake #2 68% Volume | LIQ/VAP | 0.1 | 1 |
| SL | 16 | Rake #3 64% Volume | LIQ/VAP | 0.1 | 1 |
| SL | 17 | Rake #4 60% Volume | LIQ/VAP | 0.1 | 1 |
| SL | 18 | Rake #1 56% Volume | LIQ/VAP | 0.1 | 1 |
| SL | 19 | Rake #2 54% Volume | LIQ/VAP | 0.1 | 1 |
| SL | 20 | Rake #3 52% Volume | LIQ/VAP | 0.1 | 1 |
| SL | 21 | Rake #4 50% Volume | LIQ/VAP | 0.1 | 1 |
| SL | 22 | Rake #1 48% Volume | LIQ/VAP | 0.1 | 1 |
| SL | 23 | Rake #2 44% Volume | LIQ/VAP | 0.1 | 1 |
| SL | 24 | Rake #3 40% Volume | LIQ/VAP | 0.1 | 1 |
| SL | 25 | Rake #4 36% Volume | LIQ/VAP | 0.1 | 1 |
| SL | 26 | Rake #1 32% Volume | LIQ/VAP | 0.1 | 1 |
| SL | 27 | Rake #2 28% Volume | LIQ/VAP | 0.1 | 1 |
| SL | 28 | Rake #3 24% Volume | LIQ/VAP | 0.1 | 1 |
| SL | 29 | Rake #4 20% Volume | LIQ/VAP | 0.1 | 1 |
| SL | 30 | Rake #1 16% Volume | LIQ/VAP | 0.1 | 1 |
| SL | 31 | Rake #2 12% Volume | LIQ/VAP | 0.1 | 1 |
| SL | 32 | Rake #3 8% Volume | LIQ/VAP | 0.1 | 1 |
| SL | 33 | Rake #4 4% Volume | LIQ/VAP | 0.1 | 1 |
| SL | 34 | Vent line entrance | LIQ/VAP | 0.1 | 1 |
| SL | 35 | Transfer line entrance | LIQ/VAP | 0.1 | 1 |
| SL | 36 | TVS line exit | LIQ/VAP | 0.1 | 1 |

SUPPLY MODULE PRESSURE MEASUREMENTS

| MEAS | NUM | DESCRIPTION | RANGE PSIA | INACCURACY +/- PSIA | SAMPLE FREQ (HZ) | MEAS TYPE |
|---|---|---|---|---|---|---|
| SP | 1 | Pressurization line press to supply tank | 50 | 0.23 | 0.1 EDU | Control |
| SP | 2 | Supply vent line Pressure | 50 | 0.23 | 0.1 | Control EDU |
| SP | 3 | Relief vent line pressure | 50 | 0.23 | 0.1 | Control EDU |
| SP | 4 | Active TVS line pressure to mixer | 50 | 0.37 | 0.1 | Data |
| SP | 5 | Active TVS inlet pressure to supply tank | 50 | 0.37 | 0.1 | Data |
| SP | 6 | TVS inlet pressure to visco jets | 50 | 0.37 | 0.1 | Data |
| SP | 7 | Passive TVS exit line pressure to supply tank | 50 | 0.37 | 0.1 | Data |
| SP | 8 | Supply tank LH2 transfer line pressure | 50 | 0.37 | 0.1 | Data |
| SP | 9 | Supply tank fill drain line pressure | 50 | 0.37 | 0.1 | Data |
| SP | 10 | LH2 transfer line pressure downsteam of venturi bank | 50 | 0.37 | 0.1 | Data |
| SP | 11 | LH2 transfer line pressure to vaporizer | 50 | 0.37 | 0.1 | Data |
| SP | 12 | Vaporizer B coil inlet pressure | 50 | 0.37 | 0.1 | Data |
| SP | 13 | Vaporizer B coil exit pressure | 200-2000 | 37 | 0.1 | Control |
| SP | 14 | Vaporizer A coil exit pressure | 200-2000 | 37 | 0.1 | Control |
| SP | 15 | Vaporizer B bottle pressure | 200-2000 | 37 | 0.1 | Control |
| SP | 16 | Vaporizer A bottle pressure | 200-2000 | 37 | 0.1 | Control |
| SP | 17 | Vaporizer vent line pressure | 50 | 0.37 | 0.1 | Data |
| SP | 18 | Helium bottle pressure | 3000 | 37 | 0.1 | Data safety |
| SP | 19 | Helium bottle pressure | 3000 | 37 | 0.1 | Data safety |

| MEAS | NUM | DESCRIPTION | RANGE PSIA | INACCURACY +/- PSIA | SAMPLE FREQ (HZ) | MEAS TYPE |
|---|---|---|---|---|---|---|
| SP | 20 | Pressure at Venturi flow meter bank | 50 | 0.37 | 0.1 | Data |
| SP | 21 | Supply tank active TVS flow pressure | 25 | 0.18 | 0.1 | Data |
| SP | 22 | Supply tank passive TVS flow pressure | 25 | 0.18 | 0.1 | Data |
| SP | 23 | Pressurant gas flow meter pressure | 50 | 0.37 | 0.1 | Data |
| SP | 24 | Flight Balanced vent pressure | 50 | 0.37 | 0.1 | Data |

LARGE RECEIVER (LR) TEMPERATURE MEASUREMENTS

| MEAS | NUM | DESCRIPTION | RANGE Deg (R) | INACCURACY ± Deg (R) | SAMPLE FREQ. (Hz) | PRI. EXP. |
|---|---|---|---|---|---|---|
| LRTa | 1 | 1 Pressurization line diffuser Temperature | 36-540 | < 1.5 | 0.1 | 8 |
| LRTa | 2 | 2 Internal vent line Temperature | 29-46 | < 0.2 | 0.1 | 3 |
| LRTa | 3 | Top LAD Temperature | 29-46 | < 0.2 | 0.1 | 4 |
| LRTa | 4 | Bottom LAD temp. | 29-46 | < 0.2 | 0.1 | 4 |
| LRTa | 5 | Inside LAD channel #1, 3/4 length | 29-46 | < 0.2 | 0.1 | 4 |
| LRTa | 6 | Inside LAD channel #2, 2/4 length | 29-46 | < 0.2 | 0.1 | 4 |
| LRTa | 7 | Inside LAD channel #1, 1/2 length | 29-46 | < 0.2 | 0.1 | 4 |
| LRTa | 8 | Inside LAD channel #2, 1/2 length | 29-46 | < 0.2 | 0.1 | 4 |
| LRTa | 9 | Inside LAD channel #1, 1/4 length | 29-46 | < 0.2 | 0.1 | 4 |
| LRTa | 10 | Inside LAD channel #2, 1/4 length | 29-46 | < 0.2 | 0.1 | 4 |
| LRTa | 11 | Outside LAD channel #1, 3/4 length | 29-46 | < 0.2 | 0.1 | 4 |
| LRTa | 12 | Outside LAD channel #2, 3/4 length | 29-46 | < 0.2 | 0.1 | 4 |
| LRTa | 13 | Outside LAD channel #1, 1/2 length | 29-46 | < 0.2 | 0.1 | 4 |
| LRTa | 14 | Outside LAD channel #2, 1/2 length | 29-46 | < 0.2 | 0.1 | 4 |

| MEAS | NUM | DESCRIPTION | RANGE Deg (R) | INACCURACY ± Deg (R) | SAMPLE FREQ. (Hz) | PRI. EXP. |
|---|---|---|---|---|---|---|
| LRTa | 15 | Outside LAD channel #1, 1/4 length | 29-46 | < 0.2 | 0.1 | 4 |
| LRTa | 16 | Outside LAD channel #2, 1/4 length | 29-46 | < 0.2 | 0.1 | 4 |
| LRTa | 17 | Pressurization line diffuser temperature | 29-46 | < 0.2 | 0.1 | 8 |
| LRTa | 18 | 95% volume level Rake #1 | 29-46 | < 0.2 | 0.1 | 3 |
| LRTa | 19 | 90% volume level Rake #2 | 29-46 | < 0.2 | 0.1 | 3 |
| LRTa | 20 | 85% volume level Rake #1 | 29-46 | < 0.2 | 0.1 | 3 |
| LRTa | 21 | 80% volume level Rake #2 | 36-110<br>110-540 | < 1.0<br>< 1.5 | 0.1 | 3 |
| LRTa | 22 | 75% volume level Rake #1 | 36-110<br>110-540 | < 1.0<br>< 1.5 | 0.1 | 3 |
| LRTa | 23 | 70% volume level Rake #2 | 36-110<br>110-540 | < 1.0<br>< 1.5 | 0.1 | 3 |
| LRTa | 24 | 65% volume level Rake #1 | 36-110<br>110-540 | < 1.0<br>< 1.5 | 0.1 | 3 |
| LRTa | 25 | 60% volume level Rake #2 | 36-110<br>110-540 | < 1.0<br>< 1.5 | 0.1 | 3 |
| LRTa | 26 | 55% volume level Rake #1 | 36-110<br>110-540 | < 1.0<br>< 1.5 | 0.1 | 3 |
| LRTa | 27 | 50% volume level Rake #3 | 29 - 46 | < 1.0 | 0.1 | 3 |
| LRTa | 28 | 45% volume level Rake #5 | 36-110<br>110-540 | < 1.0<br>< 1.5 | 0.1 | 3 |
| LRTa | 29 | 40% volume level Rake #4 | 36-110<br>110-540 | < 1.0<br>< 1.5 | 0.1 | 3 |
| LRTa | 30 | 35% volume level Rake #5 | 36-110<br>110-540 | < 1.0<br>< 1.5 | 0.1 | 3 |
| LRTa | 31 | 30% volume level Rake #4 | 36-110<br>110-540 | < 1.0<br>< 1.5 | 0.1 | 3 |
| LRTa | 32 | 25% volume level Rake #5 | 36-110<br>110-540 | < 1.0<br>< 1.5 | 0.1 | 3 |
| LRTa | 33 | 20% volume level Rake #4 | 36-110<br>110-540 | < 1.0<br>< 1.5 | 0.1 | 3 |
| LRTa | 34 | 15% volume level Rake #5 | 36-110<br>110-540 | < 1.0<br>< 1.5 | 0.1 | 3 |

| MEAS | NUM | DESCRIPTION | RANGE Deg (R) | INACCURACY ± Deg (R) | SAMPLE FREQ. (Hz) | PRI. EXP. |
|---|---|---|---|---|---|---|
| LRTa | 35 | 10% volume level Rake #4 | 36-110<br>110-540 | < 1.0<br>< 1.5 | 0.1 | 3 |
| LRTa | 36 | 5% volume level Rake #5 | 36-110<br>110-540 | < 1.0<br>< 1.5 | 0.1 | 3 |
| LRTa | 101 | Top axial spray line temp. at tank wall | 36-110<br>110-540 | < 1.0<br>< 1.5 | 0.1 | 3 |
| LRTa | 102 | LH2 Transfer line temp. at tank wall | 36-110<br>110-540 | < 1.0<br>< 1.5 | 0.1 | 3 |
| LRTa | 103 | Lower axial spray line temp. at tank wall | 36-110<br>110-540 | < 1.0<br>< 1.5 | 0.1 | 3 |
| LRTa | 104 | Tangential spray line temp. at tank wall | 36-110<br>110-540 | < 1.0<br>< 1.5 | 0.1 | 3 |
| LRTa | 105 | vent line temperature at outer tank wall | 36-110<br>110-540 | < 1.0<br>< 1.5 | 0.1 | 3 |
| LRTa | 106 | Pressurization line temperature | 36-110<br>110-540 | < 1.0<br>< 1.5 | 0.1 | 3 |
| LRTa | 107 | TVS line temp. at outer tank wall temp. | 36-110<br>110-540 | < 1.0<br>< 1.5 | 0.1 | 3 |
| LRTa | 108 | TVS line temperature at 50% length | 36-110<br>110-540 | < 1.0<br>< 1.5 | 0.1 | 3 |
| LRTa | 109 | TVS line temperature at 100% length | 36-110<br>110-540 | < 1.0<br>< 1.5 | 0.1 | 3 |
| LRTa | 110 | top dome warm side tank temperature | 36-110<br>110-540 | < 1.0<br>< 1.5 | 0.1 | 3 |
| LRTa | 111 | top dome cold side tank temperature | 36-110<br>110-540 | < 1.0<br>< 1.5 | 0.1 | 3 |
| LRTa | 112 | Aft dome warm side tank temperature | 36-110<br>110-540 | < 1.0<br>< 1.5 | 0.1 | 3 |
| LRTa | 113 | Aft dome cold side tank temperature | 36-110<br>110-540 | < 1.0<br>< 1.5 | 0.1 | 3 |
| LRTa | 114 | Upper barrel warm si tank temperature | 36-110<br>110-540 | < 1.0<br>< 1.5 | 0.1 | 3 |
| LRTa | 115 | Upper barrel cold si tank temperature | 36-110<br>110-540 | < 1.0<br>< 1.5 | 0.1 | 3 |
| LRTa | 116 | Central barrel, tank temperature | 36-110<br>110-540 | < 1.0<br>< 1.5 | 0.1 | 3 |
| LRTa | 117 | Lower barrel warm si tank temperature | 36-110<br>110-540 | < 1.0<br>< 1.5 | 0.1 | 3 |
| LRTa | 118 | Lower barrel cold si tank temperature | 36-110<br>110-540 | < 1.0<br>< 1.5 | 0.1 | 3 |

| MEAS | NUM | DESCRIPTION | RANGE Deg (R) | INACCURACY ± Deg (R) | SAMPLE FREQ. (Hz) | PRI. EXP. |
|---|---|---|---|---|---|---|
| LRTa | 119 | Central barrel, tank temperature | 36-110<br>110-540 | < 1.0<br>< 1.5 | 0.1 | 3 |
| LRTa | 120 | Warm side strut temperature at tank | 36-110<br>110-540 | < 1.0<br>< 1.5 | 0.1 | 3 |
| LRTa | 121 | Cold side strut temperature at tank | 36-110<br>110-540 | < 1.0<br>< 1.5 | 0.1 | 3 |
| LRTa | 122 | Warm side harness temperature at tank | 36-110<br>110-540 | < 1.0<br>< 1.5 | 0.1 | 3 |
| LRTa | 123 | Cold side harness temperature at tank | 36-110<br>110-540 | < 1.0<br>< 1.5 | 0.1 | 3 |
| LRTa | 201 | Top axial spray line temp. at panel L | 36-110<br>110-540 | < 1.0<br>< 1.5 | 0.1 | 3 |
| LRTa | 202 | LH2 Transfer line temp. at panel L | 36-110<br>110-540 | < 1.0<br>< 1.5 | 0.1 | 3 |
| LRTa | 203 | Lower axial spray line temp. at valve panel K | 36-110<br>110-540 | < 1.0<br>< 1.5 | 0.1 | 3 |
| LRTa | 204 | Tangential spray line temp. at valve panel K | 36-110<br>110-540 | < 1.0<br>< 1.5 | 0.1 | 3 |
| LRTa | 205 | Vent line temperature at valve panel L | 36-110<br>110-540 | < 1.0<br>< 1.5 | 0.1 | 3 |
| LRTa | 206 | Pressurization line temp. at panel L | 36-110<br>110-540 | < 1.0<br>< 1.5 | 0.1 | 3 |
| LRTa | 207 | TVS line temperature at valve panel L | 36-110<br>110-540 | < 1.0<br>< 1.5 | 0.1 | 3 |
| LRTb | 208 | Forward dome honeycomb warm side | 115-135 | < 1.5 | 0.1 | 3 |
| LRTb | 209 | Forward dome honeycomb cold side | 115-135 | < 1.5 | 0.1 | 3 |
| LRTb | 210 | Aft dome, honeycomb warm side | 115-135 | < 1.5 | 0.1 | 3 |
| LRTb | 211 | Aft dome, honeycomb cold side | 115-135 | < 1.5 | 0.1 | 3 |
| LRTb | 212 | Honeycomb upper barr warm side | 115-135 | < 1.5 | 0.1 | 3 |
| LRTb | 213 | Honeycomb lower barr cold side | 115-135 | < 1.5 | 0.1 | 3 |
| LRTb | 214 | Honeycomb central temperature | 115-135 | < 1.5 | 0.1 | 3 |
| LRTb | 215 | Honeycomb central temperature | 115-135 | < 1.5 | 0.1 | 3 |

| MEAS | NUM | DESCRIPTION | RANGE Deg (R) | INACCURACY ± Deg (R) | SAMPLE FREQ. (Hz) | PRI. EXP. |
|---|---|---|---|---|---|---|
| LRTb | 216 | Warm side strut temperature | 115-135 | < 1.5 | 0.1 | 3 |
| LRTb | 217 | Cold side strut temperature | 115-135 | < 1.5 | 0.1 | 3 |
| LRTb | 218 | harness at honeycomb warm side temperature | 115-135 | < 1.5 | 0.1 | 3 |
| LRTb | 219 | harness at honeycomb cold side | 115-135 | < 1.5 | 0.1 | 3 |
| LRTb | 301 | Forward dome outer M temp. on warm side | 360-520 | < 1.5 | 0.1 | 3 |
| LRTb | 302 | Aft dome cold side MLI temperature | 230-520 | < 1.5 | 0.1 | 3 |
| LRTb | 303 | Aft barrel outer MLI temp. on warm side | 360-520 | < 1.5 | 0.1 | 3 |
| LRTb | 304 | Forward barrel outer MLI temp. cold side | 230-520 | < 1.5 | 0.1 | 3 |
| LRTb | 305 | MLI temp. central side +y direction | 230-520 | < 1.5 | 0.1 | 3 |
| LRTb | 306 | MLI temp. central side temp. -y direct. | 230-520 | < 1.5 | 0.1 | 3 |
| LRTa | 307 | Receiver tank flow transfer orifice temp | 29 - 46 | < 0.2 | 0.1 | 3 |
| LRTb | 308 | Lg. Rec TVS flow meter inlet temp. | 235-525 | < 1.5 | 0.1 | 3 |

LARGE RECEIVER LIQUID VAPOR POINT MEASUREMENTS

| MEAS | NUM | DESCRIPTION | RESPONSE | SAMPLE FREQ. (Hz) | PRI. EXP. |
|---|---|---|---|---|---|
| LRL | 1 | Rake #1 98% Volume | LIQ/VAP | 0.1 | 2 |
| LRL | 2 | Rake #2 96% Volume | LIQ/VAP | 0.1 | 2 |
| LRL | 3 | Rake #1 94% Volume | LIQ/VAP | 0.1 | 2 |
| LRL | 4 | Rake #2 92% Volume | LIQ/VAP | 0.1 | 2 |
| LRL | 5 | Rake #1 90% Volume | LIQ/VAP | 0.1 | 2 |
| LRL | 6 | Rake #2 88% Volume | LIQ/VAP | 0.1 | 2 |
| LRL | 7 | Rake #1 86% Volume | LIQ/VAP | 0.1 | 2 |
| LRL | 8 | Rake #2 84% Volume | LIQ/VAP | 0.1 | 2 |
| LRL | 9 | Rake #1 82% Volume | LIQ/VAP | 0.1 | 2 |
| LRL | 10 | Rake #2 80% Volume | LIQ/VAP | 0.1 | 2 |

| MEAS | NUM | DESCRIPTION | RESPONSE | SAMPLE FREQ. (Hz) | PRI. EXP. |
|---|---|---|---|---|---|
| LRL | 11 | Rake #1 78% Volume | LIQ/VAP | 0.1 | 2 |
| LRL | 12 | Rake #2 76% Volume | LIQ/VAP | 0.1 | 2 |
| LRL | 13 | Rake #1 74% Volume | LIQ/VAP | 0.1 | 2 |
| LRL | 14 | Rake #2 72% Volume | LIQ/VAP | 0.1 | 2 |
| LRL | 15 | Rake #1 70% Volume | LIQ/VAP | 0.1 | 2 |
| LRL | 16 | Rake #2 66% Volume | LIQ/VAP | 0.1 | 2 |
| LRL | 17 | Rake #1 62% Volume | LIQ/VAP | 0.1 | 2 |
| LRL | 18 | Rake #2 58% Volume | LIQ/VAP | 0.1 | 2 |
| LRL | 19 | Rake #1 54% Volume | LIQ/VAP | 0.1 | 2 |
| LRL | 20 | Rake #3 50% Volume | LIQ/VAP | 0.1 | 2 |
| LRL | 21 | Rake #5 46% Volume | LIQ/VAP | 0.1 | 2 |
| LRL | 22 | Rake #4 42% Volume | LIQ/VAP | 0.1 | 2 |
| LRL | 23 | Rake #5 38% Volume | LIQ/VAP | 0.1 | 2 |
| LRL | 24 | Rake #4 34% Volume | LIQ/VAP | 0.1 | 2 |
| LRL | 25 | Rake #5 30% Volume | LIQ/VAP | 0.1 | 2 |
| LRL | 26 | Rake #4 26% Volume | LIQ/VAP | 0.1 | 2 |
| LRL | 27 | Rake #5 22% Volume | LIQ/VAP | 0.1 | 2 |
| LRL | 28 | Rake #4 18% Volume | LIQ/VAP | 0.1 | 2 |
| LRL | 29 | Rake #5 14% Volume | LIQ/VAP | 0.1 | 2 |
| LRL | 30 | Rake #4 10% Volume | LIQ/VAP | 0.1 | 2 |
| LRL | 31 | Rake #5 6% Volume | LIQ/VAP | 0.1 | 2 |
| LRL | 32 | Vent line exit | LIQ/VAP | 0.1 | 2 |
| LRL | 33 | Upper LAD box | LIQ/VAP | 0.1 | 4 |
| LRL | 34 | LAD channel #1 3/4 length | LIQ/VAP | 0.1 | 4 |
| LRL | 35 | LAD channel #2 3/4 length | LIQ/VAP | 0.1 | 4 |
| LRL | 36 | LAD channel #1 1/2 length | LIQ/VAP | 0.1 | 4 |
| LRL | 37 | LAD channel #2 1/2 length | LIQ/VAP | 0.1 | 4 |
| LRL | 38 | LAD channel #1 1/4 length | LIQ/VAP | 0.1 | 4 |

| MEAS | NUM | DESCRIPTION | RESPONSE | SAMPLE FREQ. (Hz) | PRI. EXP. |
|---|---|---|---|---|---|
| LRL | 39 | LAD channel #2 1/4 length | LIQ/VAP | 0.1 | 4 |
| LRL | 40 | Lower LAD box | LIQ/VAP | 0.1 | 4 |

LARGE RECEIVER PRESSURE MEASUREMENTS

| MEAS | NUM | DESCRIPTION | RANGE PSIA | ACCURACY +/- PSIA | SAMPLE FREQ. (Hz) | MEAS TYPE |
|---|---|---|---|---|---|---|
| LR | 1 | Lg Rec relief vent meter pressure | 50 | 0.23 | 0.1 | Control EDU |
| LR | 2 | Lg Rec pressurization line pressure | 50 | 0.23 | 0.1 | Control EDU |
| LR | 3 | Lg. Rec vent line pressure | 50 | 0.23 | 0.1 | Control EDU |
| LR | 4 | Top axial spray line pressure | 50 | 0.37 | 0.1 | Data |
| LR | 5 | Lg Rec LAD transfer line pressure | 50 | 0.37 | 0.1 | Data |
| LR | 6 | Aft axial spray line pressure | 50 | 0.37 | 0.1 | Data |
| LR | 7 | Tangential spray line pressure | 50 | 0.37 | 0.1 | Data |
| LR | 8 | Receiver tanks venturi pressure | 50 | 0.37 | 0.1 | Data |
| LR | 9 | Lg. Rec TVS line pressure | 25 | 0.18 | 0.1 | Data |

SMALL RECEIVER (SR) MODULE TEMPERATURE MEASUREMENTS

| MEAS | NUM | DESCRIPTION | RANGE Deg (R) | INACCURACY ± Deg (R) | SAMPLE RATE (Hz) | PRI. EXP. |
|---|---|---|---|---|---|---|
| SRTa | 1 | Pressurization line diffuser temp. | 36-110<br>110-540 | < 1.0 | 0.1 | 3 |
| SRTa | 2 | Vent line exit temperature | 29 - 46 | < 0.2 | 0.1 | 3 |
| SRTa | 3 | 97.5% volume level radial spray bar | 29 - 46 | < 0.2 | 0.1 | 3 |
| SRTa | 4 | 80.0% volume level radial spray bar | 29 - 46 | < 0.2 | 0.1 | 3 |
| SRTa | 5 | 50.0% volume level radial spray bar | 29 - 46 | < 0.2 | 0.1 | 3 |
| SRTa | 6 | 20.0% volume level radial spray bar | 29 - 46 | < 0.2 | 0.1 | 3 |

| MEAS | NUM | DESCRIPTION | RANGE Deg (R) | INACCURACY ± Deg (R) | SAMPLE RATE (Hz) | PRI. EXP. |
|---|---|---|---|---|---|---|
| SRTa | 7 | 2.5% volume level radial spray bar | 29 - 46 | < 0.2 | 0.1 | 3 |
| SRTa | 8 | Axial spray line temperature | 29 - 46 | < 0.2 | 0.1 | 3 |
| SRTa | 9 | Tangential spray line left nozzle temp. | 29 - 46 | < 0.2 | 0.1 | 3 |
| SRTa | 10 | Tangential spray line right nozzle temp. | 29 - 46 | < 0.2 | 0.1 | 3 |
| SRTa | 11 | Tangential spray line center left temp. | 29 - 46 | < 0.2 | 0.1 | 3 |
| SRTa | 12 | Tangential spray line center right temp. | 29 - 46 | < 0.2 | 0.1 | 3 |
| SRTa | 13 | Rake V-1, 5% level | 29 - 46 | < 0.2 | 0.1 | 3 |
| SRTa | 14 | Rake V-1, 75% level | 29 - 46 | < 0.2 | 0.1 | 3 |
| SRTa | 15 | Rake V-1, 75% level | 36-110<br>110-540 | < 1.0<br>< 1.5 | 0.1 | 3 |
| SRTa | 16 | Rake V-1, 95% level | 36-110<br>110-540 | < 1.0<br>< 1.5 | 0.1 | 3 |
| SRTa | 17 | Rake V-2, 5% level | 36-110<br>110-540 | < 1.0<br>< 1.5 | 0.1 | 3 |
| SRTa | 18 | Rake V-2, 25% level | 36-110<br>110-540 | < 1.0<br>< 1.5 | 0.1 | 3 |
| SRTa | 19 | Rake V-2, 75% level | 36-110<br>110-540 | < 1.0<br>< 1.5 | 0.1 | 3 |
| SRTa | 20 | Rake V-2, 95% level | 29 - 46 | < 0.2 | 0.1 | 3 |
| SRTa | 21 | Rake H-2 center right temperature | 36-110<br>110-540 | < 1.0<br>< 1.5 | 0.1 | 3 |
| SRTa | 22 | Rake H-2 center left temperature | 36-110<br>110-540 | < 1.0<br>< 1.5 | 0.1 | 3 |
| SRTa | 23 | Rake H-1 center right temperature | 36-110<br>110-540 | < 1.0<br>< 1.5 | 0.1 | 3 |
| SRTa | 24 | Rake H-1 center left temperature | 36-110<br>110-540 | < 1.0<br>< 1.5 | 0.1 | 3 |

SMALL RECEIVER TANK OUTER WALL TEMPERATURE MEASUREMENTS

| MEAS | NUM | DESCRIPTION | RANGE Deg (R) | ACCURACY ± Deg (R) | SAMPLE RATE (Hz) | PRI. EXP. |
|---|---|---|---|---|---|---|
| SRTa | 101 | Top axial spray line temp. at tank wall | 36-110<br>110-540 | < 1.0<br>< 1.5 | 0.1 | 3 |

| MEAS | NUM | DESCRIPTION | RANGE Deg (R) | ACCURACY ± Deg (R) | SAMPLE RATE (Hz) | PRI. EXP. |
|---|---|---|---|---|---|---|
| SRTa | 102 | Radial spray line temp. at tank wall | 36-110<br>110-540 | < 1.0<br>< 1.5 | 0.1 | 3 |
| SRTa | 103 | Tangential spray line temp. at tank wall | 36-110<br>110-540 | < 1.0<br>< 1.5 | 0.1 | 3 |
| SRTa | 104 | Vent line temp. at outer tank wall | 36-110<br>110-540 | < 1.0<br>< 1.5 | 0.1 | 3 |
| SRTa | 105 | Pressurization line temperature | 36-110<br>110-540 | < 1.0<br>< 1.5 | 0.1 | 3 |
| SRTa | 106 | TVS line temperature downstream of JT device | 29 - 46 | < 0.2 | 0.1 | 3 |
| SRTa | 107 | TVS line temperature 50% length | 29 - 46 | < 0.2 | 0.1 | 3 |
| SRTa | 108 | TVS line temperature 100% length | 29 - 46 | < 0.2 | 0.1 | 3 |
| SRTa | 109 | Top dome, quadrant 1 temperature | 36-110<br>110-540 | < 1.0<br>< 1.5 | 0.1 | 3 |
| SRTa | 110 | Top dome, quadrant 2 temperature | 36-110<br>110-540 | < 1.0<br>< 1.5 | 0.1 | 3 |
| SRTa | 111 | Top dome, quadrant 3 temperature | 36-110<br>110-540 | < 1.0<br>< 1.5 | 0.1 | 3 |
| SRTa | 112 | Aft dome, quadrant 4 temperature | 36-110<br>110-540 | < 1.0<br>< 1.5 | 0.1 | 3 |
| SRTa | 113 | Aft dome, quadrant 5 temperature | 36-110<br>110-540 | < 1.0<br>< 1.5 | 0.1 | 3 |
| SRTa | 114 | Aft dome, quadrant 6 temperature | 36-110<br>110-540 | < 1.0<br>< 1.5 | 0.1 | 3 |
| SRTa | 115 | Tangential spray are tank temperature | 36-110<br>110-540 | < 1.0<br>< 1.5 | 0.1 | 3 |
| SRTa | 116 | Tangential spray are tank temperature | 36-110<br>110-540 | < 1.0<br>< 1.5 | 0.1 | 3 |
| SRTa | 117 | Barrel Section 90 de from spary | 36-110<br>110-540 | < 1.0<br>< 1.5 | 0.1 | 3 |
| SRTa | 118 | Barrel Section 90 de from spary | 36-110<br>110-540 | < 1.0<br>< 1.5 | 0.1 | 3 |
| SRTa | 119 | Warm side harness temperature at tank | 36-110<br>110-540 | < 1.0<br>< 1.5 | 0.1 | 3 |
| SRTa | 120 | Cold side harness temperature at tank | 36-110<br>110-540 | < 1.0<br>< 1.5 | 0.1 | 3 |
| SRTa | 121 | Warm side strut temperature at tank | 36-110<br>110-540 | < 1.0<br>< 1.5 | 0.1 | 3 |

| MEAS | NUM | DESCRIPTION | RANGE Deg (R) | ACCURACY ± Deg (R) | SAMPLE RATE (Hz) | PRI. EXP. |
|---|---|---|---|---|---|---|
| SRTa | 122 | Cold side strut temperature at tank | 36-110<br>110-540 | < 1.0<br>< 1.5 | 0.1 | 3 |
| SRTa | 201 | LH2 Transfer line temp. at panel M | 36-110<br>110-540 | < 1.0<br>< 1.5 | 0.1 | 3 |
| SRTa | 202 | Lower axial spray line temp. at valve panel M | 36-110<br>110-540 | < 1.0<br>< 1.5 | 0.1 | 3 |
| SRTa | 203 | Radial spray line temperature at panel M | 36-110<br>110-540 | < 1.0<br>< 1.5 | 0.1 | 3 |
| SRTa | 204 | Tangential spray line temp. at panel N valve | 36-110<br>110-540 | < 1.0<br>< 1.5 | 0.1 | 3 |
| SRTa | 205 | vent line temperature at valve panel N | 36-110<br>110-540 | < 1.0<br>< 1.5 | 0.1 | 3 |
| SRTa | 206 | Pressurization line temperature at panel N | 36-110<br>110-540 | < 1.0<br>< 1.5 | 0.1 | 3 |
| SRTb | 207 | Top dome, honeycomb quadrant 1 | 117-135 | < 1.5 | 0.1 | 3 |
| SRTb | 208 | Top dome, honeycomb quadrant 2 | 117-135 | < 1.5 | 0.1 | 3 |
| SRTb | 209 | Top dome, honeycomb quadrant 3 | 117-135 | < 1.5 | 0.1 | 3 |
| SRTb | 210 | Aft dome, honeycomb quadrant 4 | 117-135 | < 1.5 | 0.1 | 3 |
| SRTb | 211 | Aft dome, honeycomb quadrant 5 | 117-135 | < 1.5 | 0.1 | 3 |
| SRTb | 212 | Aft dome, honeycomb quadrant 6 | 117-135 | < 1.5 | 0.1 | 3 |
| SRTb | 213 | Honeycomb barrel temperature +y | 117-135 | < 1.5 | 0.1 | 3 |
| SRTb | 214 | Honeycomb barrel temperature -y | 117-135 | < 1.5 | 0.1 | 3 |
| SRTb | 215 | Honeycomb barrel temperature +z | 117-135 | < 1.5 | 0.1 | 3 |
| SRTb | 216 | Honeycomb barrel temperature +z | 117-135 | < 1.5 | 0.1 | 3 |
| SRTb | 217 | Warm side harness temperature at IMLI | 117-135 | < 1.5 | 0.1 | 3 |
| SRTb | 218 | Cold side harness temperature at IMLI | 117-135 | < 1.5 | 0.1 | 3 |
| SRTb | 219 | Warm side strut temperature at IMLI | 117-135 | < 1.5 | 0.1 | 3 |

| MEAS | NUM | DESCRIPTION | RANGE Deg (R) | ACCURACY ± Deg (R) | SAMPLE RATE (Hz) | PRI. EXP. |
|---|---|---|---|---|---|---|
| SRTb | 220 | Cold side strut temperature at IMLI | 117-135 | < 1.5 | 0.1 | 3 |
| SRTa | 301 | Dump vent line temperature | 36-110<br>110-540 | < 1.0<br>< 1.5 | 0.1 | 3 |
| SRTb | 302 | Top dome, outer MLI quadrant 1 | 235-525 | < 1.5 | 0.1 | 3 |
| SRTb | 303 | Top dome, outer MLI quadrant 2 | 235-525 | < 1.5 | 0.1 | 3 |
| SRTb | 304 | Aft doem, outer MLI quadrant 4 | 235-525 | < 1.5 | 0.1 | 3 |
| SRTb | 305 | Aft doem, outer MLI quadrant 5 | 235-525 | < 1.5 | 0.1 | 3 |
| SRTb | 306 | Outer MLI barrel temperature | 235-525 | < 1.5 | 0.1 | 3 |
| SRTb | 307 | Outer MLI barrel temperature | 235-525 | < 1.5 | 0.1 | 3 |
| SRTb | 309 | Outer MLI barrel temperature | 235-525 | < 1.5 | 0.1 | 3 |
| SRTb | 310 | Sm. Rec TVs flow meter inlet temperature | 235-525 | < 1.5 | 0.1 | 3 |

SMALL RECEIVER TANK MODULE LIQUID VAPOR POINT MEASUREMENTS

| MEAS | NUM | DESCRIPTION | RESPONSE Deg (R) | SAMPLE FREQ. (Hz) | PRI. EXP. |
|---|---|---|---|---|---|
| SRL | 1 | Radial Spray Rake 95.5% level | LIQ/VAP | 0.1 | 2 |
| SRL | 2 | Rake H-1, -8.2 inch from center | LIQ/VAP | 0.1 | 2 |
| SRL | 3 | Rake H-1, -4.1 inch from center | LIQ/VAP | 0.1 | 2 |
| SRL | 4 | Rake H-1, center | LIQ/VAP | 0.1 | 2 |
| SRL | 5 | Rake H-1, 8.2 inch from center | LIQ/VAP | 0.1 | 2 |
| SRL | 6 | Rake H-1, 4.1 inch from center | LIQ/VAP | 0.1 | 2 |
| SRL | 7 | Radial Spray Rake 92.5% level | LIQ/VAP | 0.1 | 2 |
| SRL | 8 | Rake V-1, 90%level | LIQ/VAP | 0.1 | 2 |
| SRL | 9 | Radial bar, 88% | LIQ/VAP | 0.1 | 2 |
| SRL | 10 | Rake V-2, 86% level | LIQ/VAP | 0.1 | 2 |

| MEAS | NUM | DESCRIPTION | RESPONSE Deg (R) | SAMPLE FREQ. (Hz) | PRI. EXP. |
|---|---|---|---|---|---|
| SRL | 11 | Rake V-1, 84% level | LIQ/VAP | 0.1 | 2 |
| SRL | 12 | Radial bar, 82% | LIQ/VAP | 0.1 | 2 |
| SRL | 13 | Rake V-2, 80% level | LIQ/VAP | 0.1 | 2 |
| SRL | 14 | Rake V-1, 78% level | LIQ/VAP | 0.1 | 2 |
| SRL | 15 | Radial bar, 76% | LIQ/VAP | 0.1 | 2 |
| SRL | 16 | Rake V-2, 74% level | LIQ/VAP | 0.1 | 2 |
| SRL | 17 | Rake V-1, 72% level | LIQ/VAP | 0.1 | 2 |
| SRL | 18 | Radial bar, 70% | LIQ/VAP | 0.1 | 2 |
| SRL | 19 | Rake V-1, 65% level | LIQ/VAP | 0.1 | 2 |
| SRL | 20 | Radial bar, 60% | LIQ/VAP | 0.1 | 2 |
| SRL | 21 | Rake V-2, 55% level | LIQ/VAP | 0.1 | 2 |
| SRL | 22 | Tangential Rake -13.3 in from center | LIQ/VAP | 0.1 | 2 |
| SRL | 23 | Tangential Rake -9.7 in from center | LIQ/VAP | 0.1 | 2 |
| SRL | 24 | Tangential Rake center | LIQ/VAP | 0.1 | 2 |
| SRL | 25 | Tangential Rake 13.3 in from center | LIQ/VAP | 0.1 | 2 |
| SRL | 26 | Tangential Rake 9.7 in from center | LIQ/VAP | 0.1 | 2 |
| SRL | 27 | Rake V-1, 45% level | LIQ/VAP | 0.1 | 2 |
| SRL | 28 | Radial bar, 40% | LIQ/VAP | 0.1 | 2 |
| SRL | 29 | Rake, V-2, 35% level | LIQ/VAP | 0.1 | 2 |
| SRL | 30 | Rake V-1, 30% level | LIQ/VAP | 0.1 | 2 |
| SRL | 31 | Radial bar, 25% | LIQ/VAP | 0.1 | 2 |
| SRL | 32 | Rake V-2, 20% level | LIQ/VAP | 0.1 | 2 |
| SRL | 33 | Rake V-1, 15% level | LIQ/VAP | 0.1 | 2 |
| SRL | 34 | Rake V-2, 10% level | LIQ/VAP | 0.1 | 2 |
| SRL | 35 | Rake H-2, -8.2 inch from center | LIQ/VAP | 0.1 | 2 |
| SRL | 36 | Rake H-2, -4.1 inch from center | LIQ/VAP | 0.1 | 2 |
| SRL | 37 | Rake H-2, center | LIQ/VAP | 0.1 | 2 |

| MEAS | NUM | DESCRIPTION | RESPONSE Deg (R) | | SAMPLE FREQ. (Hz) | PRI. EXP. |
|---|---|---|---|---|---|---|
| SRL | 38 | Rake H-2, 8.2 inch from center | LIQ/VAP | | 0.1 | 2 |
| SRL | 39 | Rake H-2, 4.1 inch from center | LIQ/VAP | | 0.1 | 2 |
| SRL | 40 | Vent eixt line | LIQ/VAP | | 0.1 | 2 |

SMALL RECEIVER MODULE PRESSURE MEASUREMNTS

| MEAS | NUM | DESCRIPTION | RANGE PSIA | ACCURACY +/- PSIA | SAMPLE RATE (HZ) | MEAS TYPE |
|---|---|---|---|---|---|---|
| SRP | 1 | Sm Rec pressurization line pressure | 50 | 0.23 | 0.1 | Control EDU |
| SRP | 2 | Sm. Rec vent line pressure | 50 | 0.23 | 0.1 | Control EDU |
| SRP | 3 | Sm Rec dump vent line pressure | 50 | 0.23 | 0.1 | Control EDU |
| SRP | 4 | LH2 transfer line pressure | 50 | 0.37 | 0.1 | Data |
| SRP | 5 | axial spray line pressure | 50 | 0.37 | 0.1 | Data |
| SRP | 6 | radial spray line pressure | 50 | 0.37 | 0.1 | Data |
| SRP | 7 | Tangential spray line pressure | 50 | 0.37 | 0.1 | Data |
| SRP | 8 | Pressure downstream of JT device | 50 | 0.37 | 0.1 | Data |
| SRP | 9 | Sm Rec TVS flow line pressure | 25 | 0.18 | 0.1 | Data |

COLD-SAT EXPERIMENT SUBSYSTEM ACCELERATION MEASUREMENTS

| MEAS | NUM | DESCRIPTION | RANGE (MICRO-G) | ACCURACY RATE (Hz) | SAMPLE | PRI EXP |
|---|---|---|---|---|---|---|
| SA | 1 | X-axis acceleration | 1-100 | TBD | 10 | 3 |
| SA | 2 | Y-axis acceleration | 1-100 | TBD | 10 | 3 |
| SA | 3 | Z-axis acceleraiton | 1-100 | TBD | 10 | 3 |

COLD-SAT EXPERIMENT SUBSYSTEM POWER (W) MEASUREMENTS

| MEAS | NUM | DESCRIPTION | RANGE WATTS | ACCURACY | SAMPLE RATE (Hz) | PRI. EXP. |
|---|---|---|---|---|---|---|
| W | 1 | Supply tank heater power | 8-21 | TBD | 1 | 1 |

| MEAS | NUM | DESCRIPTION | RANGE WATTS | ACCURACY | SAMPLE RATE (Hz) | PRI. EXP. |
|---|---|---|---|---|---|---|
| W | 2 | Vaporizer A | 100 | TBD | 1 | Eng |
| W | 3 | Vaporizer B | 100 | TBD | 1 | Eng |
| W | 4 | Large receiver heater power | 50 | TBD | 1 | 3 |
| W | 5 | Small reciever heater power | 50 | TBD | 1 | 3 |
| W | 6 | Flight vent | 7 | TBD | 1 | 3 |
| W | 7 | TVS vent | 7 | TBD | 1 | 1 |
| W | 8 | Vaporizer panel A | 6 | TBD | 1 | Eng |
| W | 9 | Vaporizer panel B | 6 | TBD | 1 | Eng |
| W | 10 | Connector panel A | 2 | TBD | 1 | Eng |
| W | 11 | Connector panel B | 2 | TBD | 1 | Eng |

COLD-SAT EXPERIMENTAL SUBSYSTEM FLOW MEASUREMENTS

| MEAS | NUM | DESCRIPTION | RANGE (LBM/HR) | INACCURACY FREQ. | SAMPLE | PRI EXP |
|---|---|---|---|---|---|---|
| F | 1 | LH2 transfer flow from supply tank | 50-350 | 0.5% read | TBD | 3 |
| F | 2 | LH2 low flow rate | 15-50 | 0.5% span | TBD | 3 |
| F | 3 | LH2 medium flow rate | 30-100 | 0.5% span | TBD | 3 |
| F | 4 | LH2 high flow rate | 60-200 | 0.5% span | TBD | 3 |
| F | 5 | Supply tank passive TVS flow rate | 0.16 | 1.0% span | TBD | 1 |
| F | 6 | Supply tank active TVS flow rate | 5.6 | 1.0% span | TBD | 1 |
| F | 7 | Lg. Rec. tank passive TVS flow rate | 0.21 | 1.0% span | TBD | 3 |
| F | 8 | Sm. Rec. tank passive TVS flow rate | 0.15 | 1.0% span | TBD | 3 |
| F | 9 | Pressurant flow rate | 1-10 | 1.0% span | TBD | 3 |
| F | 10 | LH2 transfer flow between receivers | 60-200 | 0.5% span | TBD | 3 |
| F | 11 | Flight balanced Vent flow rate | TBD | TBD | TBD | 8 |

TABLE 1.— EXPERIMENT ELECTRICAL AND ELECTRONICS BOX DEFINITION

| Type of measurement unit | Number of units required | Electronics bay location | Unit weight, lb | Unit power, W |
|---|---|---|---|---|
| Experimental data | 3 | 2 | 7 | 15 |
| Accelerometer data | 1 | 2 | 6 | 10 |
| Mixer motor power | 1 | 2 | 7.5 | 15 |
| Capacitive probe signal conditioning power | 1 | 2 | 12 | 15 |

TABLE 2.—8-BIT DATA ACQUISITION SYSTEM VOLTAGE MEASUREMENT UNCERTAINTY ESTIMATES

| Voltage range, mV | Uncertainty, mV | rss uncertainty, percent |
|---|---|---|
| 0-10 | ±0.18 | 1.80 |
| 0-30 | ±.20 | .67 |
| 0-125 | ±.45 | .36 |
| 0-1250 | ±3.34 | .27 |

TABLE 3.—COLD-SAT EXPERIMENT SUBSYSTEM MEASUREMENT REQUIREMENT SUMMARY

| Measurement requirement | Measurement range | Transistor type | Measurement error | Resolution, bit | Sample frequency, Hz | Number required |
|---|---|---|---|---|---|---|
| High-accuracy fluid temperature | 30.0–50.0 °R | Type A PRT | ≤±0.2 R | 8 | 0.1 | 90 |
| Structure temperature | 30.0–50.0 °R | Type A PRT | ≤±0.2 R | 8 | 0.1 | 49 |
| Structure temperatures | 36.0–540 °R | Type AB PRT | ≤±2.0 R | 8 | 0.1 | 162 |
| Hydrogen liquid/vapor level detection | Tank volume | Thermistor | ±1.0 percent | 1 | 0.1 | 106 |
| Two-phase flow detection | Liquid to vapor | Thermistor | NA | 1 | 0.1 | 10 |
| High resolution tank pressures | 0–50 psia | Cryogenic strain gauge | ±0.23 psia | 12 | 0.1 | 9 |
| Plumbing system pessures | 0–5000 psia | Cryogenic strain gauge | ±1.0% | 8 | 0.1 | 33 |
| LH2 Transfer Flow Rates | 50, 100, 200 lbm/hr | Venturi/ΔP | <±2.0% | 12 | 0.1 | 4 |
| Mixer flow rates | TBD | rpm | TBD | 12 | 0.1 | 2 |
| TVS flow rates: | lbm/hr | Turbine meters | <±5.0% | | | |
| Supply tank | 0.16–5.6 | | | 12 | 0.1 | 2 |
| Large receiver | 0.21 | | | 12 | .1 | 1 |
| Small receiver | 0.15 | | | 12 | .1 | 1 |
| Vent flow rates | 5–50 lbm/hr | Sonic flow nozzle | <±5.0% | 8 | 10 | 3 |
| Acceleration | ≤ 100 μg | Accelerometer | TBD | 12 | 10 | 3 |
| Valve status | Open/close | Switch | N/A | 1 | 0.1 | 61 |

TABLE 4.—TEMPERATURE SENSOR CANDIDATE REQUIREMENTS AND ERRORS

| Sensor type | Temperature range, °R | Excitation level, mA | Excitation error, percent | Sensor output, mV | Total 8-bit measurement error, mV |
|---|---|---|---|---|---|
| GRT | 20–50 | (a) | ±0.1 | ≤10 | 0.18 |
| PRT $R_o$ = 1000 | 29–47 | 10 | ±0.1 | 33–125 | 0.45 |
| | 29–540 | 1.0 | ±0.1<br>.11 | 3.3–125<br>125–1250 | 0.45<br>3.3 |
| Silicon diode | 20–540 | 0.01 | ±0.1 | 1300–520 | 3.3 |

[a]Variable.

TABLE 5.—ERROR ANALYSIS FOR 1000-OHM PLATINUM RESISTANCE THERMOMETER IN 8-BIT DATA ACQUITISION SYSTEM

[DAS error, ±0.45 mV; excitation current, 10 mA.]

| Temperature, °R | Resistance, Ω | Sensivity of resistance to temperature, ΔΩ/Δ°R | Sensitivity of temperature to voltage, °R/mV | Temperature error °R | Error, percent |
|---|---|---|---|---|---|
| 29.07 | 3.39 | 0.23 | 0.43 | ±0.20 | ±0.68 |
| 3.87 | 3.84 | .27 | .37 | ±.17 | ±.54 |
| 32.67 | 4.37 | .32 | .31 | ±.14 | ±.44 |
| 34.47 | 4.99 | .37 | .27 | ±.12 | ±.36 |
| 36.27 | 5.70 | .42 | .24 | ±.11 | ±.30 |
| 38.07 | 6.51 | .48 | .21 | ±.10 | ±.25 |
| 39.87 | 7.42 | .54 | .19 | ±.08 | ±.21 |
| 41.67 | 8.45 | .73 | .14 | ±.06 | ±.15 |
| 50.67 | 15.33 | .93 | .11 | ±.05 | ±.10 |

TABLE 6.—8-BIT DATA ACQUISITION SYSTEM INACCURACY INFLUENCE ON GRT TEMPERATURE MEASUREMENT ERROR

[Voltage measurement error, ±0.18 mV.]

| Temperature, °R | Resistance, Ω | Sensitivity of resistance to temperature, Ω/°R | Current, mA | Sensitivity of temperature to voltage, °R/mV | Temperature error, percent | Error, percent |
|---|---|---|---|---|---|---|
| 18 | 149.16 | −21.89 | 0.067 | 0.681 | ±0.1 | ±0.67 |
| 36 | 23.57 | −1.58 | .424 | 1.490 | ±.27 | ±.75 |
| 54 | 9.46 | −.36 | 1.058 | 2.647 | ±.48 | ±.89 |
| 72 | 5.44 | −.13 | 1.839 | 4.130 | ±.74 | ±1.0 |
| 180 | 1.695 | −.007 | 5.900 | 25.45 | ±4.6 | ±2.6 |

TABLE 7.—UNCERTAINTY IN SATURATION TEMPERATURE DUE TO PRESSURE MEASUREMENT UNCERTAINTY (*UP*)

[Uncertainty in saturation pressure, *UP*, ±0.23 psi.]

| Temperature, °R | Pressure, psia | Sensitivity of temperature to pressure, $\delta T/\delta P$, °R/psi | Uncertainty in saturation temperature, *UT*, °R |
|---|---|---|---|
| 30.806 | 5 | 0.7836 | ±0.18 |
| 36.608 | 15 | .4231 | ±0.10 |
| 41.299 | 30 | .2431 | ±0.06 |
| 45.406 | 50 | .1385 | ±0.03 |

TABLE 8.—FLIGHT QUALIFIED CRYOGENIC PRESSURE SENSOR CANDIDATE SPECIFICATIONS

| | |
|---|---|
| Transducer type | Cryogenic strain gauge |
| Temperature range, °R | 36–186 |
| Full scale inaccuracy, percent | ±0.25 |
| Thermal zero shift, percent of FS/°R | ±0.015 |
| Thermal span shift, percent/°R | ±0.005 |
| Natural frequency (at 15 psi), kHz | 3 |

Table 9.—PRESSURE MEASUREMENT INACCURACY AND RESOLUTION VALUES

| Full scale pressure, psia | 8-bit system error, psia | 8-bit resolution, psi | 12-bit system error, psia | 12-bit resolution, psi |
|---|---|---|---|---|
| 15 | ±0.11 | 0.06 | ±0.07 | 0.004 |
| 25 | ±.18 | .10 | ±.11 | .006 |
| 30 | ±.21 | .12 | ±.13 | .007 |
| 50 | ±.36 | .20 | ±.23 | .012 |

TABLE 10.—LIQUID HYDROGEN FLOW MEASUREMENT ERROR ANALYSIS

[Calibration, ±0.5 percent; density, ±0.2 percent.]

(a) Orifice differential pressure

| Flow range, percent | $\Delta P$ error, percent | EDU error, percent | Mass flow rate rss error, percent |
|---|---|---|---|
| 100 | ±0.25 | ±0.20 | ±0.63 |
| 90 | ±.31 | ±.25 | ±.67 |
| 80 | ±.39 | ±.31 | ±.74 |
| 70 | ±.51 | ±.41 | ±.85 |
| 60 | ±.69 | ±.56 | ±1.04 |
| 50 | ±1.00 | ±.80 | ±1.39 |
| 40 | ±1.56 | ±1.25 | ±2.07 |

(b) Turbine flowmeter

| Flow range, percent | EDU error, percent | Mass flow rate rss error, percent |
|---|---|---|
| 100 | ±0.40 | ±0.67 |
| 90 | ±.44 | ±.72 |
| 80 | ±.50 | ±.74 |
| 70 | ±.57 | ±.79 |
| 60 | ±.67 | ±.85 |
| 50 | .80 | ±.96 |
| 40 | ±1.00 | ±1.16 |

TABLE 11.–THERMODYNAMIC VENT SYSTEM (TVS) FLOW RATE RANGE AND TURBINE METER SIZING

| Location | TVS type | Mass flow rate, lb/hr | Meter inlet temperature and pressure | | Turbine meter diameter required, in. | Flow range, $ft^3$/hr |
|---|---|---|---|---|---|---|
| | | | 180 °R, 20 psia | 360 °R, 5 psia | | |
| | | | Equivalent volume flow rate, $ft^3$/min | | | |
| Small receiver | Passive | 0.15 | 0.12 | 0.96 | 0.5 | 0.1–1.0 |
| Large receiver | Passive | .21 | .17 | 1.34 | .5 | 0.25–2.5 |
| Supply tank | Passive | .16 | .13 | 1.02 | .5 | 0.1–1.0 |
| Supply tank | Active | 5.6 | 4.47 | 35.84 | 1.0 | 5–50 |

TABLE 12.–TVS FLOW MEASUREMENT ERROR ANALYSIS

| Meter range, percent | Turbine inaccuracy, percent | EDU error, percent | Density error, percent | Mass flow rate rss error, percent |
|---|---|---|---|---|
| 100 | ±1.05 | ±0.4 | ±3.66 | ±3.83 |
| 50 | ±2.10 | ±0.8 | ±3.66 | ±4.29 |

TABLE 13.–TEMPERATURE INFLUENCE ON NOZZLE DIAMETER

| Temperature °R | Density, lb/$ft^3$ | Velocity, $V_s$, ft/sec | Area, in.$^2$ | Diameter, in. | Volume flow rate, $ft^3$/min |
|---|---|---|---|---|---|
| 50 | 0.222 | 1334 | $6.75\times10^{-3}$ | 0.093 | 3.75 |
| 140 | .0675 | 2320 | $1.28\times10^{-2}$ | .128 | 12.37 |
| 240 | .0391 | 2842 | $1.80\times10^{-2}$ | .151 | 21.32 |
| 340 | .0276 | 3363 | $2.16\times10^{-2}$ | .166 | 30.2 |
| 440 | .0213 | 3860 | $2.43\times10^{-2}$ | .176 | 39.13 |

TABLE 14.—LARGE RECEIVER ESTIMATED VENT TIMES

| Temperature °R | Mass, lb, at — | | Mass difference, lb | Vent time, sec |
|---|---|---|---|---|
| | 30 psia | 35 psia | | |
| 440 | 0.267 | 0.222 | 0.045 | 8 |
| 340 | .345 | .288 | .057 | 9 |
| 240 | .489 | .408 | .081 | 11 |
| 140 | .838 | .698 | .140 | 13 |

TABLE 15.—VENT FLOW RATE MEASUREMENT ERROR ANALYSIS RESULTS

| Temperature, °R | Pressure error, percent, at— | | | | |
|---|---|---|---|---|---|
| | 50 psia | 35 psia | 25 psia | 15 psia | 5 psia |
| 140 | ±1.01 | ±1.12 | ±1.24 | ±1.78 | ±4.70 |
| 440 | ±.90 | ±1.01 | ±1.20 | ±1.71 | ±4.67 |

TABLE 16.—SUPPLY MODULE INSTRUMENTATION LISTING

| Sensor location | Sensor type | | | | | | | | |
|---|---|---|---|---|---|---|---|---|---|
| | Temperature sensors | Liquid-vapor sensors | Pressure sensors | Differential pressure venturi | Turbine meters | Cryogen valve discretes | Gas valve discretes | Speed sensors | Capacitance probe |
| Inside pressure vessel | 54 | 34 | 0 | 0 | 0 | 0 | 0 | 0 | 1 |
| Liquid acquisition device | 10 | 2 | 0 | 0 | 0 | 0 | 0 | 0 | 0 |
| Outer tank wall | 10 | 0 | 0 | 0 | 0 | 0 | 0 | 0 | 0 |
| Tank wall plumbing | 5 | 0 | 0 | 0 | 0 | 0 | 0 | 0 | 0 |
| Tank wall struts | 2 | 0 | 0 | 0 | 0 | 0 | 0 | 0 | 0 |
| Tank wall harnesses | 2 | 0 | 0 | 0 | 0 | 0 | 0 | 0 | 0 |
| Panel E inside MLI | 1 | 0 | 1 | 0 | 0 | 2 | 0 | 0 | 0 |
| Panel F inside MLI | 2 | 0 | 2 | 0 | 0 | 3 | 0 | 2 | 0 |
| Panel G inside MLI | 1 | 0 | 2 | 0 | 0 | 2 | 0 | 0 | 0 |
| Panel H inside MLI | 3 | 0 | 2 | 0 | 0 | 3 | 0 | 0 | 0 |
| Panel I inside MLI | 2 | 0 | 1 | 4 | 0 | 3 | 0 | 0 | 0 |
| Panel J inside MLI | 2 | 0 | 3 | 0 | 1 | 5 | 0 | 0 | 0 |
| Struts inside MLI | 2 | 0 | 0 | 0 | 0 | 0 | 0 | 0 | 0 |
| Harnesses inside MLI | 2 | 0 | 0 | 0 | 0 | 0 | 0 | 0 | 0 |
| Honeycomb wall | 10 | 0 | 0 | 0 | 0 | 0 | 0 | 0 | 0 |
| Outside MLI can | 10 | 0 | 0 | 0 | 0 | 0 | 0 | 0 | 0 |
| Tray | 1 | 0 | 1 | 0 | 1 | 4 | 0 | 0 | 0 |
| Hydrogen vaporizers | 10 | 0 | 7 | 0 | 0 | 4 | 8 | 0 | 0 |
| Helium tanks | 5 | 0 | 3 | 0 | 1 | 0 | 4 | 0 | 0 |
| Vent panel O | 2 | 0 | 2 | 0 | 1 | 0 | 0 | 0 | 0 |
| Accelerometer | 3 | 0 | 0 | 0 | 0 | 0 | 0 | 0 | 0 |
| Total: | 139 | 36 | 24 | 4 | 4 | 26 | 12 | 2 | 1 |

TABLE 17 - LARGE RECEIVER MODULE INSTRUMENTATION LISTING

| Location | Sensor type | | | | | |
|---|---|---|---|---|---|---|
| | Temper-ature sensors | Liquid-vapor sensors | Pressure sensors | Differ-ential pressure venturi | Turbine meters | Cryogen valve discretes |
| Inside Pressure vessel | 22 | 32 | 0 | 0 | 0 | 0 |
| Liquid acquisition devise | 14 | 8 | 0 | 0 | 0 | 0 |
| Outer tank wall | 10 | 0 | 0 | 0 | 0 | 0 |
| Tank wall plumbing & TVS | 9 | 0 | 0 | 0 | 0 | 0 |
| Tank wall struts | 2 | 0 | 0 | 0 | 0 | 0 |
| Tank wall harnesses | 2 | 0 | 0 | 0 | 0 | 0 |
| Panel K inside MLI | 3 | 0 | 3 | 0 | 0 | 3 |
| Panel L inside MLI | 4 | 0 | 5 | 0 | 1 | 4 |
| Struts inside MLI | 2 | 0 | 0 | 0 | 0 | 0 |
| Harnesses inside MLI | 2 | 0 | 0 | 0 | 0 | 0 |
| Honeycomb wall | 8 | 0 | 0 | 0 | 0 | 0 |
| Outside MLI wall | 6 | 0 | 0 | 0 | 0 | 0 |
| Tray | 2 | 0 | 1 | 2 | 0 | 2 |
| Total: | 86 | 40 | 9 | 2 | 1 | 9 |

TABLE 18.—SMALL RECEIVER MODULE INSTRUMENTATION LISTING

| Location | Sensor type | | | | | |
|---|---|---|---|---|---|---|
| | Temper-ature sensors | Liquid-vapor sensors | Pres-sure sensors | Differ-ential pressure venturi | Turbine meters | Cryogen valve discretes |
| Inside pressure vessel | 24 | 40 | 0 | 0 | 0 | 0 |
| Outer tank wall | 10 | 8 | 0 | 0 | 0 | 0 |
| Tank wall plumbing & TVS | 8 | 0 | 0 | 0 | 0 | 0 |
| Tank wall struts | 2 | 0 | 0 | 0 | 0 | 0 |
| Tank wall harnesses | 2 | 0 | 0 | 0 | 0 | 0 |
| Panel M inside MLI | 3 | 0 | 4 | 0 | 0 | 4 |
| Panel N inside MLI | 3 | 0 | 4 | 0 | 1 | 4 |
| Struts inside MLI | 2 | 0 | 0 | 0 | 0 | 0 |
| Harnesses inside MLI | 2 | 0 | 0 | 0 | 0 | 0 |
| Honeycomb wall | 10 | 0 | 0 | 0 | 0 | 0 |
| Outside MLI wall | 8 | 0 | 0 | 0 | 0 | 0 |
| Tray | 2 | 0 | 1 | 0 | 0 | 2 |
| Total: | 86 | 40 | 9 | 2 | 1 | 9 |

TABLE 19.—ESTIMATED WIRE HARNESS WEIGHT

| Wire size | Conductor | Insulation material | Wire diameter, in. | Estimated weight, lb/1000 ft |
|---|---|---|---|---|
| 24 AWG | Manganin | Polyimide | 0.037 | 2.0 |
| 18 AWG | Phosphor-bronze | Polyimide | .062 | 6.6 |

TABLE 20.— ESTIMATED WIRE BUNDLE SIZE

| Wire size | Conductor material | Number of wires | Estimated bundle diameter, in. |
|---|---|---|---|
| 24 AWG | Manganin | 45<br>50<br>55 | 0.284<br>.299<br>.313 |
| 18 AWG | Phosphor-bronze | 40<br>35<br>45 | 0.451<br>.422<br>.477 |

TABLE 21.—COLD-SAT EXPERIMENT SUBSYSTEM WIRING SUMMARY

| Module | Number of instrumentation wires | | Number of power wires | | Total wires |
|---|---|---|---|---|---|
| | 24-AWG manganin | 24-AWG copper | 18-AWG phorphor-bronze | 24-AWG copper | |
| Supply module | 547 | 188 | 66 | 160 | 963 |
| Large receiver module | 391 | 0 | 40 | 0 | 431 |
| Small receiver module | 370 | 0 | 44 | 0 | 414 |
| Total: | 1308 | 188 | 152 | 160 | 1808 |

TABLE 22.—SUPPLY MODULE INSTRUMENTATION WIRE ALLOCATION

| Location | Sensor or hardware type | | | | | | | | | |
|---|---|---|---|---|---|---|---|---|---|---|
| | Temperature wires | Liquid-vapor wires | Pressure wires | Differential pressure wires | Turbine wires | Cryogen valve wires | Gas valve wires | Speed sensor wires | Capacitance probe | Total wires |
| Inside pressure vessel | 164 | 21 | 0 | 0 | 0 | 0 | 0 | 0 | 4 | 189 |
| Outer tank wall | 40 | 0 | 0 | 0 | 0 | 0 | 0 | 0 | 0 | 40 |
| Tank wall plumbing | 20 | 0 | 0 | 0 | 0 | 0 | 0 | 0 | 0 | 20 |
| Tank wall struts | 8 | 0 | 0 | 0 | 0 | 0 | 0 | 0 | 0 | 8 |
| Tank wall harnesses | 8 | 0 | 0 | 0 | 0 | 0 | 0 | 0 | 0 | 8 |
| Panel E inside MLI | 4 | 0 | 4 | 0 | 0 | 6 | 0 | 0 | 0 | 14 |
| Panel F inside MLI | 8 | 0 | 8 | 0 | 0 | 9 | 0 | 4 | 0 | 29 |
| Panel G inside MLI | 4 | 0 | 8 | 0 | 0 | 6 | 0 | 0 | 0 | 18 |
| Panel H inside MLI | 12 | 0 | 8 | 0 | 0 | 9 | 0 | 0 | 0 | 29 |
| Panel I inside MLI | 8 | 0 | 4 | 16 | 0 | 9 | 0 | 0 | 0 | 37 |
| Panel J inside MLI | 8 | 0 | 12 | 0 | 2 | 15 | 0 | 0 | 0 | 37 |
| Struts inside MLI | 8 | 0 | 0 | 0 | 0 | 0 | 0 | 0 | 0 | 8 |
| Harnesses inside MLI | 8 | 0 | 0 | 0 | 0 | 0 | 0 | 0 | 0 | 8 |
| Honeycomb wall | 40 | 0 | 0 | 0 | 0 | 0 | 0 | 0 | 0 | 40 |
| Outside MLI can | 40 | 0 | 0 | 0 | 0 | 0 | 0 | 0 | 0 | 40 |
| Tray | 4 | 0 | 4 | 0 | 2 | 12 | 0 | 0 | 0 | 22 |
| Hydrogen vaporizers (Cu) | 20 | 0 | 28 | 0 | 0 | 12 | 48 | 0 | 0 | 108 |
| Helium tanks (Cu) | 10 | 0 | 12 | 0 | 2 | 0 | 24 | 0 | 0 | 48 |
| Vent panel O (Cu) | 4 | 0 | 8 | 0 | 2 | 12 | 0 | 0 | 0 | 26 |
| Accelerometer (Cu) | 6 | 0 | 0 | 0 | 0 | 0 | 0 | 0 | 0 | 6 |
| Total: | 424 | 21 | 96 | 16 | 8 | 90 | 72 | 4 | 4 | 735 |

TABLE 23.—LARGE RECEIVER MODULE INSTRUMENTATION WIRE ALLOCATIONS

| Location | Sensor type | | | | | | |
|---|---|---|---|---|---|---|---|
| | Temperature wires | Liquid-vapor wires | Pressure wires | Differential pressure wires | Turbine meters | Cryogen valve wires | Total wires |
| Inside pressure vessel | 96 | 22 | 0 | 0 | 0 | 0 | 118 |
| Outer tank wall | 40 | 0 | 0 | 0 | 0 | 0 | 40 |
| Tank wall plumbing & TVS | 36 | 0 | 0 | 0 | 0 | 0 | 36 |
| Tank wall struts | 8 | 0 | 0 | 0 | 0 | 0 | 8 |
| Tank Wall harnesses | 8 | 0 | 0 | 0 | 0 | 0 | 8 |
| Panel K inside MLI | 12 | 0 | 12 | 0 | 0 | 9 | 33 |
| Panel L inside MLI | 16 | 0 | 20 | 0 | 2 | 12 | 50 |
| Struts inside MLI | 8 | 0 | 0 | 0 | 0 | 0 | 8 |
| Harnesses inside MLI | 8 | 0 | 0 | 0 | 0 | 0 | 8 |
| Honeycomb wall | 32 | 0 | 0 | 0 | 0 | 0 | 32 |
| Outside MLI wall | 24 | 0 | 0 | 0 | 0 | 0 | 24 |
| Tray & flowmeter | 8 | 0 | 4 | 8 | 0 | 6 | 26 |
| Total: | 296 | 22 | 36 | 8 | 2 | 27 | 391 |

TABLE 24.—SMALL RECEIVER MODULE INSTRUMENTATION WIRE ALLOCATION

| Location | Sensor type | | | | | | |
|---|---|---|---|---|---|---|---|
| | Wires | Liquid-vapor wires | Pressure wires | Differential pressure wires | Turbine meters | Cryogen valve wires | Total wires |
| Inside pressure vessel | 72 | 22 | 0 | 0 | 0 | 0 | 94 |
| Outer tank wall | 40 | 0 | 0 | 0 | 0 | 0 | 40 |
| Tank wall plumbing & TVS | 32 | 0 | 0 | 0 | 0 | 0 | 32 |
| Tank wall struts | 8 | 0 | 0 | 0 | 0 | 0 | 8 |
| Tank wall harnesses | 8 | 0 | 0 | 0 | 0 | 0 | 8 |
| Panel M inside MLI | 12 | 0 | 16 | 0 | 0 | 12 | 40 |
| Panel N inside MLI | 12 | 0 | 16 | 0 | 0 | 12 | 40 |
| Struts inside MLI | 8 | 0 | 0 | 0 | 2 | 0 | 10 |
| Harnesses inside MLI | 8 | 0 | 0 | 0 | 0 | 0 | 8 |
| Honeycomb wall | 40 | 0 | 0 | 0 | 0 | 0 | 40 |
| Outside MLI wall | 32 | 0 | 0 | 0 | 0 | 0 | 32 |
| Tray & TVS meter | 8 | 0 | 4 | 0 | 0 | 6 | 18 |
| Total: | 280 | 22 | 36 | 0 | 2 | 30 | 370 |

TABLE 25 COLD-SAT INSTRUMENTATION WIRING SUMMARY

(a) Supply tank

| Wire location | CTU wires | RCTU 1 wires | RCTU 2 wires | EDU 1 | EDU 2 | EDU 3 | Total |
|---|---|---|---|---|---|---|---|
| Penetrating tank | 67 | 70 | 48 | 0 | 0 | 4 | 189 |
| Thermally bonded to tank | 68 | 59 | 79 | 16 | 10 | 8 | 240 |
| Inside MLI | 16 | 16 | 24 | 0 | 0 | 0 | 56 |
| Outside MLI & tray | 19 | 22 | 19 | 2 | 0 | 0 | 62 |
| Total: | 170 | 167 | 170 | 18 | 10 | 12 | 547 |

(b) Large receiver

| Wire location | CTU wires | RCTU 1 wires | RCTU 2 wires | EDU 1 | EDU 2 | EDU 3 | Total |
|---|---|---|---|---|---|---|---|
| Penetrating tank | 48 | 46 | 24 | 0 | 0 | 0 | 118 |
| Thermally bonded to tank | 49 | 42 | 70 | 4 | 4 | 4 | 173 |
| Inside MLI | 16 | 16 | 16 | 0 | 0 | 0 | 48 |
| Outside MLI & tray | 12 | 19 | 11 | 0 | 6 | 4 | 52 |
| Total: | 125 | 123 | 121 | 4 | 10 | 8 | 391 |

(c) Small receiver module

| Wire location | CTU wires | RCTU 1 wires | RCTU 2 wires | EDU 1 | EDU 2 | EDU 3 | Total |
|---|---|---|---|---|---|---|---|
| Penetrating tank | 24 | 24 | 46 | 0 | 0 | 0 | 94 |
| Thermally bonded to tank | 57 | 65 | 38 | 4 | 4 | 6 | 174 |
| Inside MLI | 20 | 20 | 16 | 0 | 0 | 0 | 56 |
| Outside MLI & tray | 12 | 12 | 22 | 0 | 0 | 0 | 46 |
| Total: | 113 | 121 | 122 | 4 | 4 | 6 | 370 |

TABLE 26.—COLD-SAT POWER WIRING SOURCE SUMMARY

| Wire source destination | Supply tank | | Large receiver | | Small receiver | | Total |
|---|---|---|---|---|---|---|---|
| | SEQ 1 wires | SEQ 2 wires | SEQ 1 wires | SEQ 2 wires | SEQ 1 wires | SEQ 2 wires | |
| Thermally bonded to tank (valves) | 36 | 0 | 20 | 8 | 20 | 12 | 96 |
| Thermally bonded to tank (heater) | 4 | 0 | 0 | 4 | 0 | 4 | 12 |
| Outside MLI & tray valves | 16 | 0 | 0 | 8 | 0 | 8 | 32 |
| Total: | 56 | 0 | 20 | 20 | 20 | 24 | 140 |

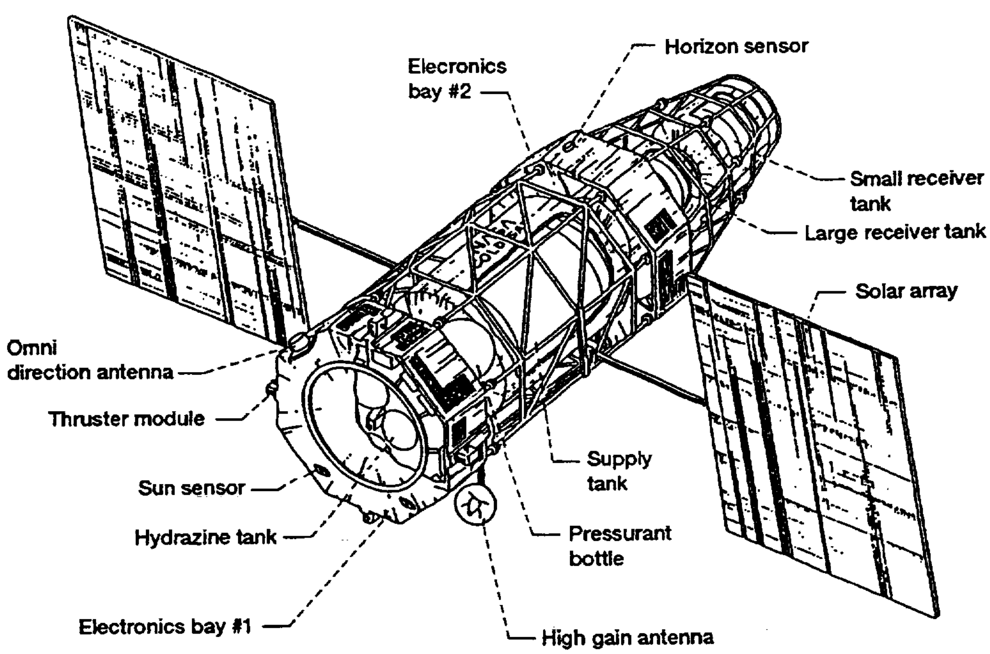


Figure 1.—Cryogenic on-orbit liquid depot-storage, acquisition, transfer (COLD-SAT) spacecraft.

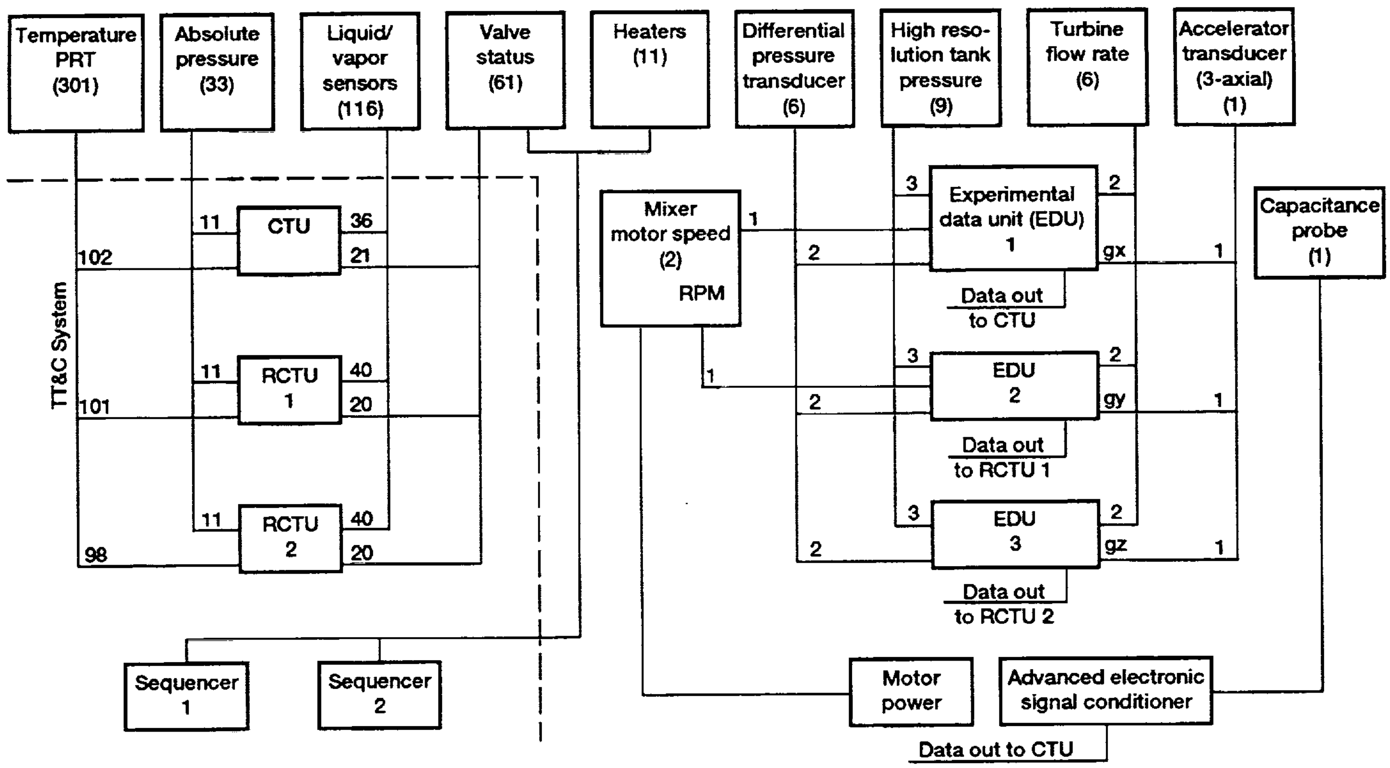


Figure 2.—Instrumentation and electronics system and TT&C interface block diagram.

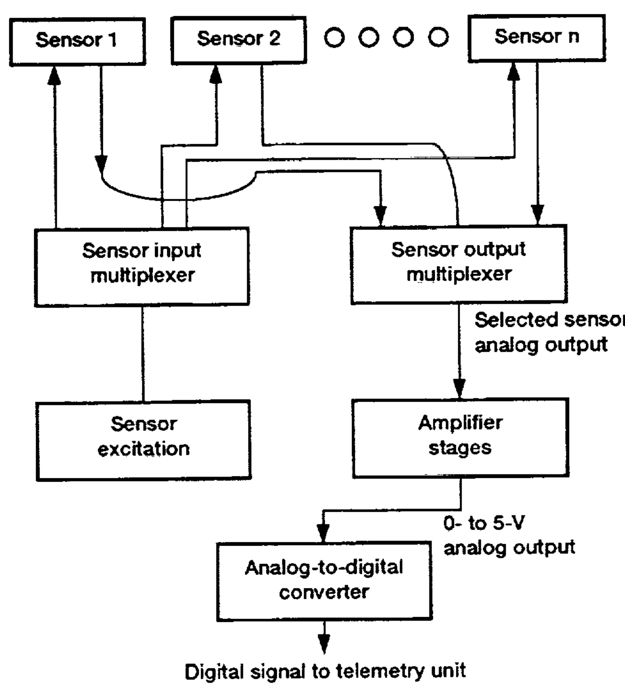


Figure 3.—Simplified data acquisition system block diagram.

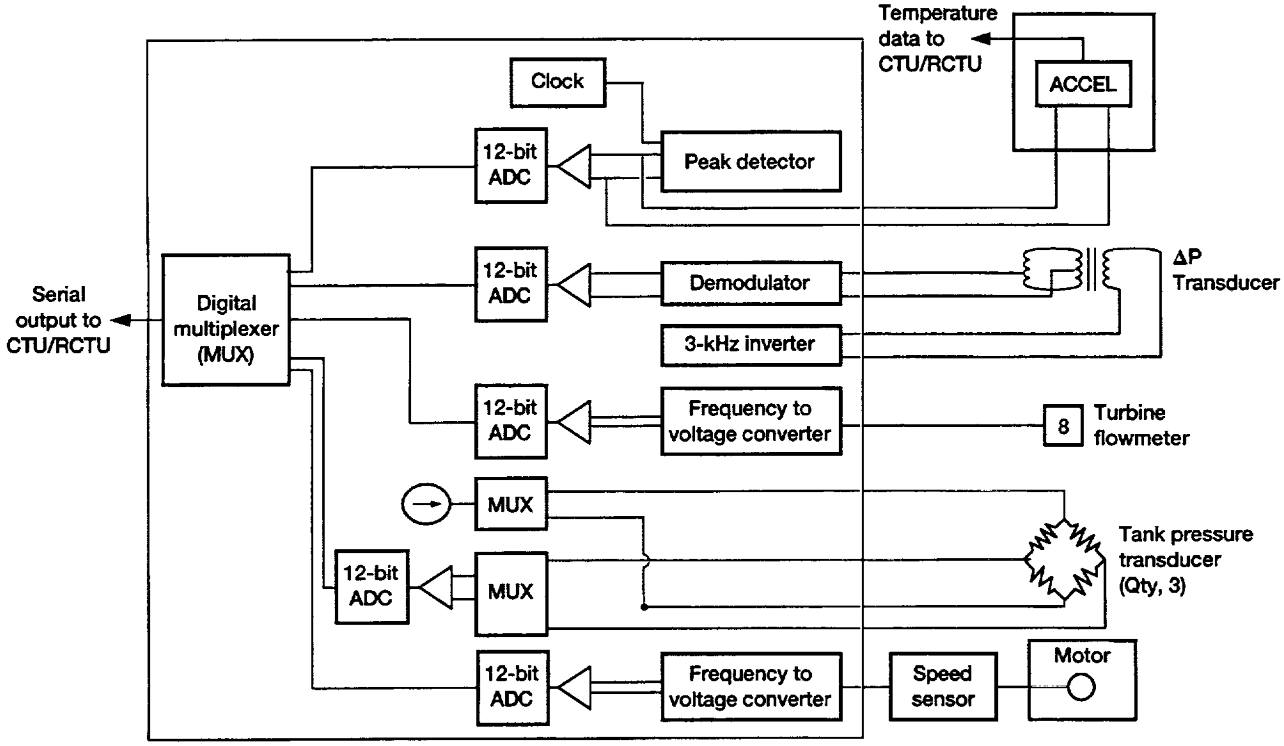


Figure 4.—Simplified experiment data unit (EDU) block diagram.

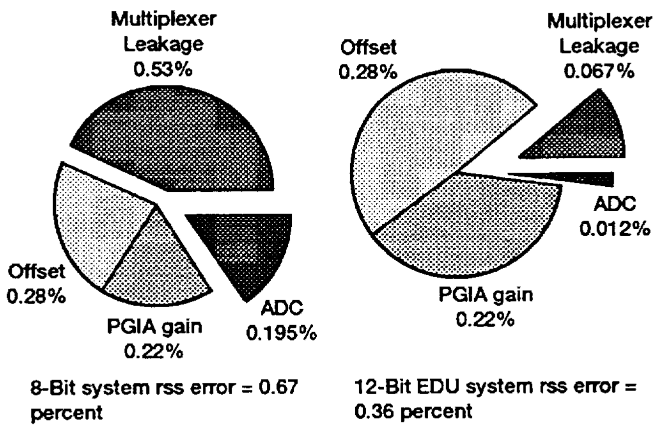


Figure 5.—Data Acquisition system estimated range error for 8-Bit TT&C and 12-Bit EDU systems.

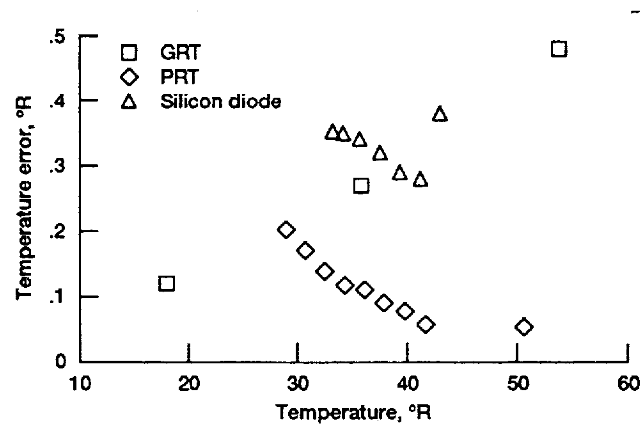


Figure 6.—High-accuracy temperature measurement errors.

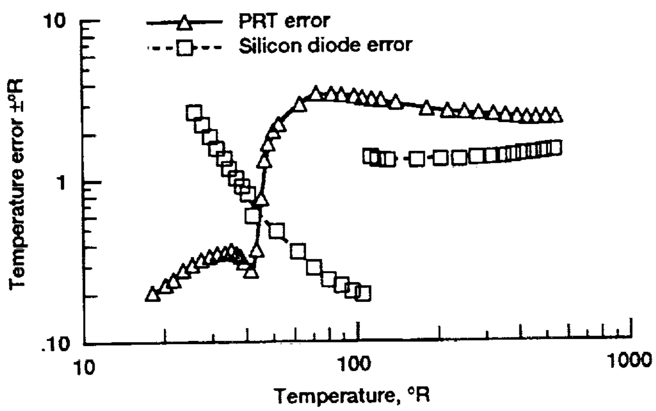


Figure 7.—Type AB temperature measurement system error.

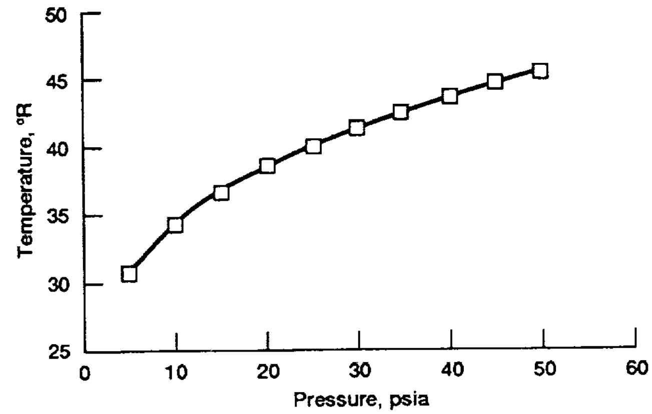


Figure 10.—Saturation temperature versus pressure of $LH_2$.

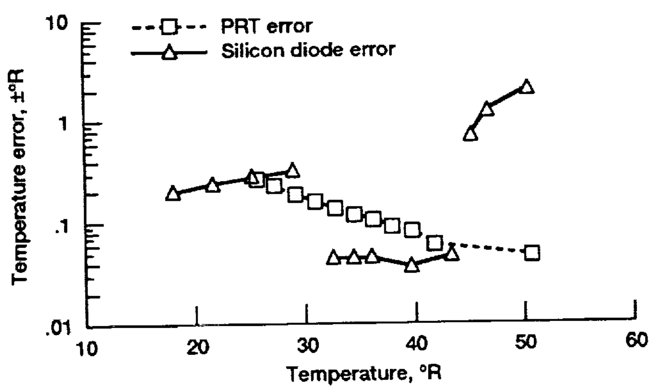


Figure 8.—Dual range diode temperature measurement system errors. 1.13-V offset (diode) for 32 to 43 °R range.

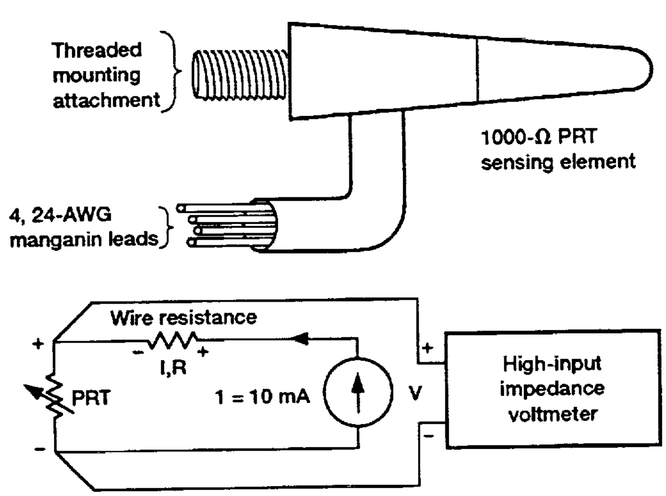


Figure 9.—1000-Ohm PRT probe and simplified operation schematic.

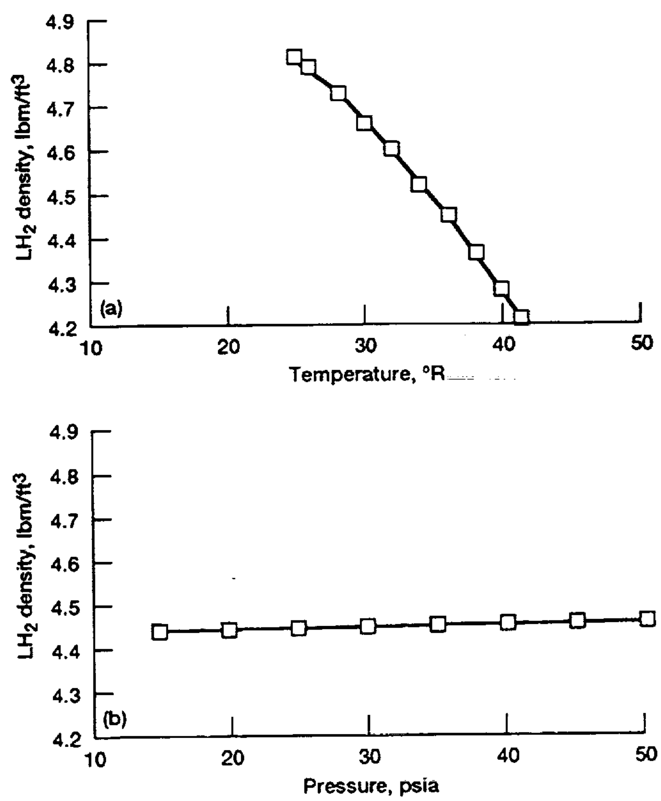


Figure 11.—Influence on $LH_2$ density of (a) temperature at 30 psia and of (b) pressure at 36 °R.

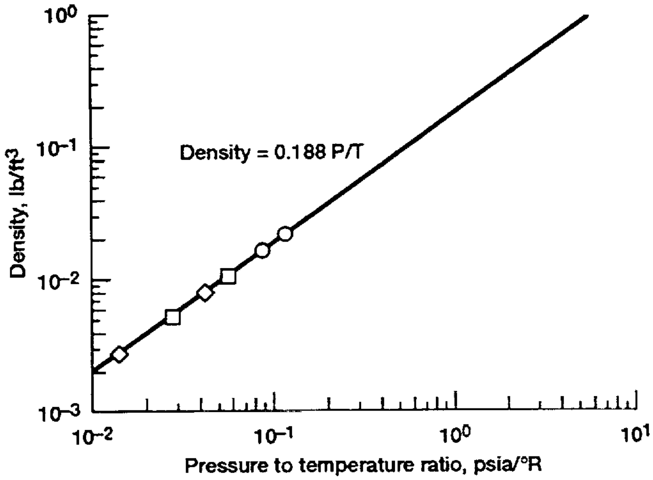


Figure 12.—$GH_2$ density versus pressure to temperature ratio. Temperature, range, 180 to 360 °R; pressure range, 5 to 20 psia.

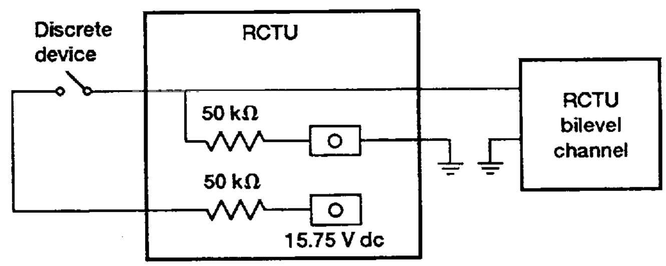


Figure 14.—Discrete measurement schematic.

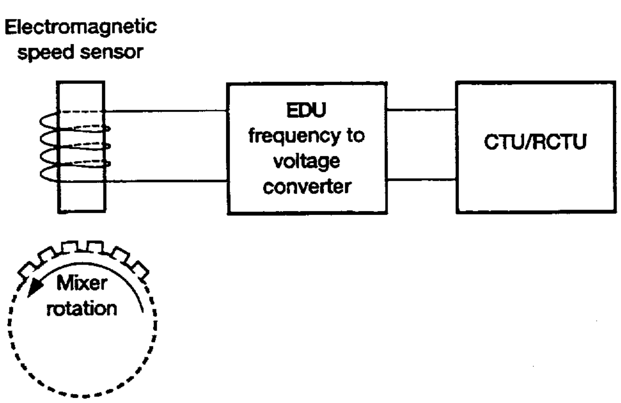


Figure 13.—Rotational speed sensor schematic.

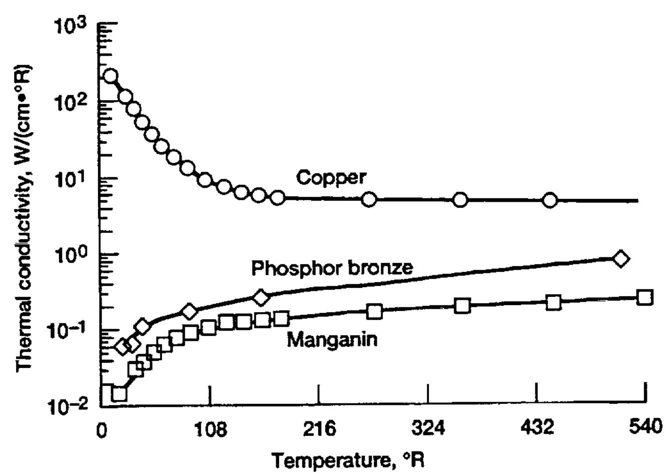


Figure 15.—Thermal conductivity of metals.

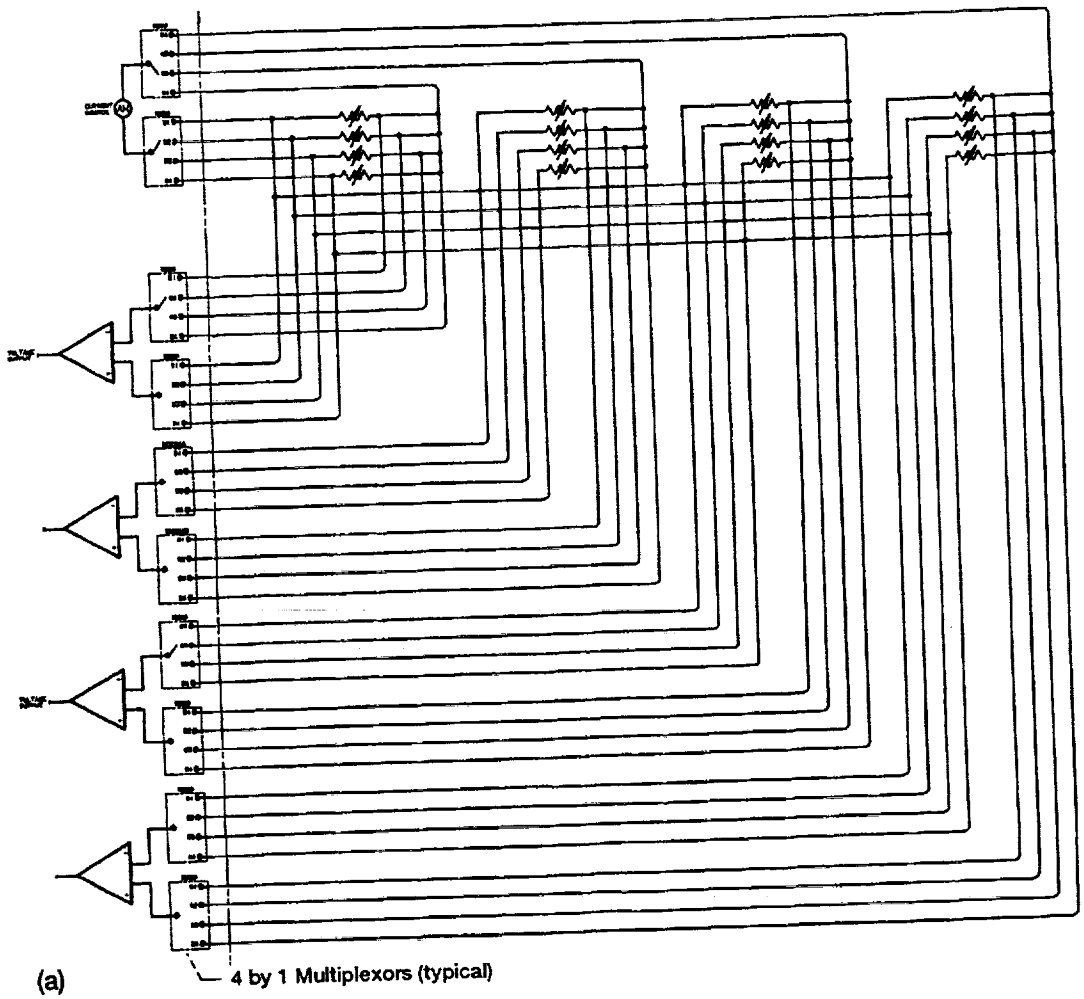


(a)

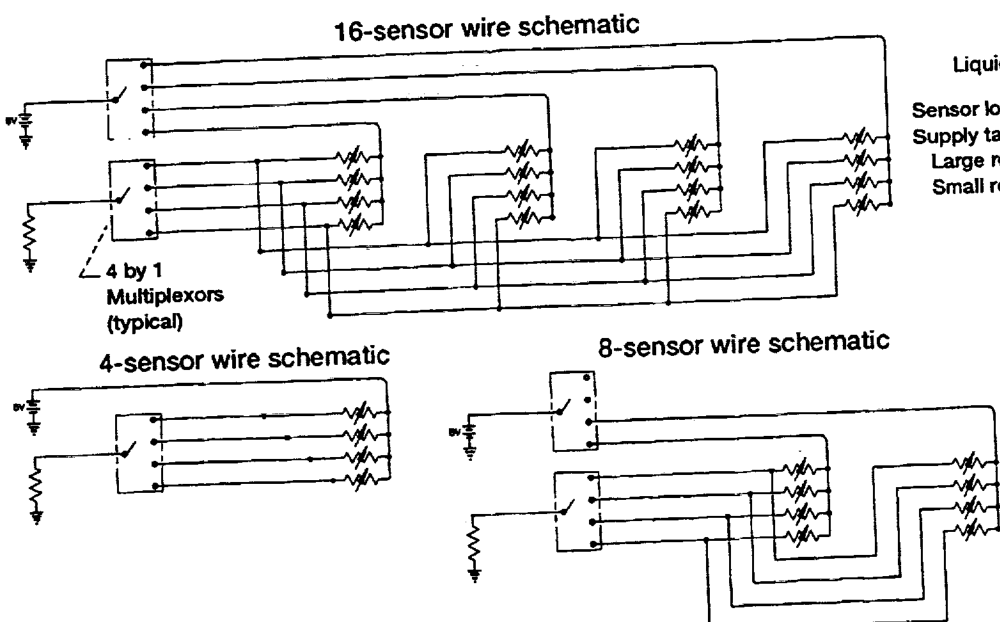


Liquid/vapor sensor wire allocations

| Sensor location | RCTU 1 | RCTU 2 | RCTU 3 |
|---|---|---|---|
| Supply tank | 5 | 8 | 8 |
| Large receiver | 8 | 6 | 8 |
| Small receiver | 8 | 8 | 6 |

(b)

Figure 16.—Multiplex use of common excitation wiring to reduce wire penetrations. (a) Temperature sensor wiring. (b) Liquid/vapor sensor multiplexed wire reduction technique.

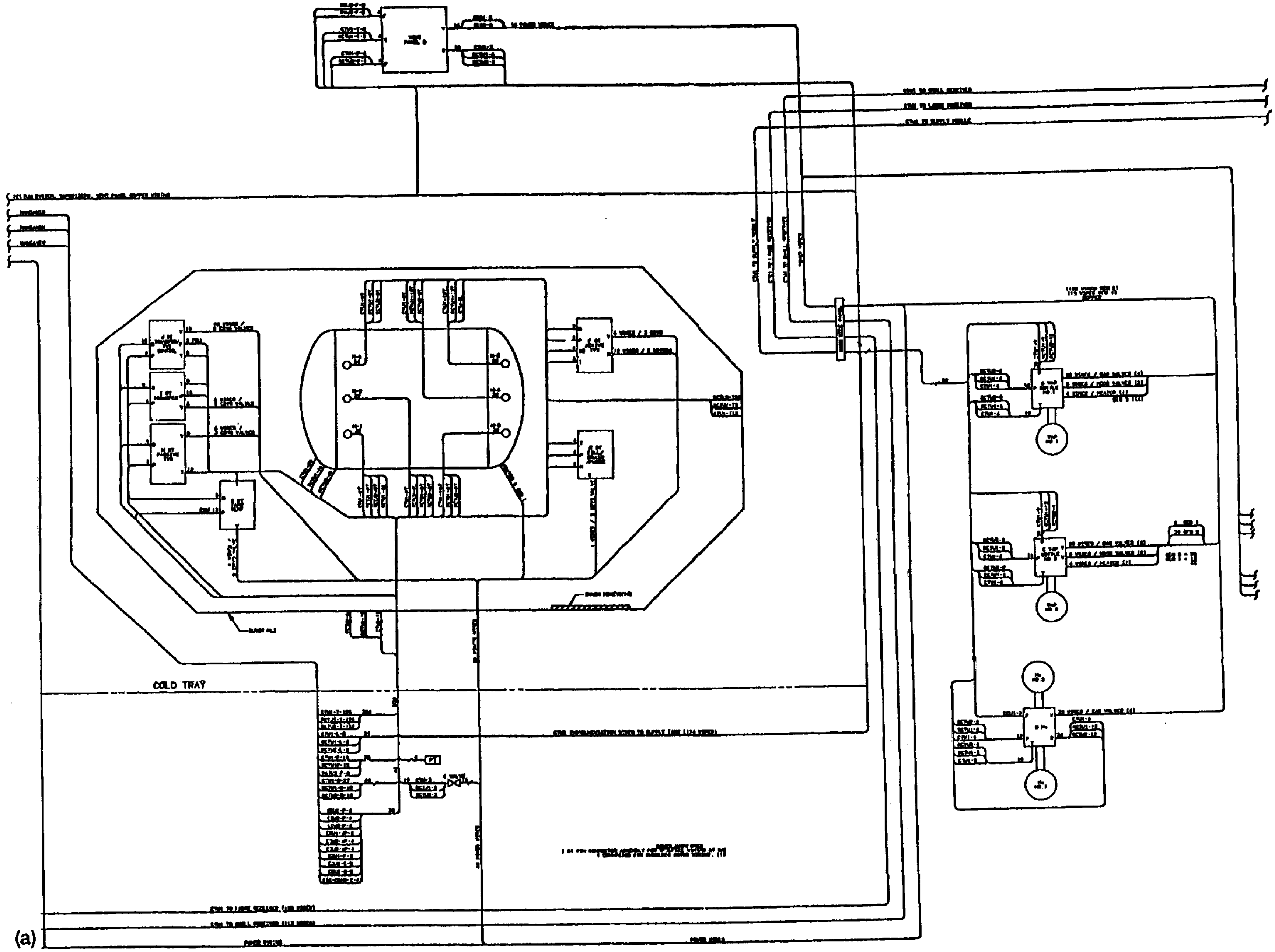


(a)

Figure 17.—Wire schematics. (a) Supply tank module wire harness. (b) Large receiver tank module wire harness. (c) Small receiver tank module wire harness. (d) Electronics bay wire harness. (e) Electronics bay 2 wire harness.

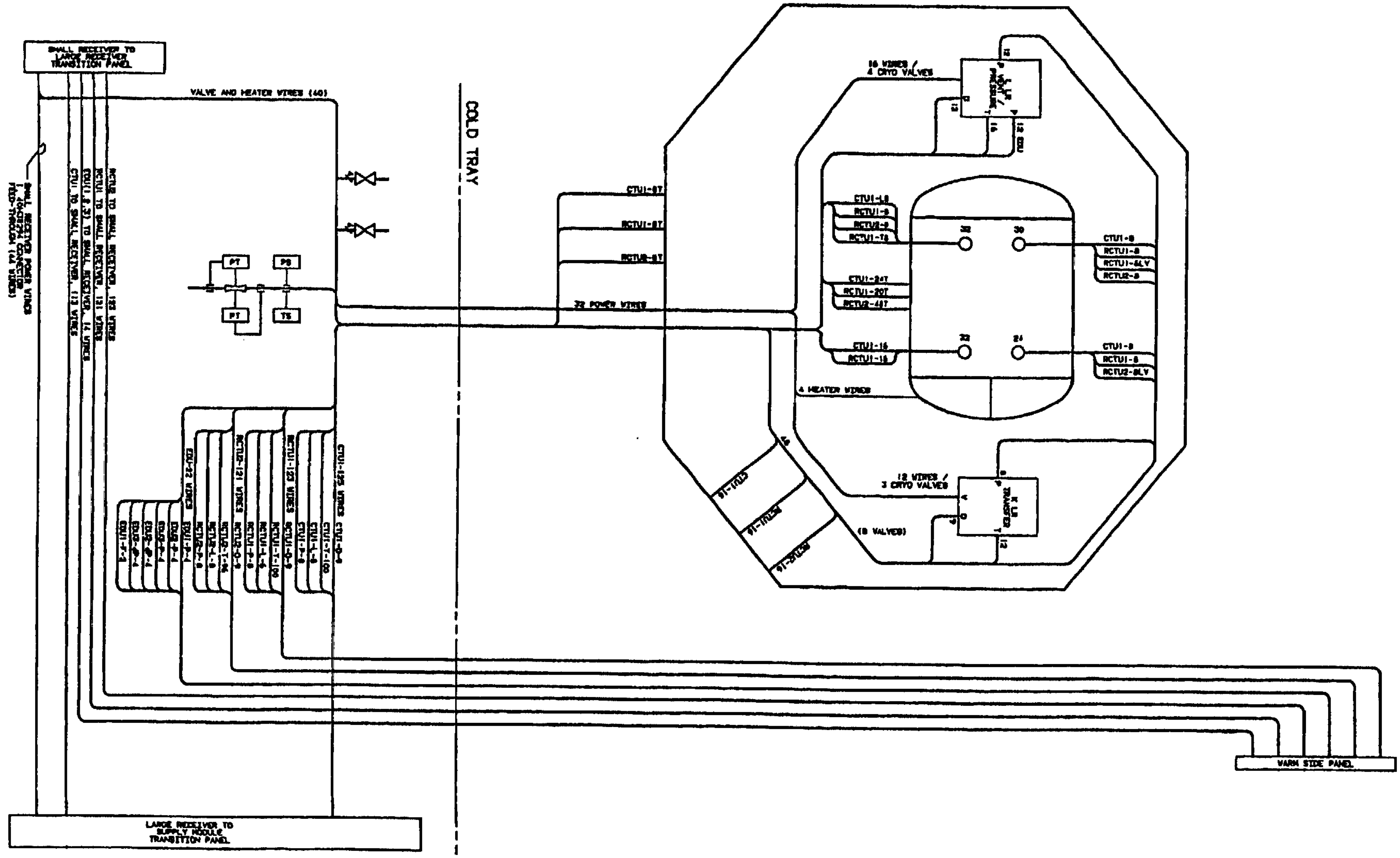


(b)

Figure 17.—Continued.

Small receiver instrumentation summary

| Sensor location | Temperature | Liquid/vapor | Pressure | Valves |
|---|---|---|---|---|
| Inside pressure vessel | 24 | 40 | 0 | 0 |
| Outer tank wall | 22 | 0 | 0 | 0 |
| Inside MLI | 20 | 0 | 8 | 9 |
| Outer MLI | 8 | 0 | 0 | 0 |
| Tray | 2 | 0 | 1 | 1 |
| Total | 76 | 40 | 9 | 10 |

Small receiver harness summary

| Wire purpose | Number | Type |
|---|---|---|
| Internal tank instrumentation | 92 | 24AWG manganin |
| External tank instrumentation | 260 | 24AWG manganin |
| Power | 44 | 18AWG phosphor bronze |
| Total | 414 | |

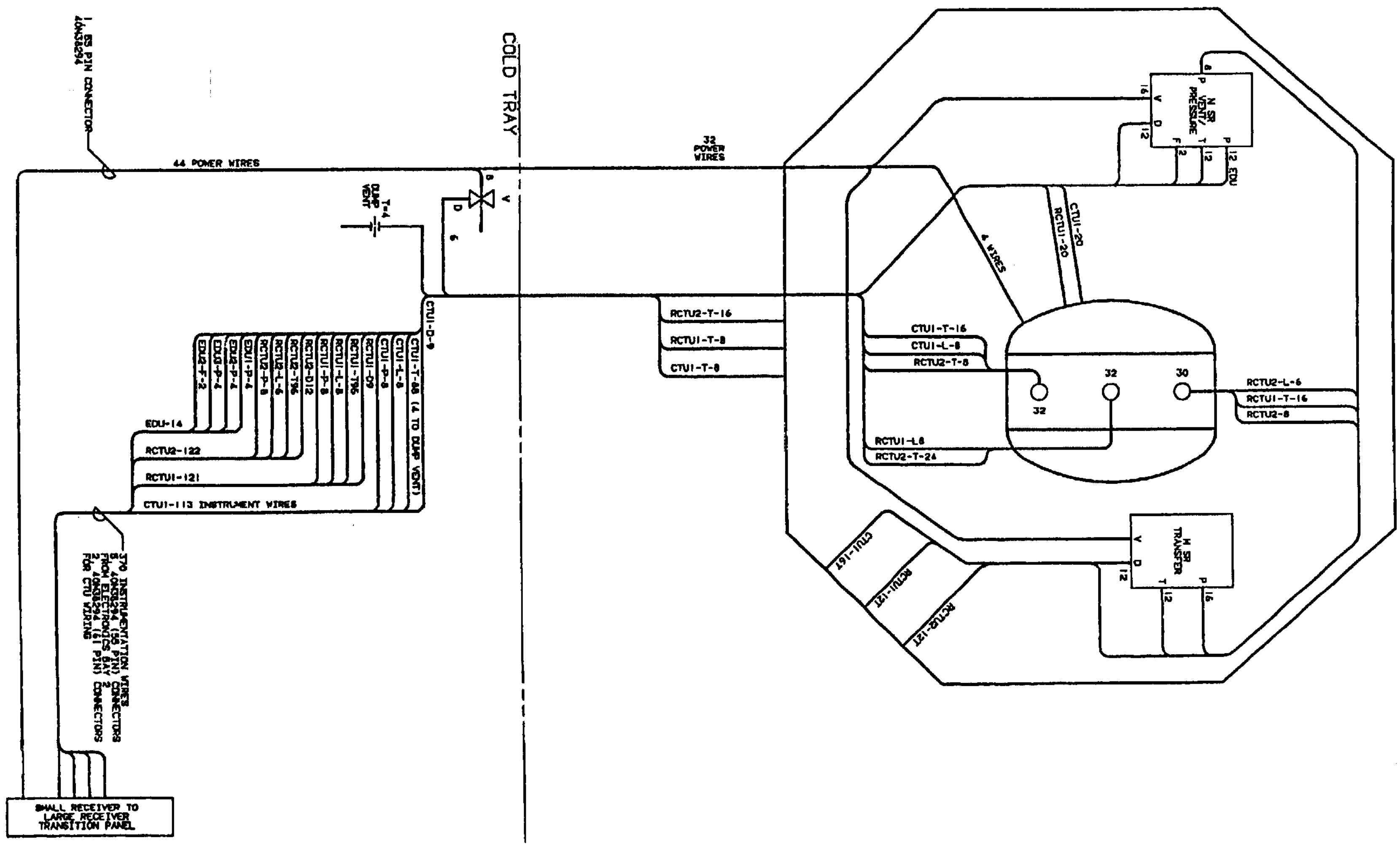


(c)

Figure 17.—Continued.

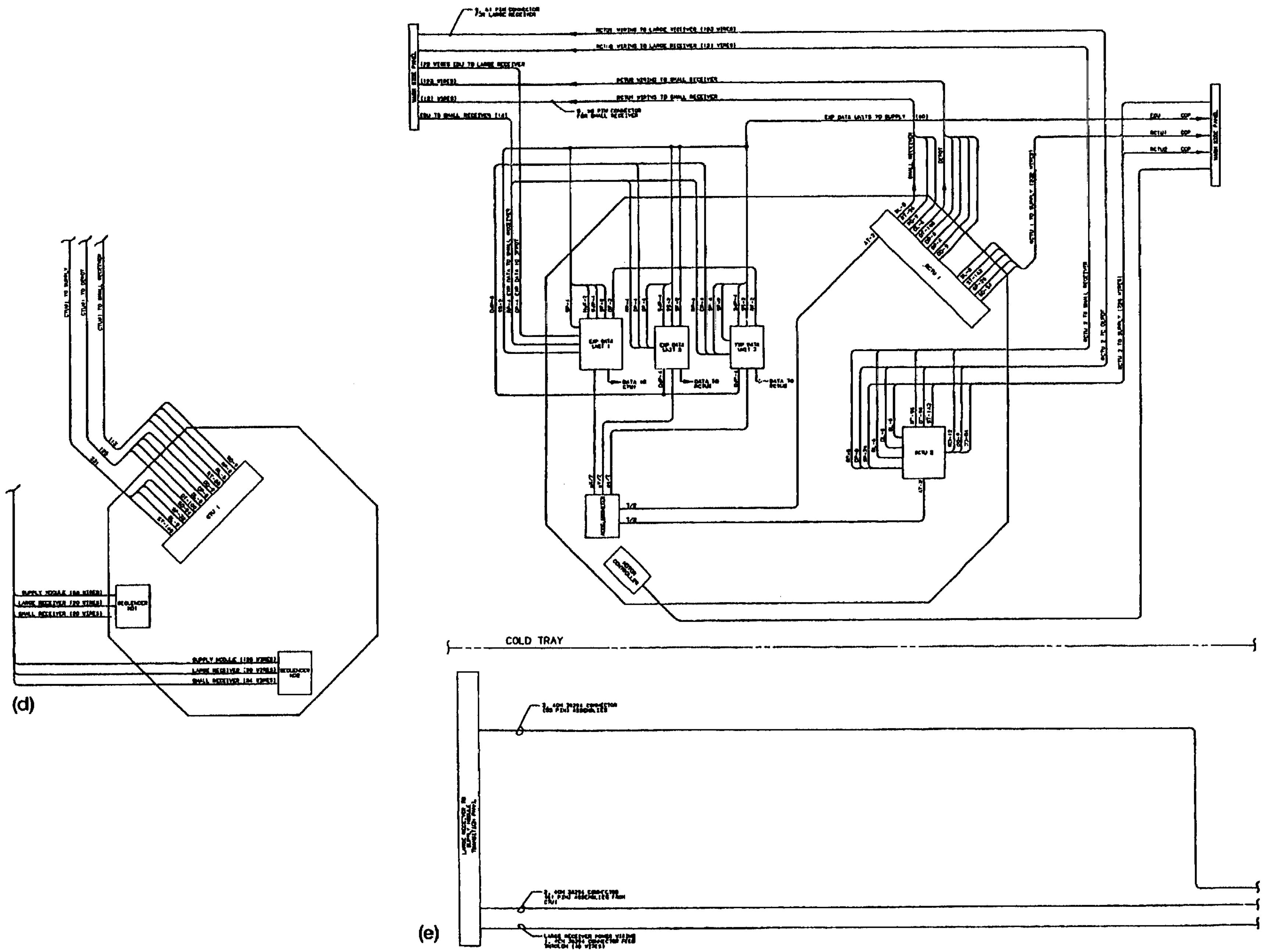


Figure 17.—Concluded.

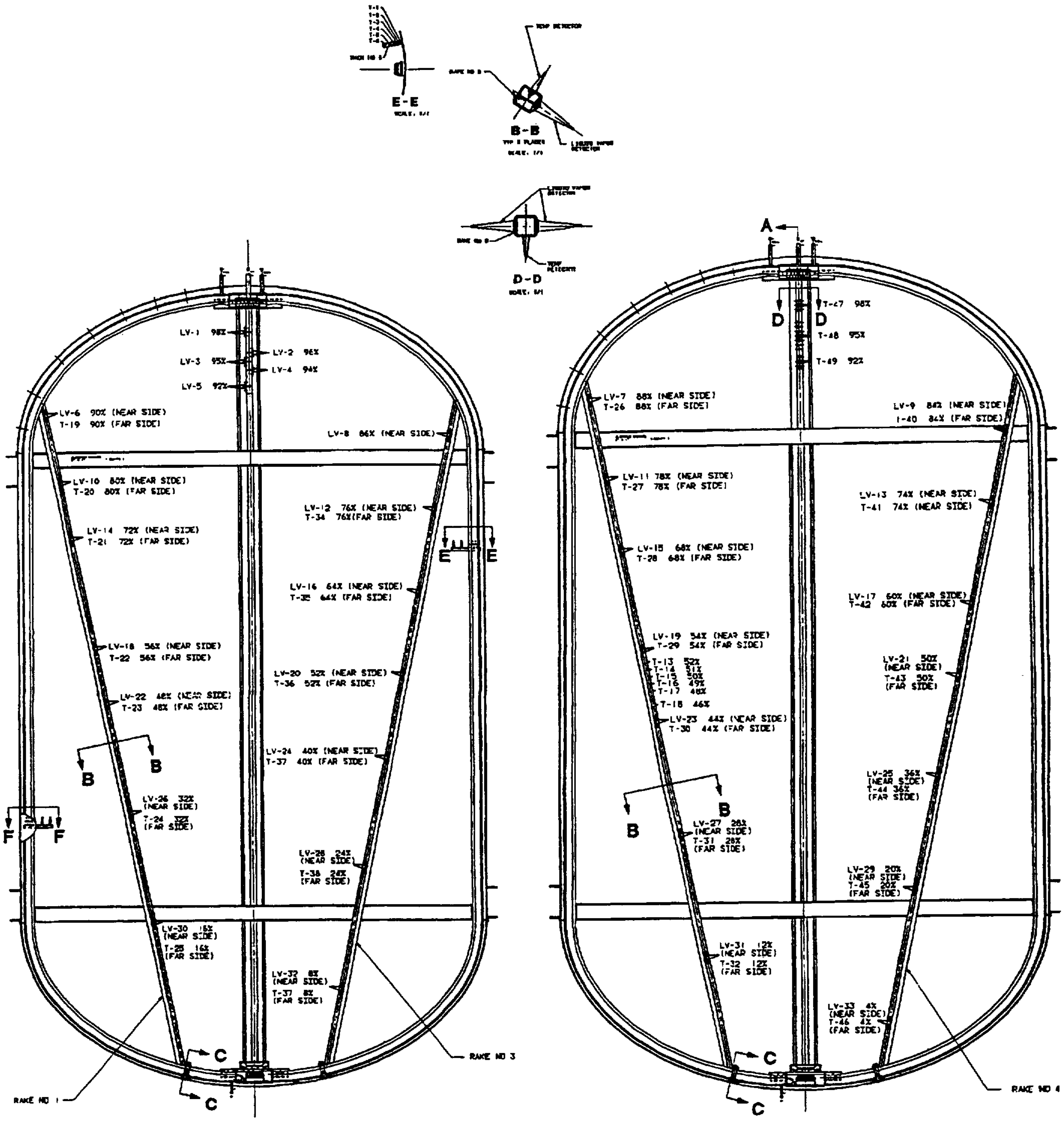


(a)

Figure 18.—Supply tank internal instrumentation. (a) Temperature and liquid vapor sensors. (b) Supply tank temperature sensors.

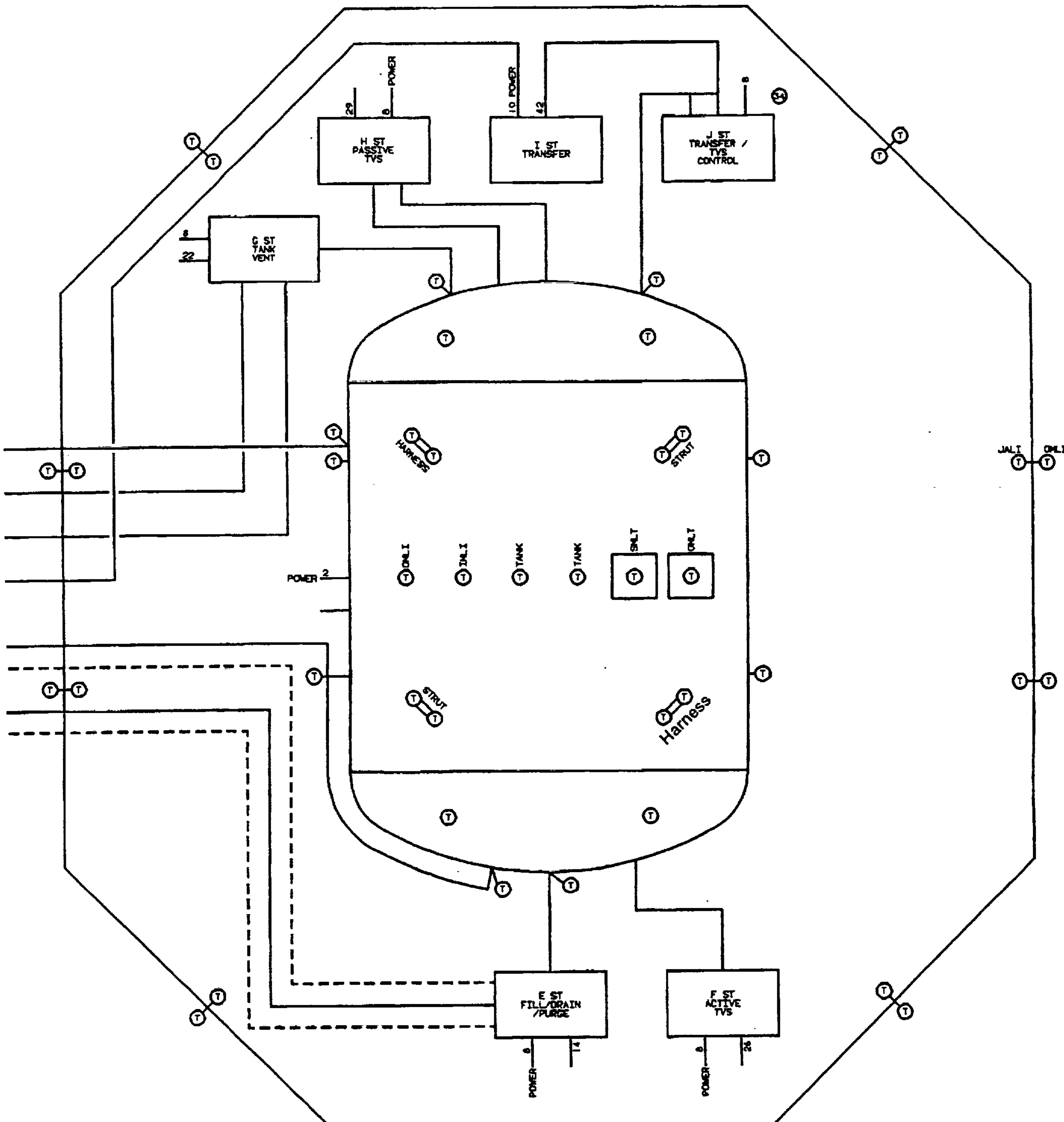


(b)

Figure 18.—Concluded.

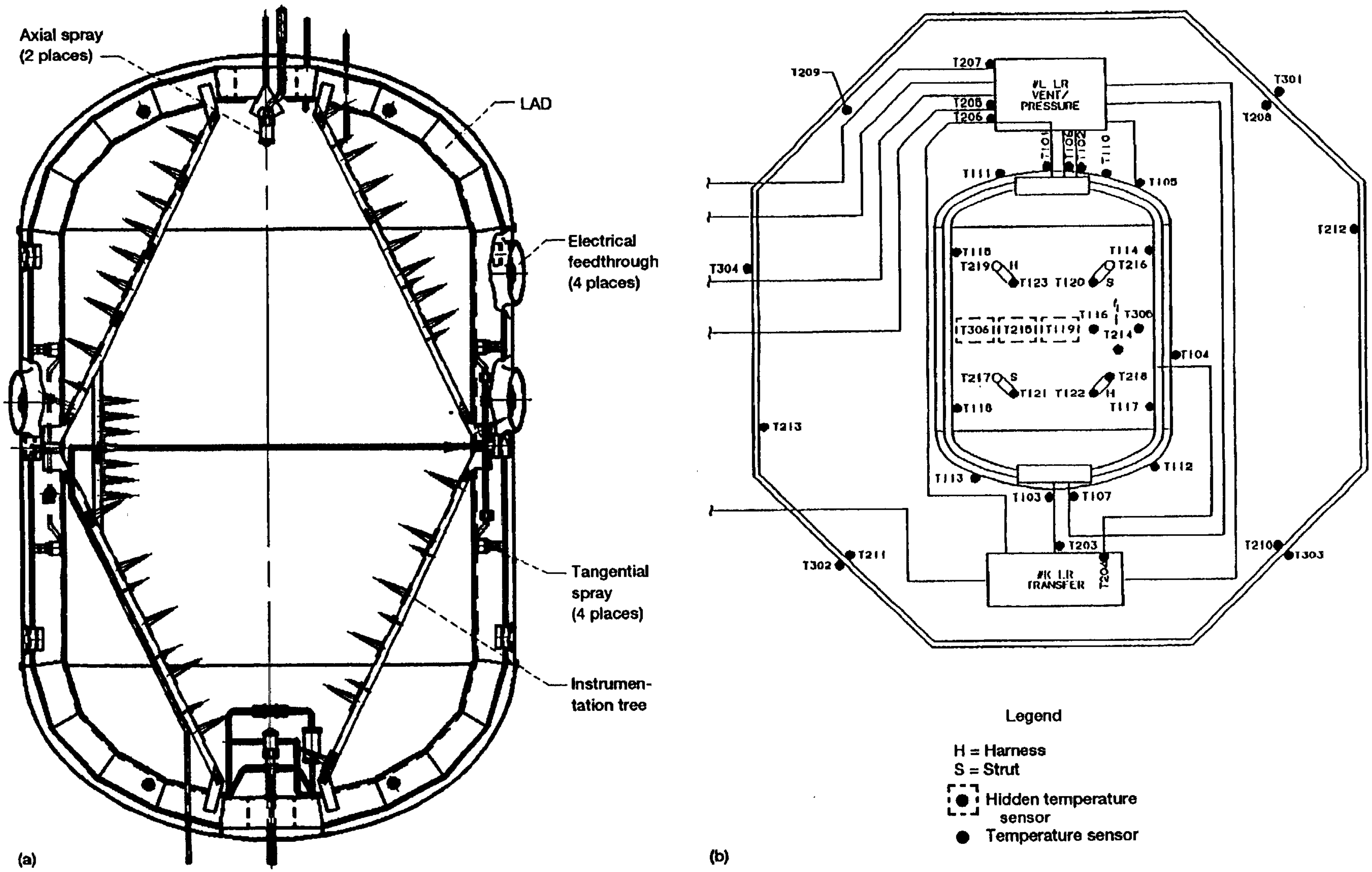


Figure 19.—COLD-SAT experiment subsystem. Large receiver tank instrumentation locations. (a) Internal instrumentation locations. (b) External temperature sensor locations.

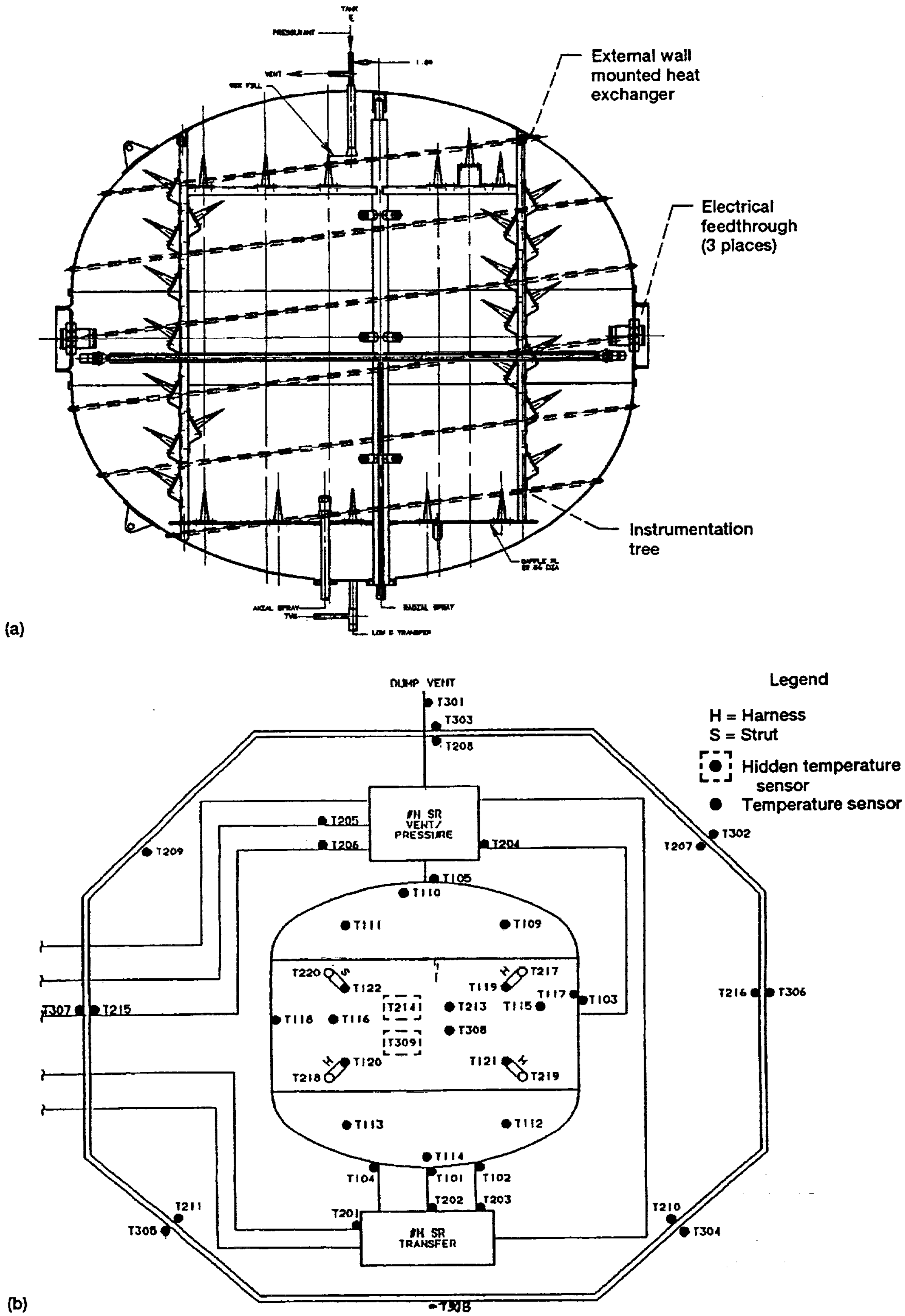


Figure 20.—COLD-SAT experiment subsystem small receiver tank instrumentation locations. (a) Internal instrumentation locations. (b) External temperature sensor locations.

# REPORT DOCUMENTATION PAGE

*Form Approved*
*OMB No. 0704-0188*



| 1. AGENCY USE ONLY (*Leave blank*) | 2. REPORT DATE | 3. REPORT TYPE AND DATES COVERED |
|---|---|---|
| | March 1994 | Final Contractor Report |

**4. TITLE AND SUBTITLE**
Cryogenic On-Orbit Liquid Depot Storage Acquisition and Transfer (COLD-SAT) Experiment Subsystem Instrumentation and Wire Harness Design Report

**5. FUNDING NUMBERS**
WU-506-48-00
C-NAS3-25776

**6. AUTHOR(S)**
Lawrence G. Edwards

**7. PERFORMING ORGANIZATION NAME(S) AND ADDRESS(ES)**
Analex Corporation
3001 Aerospace Parkway
Brook Park, Ohio 44142

**8. PERFORMING ORGANIZATION REPORT NUMBER**
E-8098

**9. SPONSORING/MONITORING AGENCY NAME(S) AND ADDRESS(ES)**
National Aeronautics and Space Administration
Lewis Research Center
Cleveland, Ohio 44135–3191

**10. SPONSORING/MONITORING AGENCY REPORT NUMBER**
NASA CR-189172

**11. SUPPLEMENTARY NOTES**
Project Manager, James R. Faddoul, Space Experiments Division, organization code 6780, (216) 433-6322.

**12a. DISTRIBUTION/AVAILABILITY STATEMENT**
Unclassified - Unlimited
Subject Categories 15, 16, 18, 19, 20, and 28

**12b. DISTRIBUTION CODE**

**13. ABSTRACT *(Maximum 200 words)***

Subcritical cryogens such as liquid hydrogen ($LH_2$) and liquid oxygen ($LO_2$) are required for space based transportation propellant, reactant, and life support systems. Future long-duration space missions will require on-orbit systems capable of long-term cryogen storage and efficient fluid transfer capabilities. COLD–SAT, which stands for cryogenic orbiting liquid depot-storage acquisition and transfer, is a free-flying liquid-hydrogen-management flight experiment. Experiments to determine optimum methods of fluid storage and transfer will be performed on the COLD–SAT mission. The success of the mission is directly related to the type and accuracy of measurements made. The instrumentation and measurement techniques used are therefore critical to the success of the mission. This paper presents the results of the COLD–SAT experiment subsystem instrumentation and wire harness design effort. Candidate transducers capable of fulfilling the COLD–SAT experiment measurement requirements are identified. Signal conditioning techniques, data acquisition requirements, and measurement uncertainty analysis are presented. Electrical harnessing materials and wiring techniques for the instrumentation designed to minimize heat conduction to the cryogenic tanks and provide optimum measurement accuracy are listed.

**14. SUBJECT TERMS**
COLD-SAT; Cryogenic; Liquid hydrogen; Instrumentation; Transducers; Signal conditioner; Data acquisition system; Binary digit (Bit); Resolution uncertainty; Manganin; Phosphor-Bronze; Wire harness; Thermal conductivity

**15. NUMBER OF PAGES**
72

**16. PRICE CODE**
A04

| 17. SECURITY CLASSIFICATION OF REPORT | 18. SECURITY CLASSIFICATION OF THIS PAGE | 19. SECURITY CLASSIFICATION OF ABSTRACT | 20. LIMITATION OF ABSTRACT |
|---|---|---|---|
| Unclassified | Unclassified | Unclassified | |

NSN 7540-01-280-5500

Standard Form 298 (Rev. 2-89)
Prescribed by ANSI Std. Z39-18
298-102